

KWAME NKRUMAH UNIVERSITY OF SCIENCE AND  
TECHNOLOGY, KUMASI, GHANA

Incorporating Joint Flexibility in Collapse Risk Assessment

KNUST

by

Osei Jack Banahene (BSc Civil Engineering)

A Thesis submitted to the Department of Civil Engineering  
College of Engineering

in partial fulfilment of the requirement for the degree of

MASTER OF PHILOSOPHY

SEPTEMBER, 2016

**DECLARATION**

I

I thereby declare that this submission is my own work towards MPHIL and that, to the best of my knowledge, it contains no material previously published by another person nor material which has been accepted for the award of any other degree of the University, except where due acknowledge has been made in the text.

# KNUST

Certified By: .....

OSEI JACK BANAHENE

Signature

Date

(PG 2208114)

Certified By: .....

Prof. Mark Adom-Asamoah

Signature

Date (Supervisor)

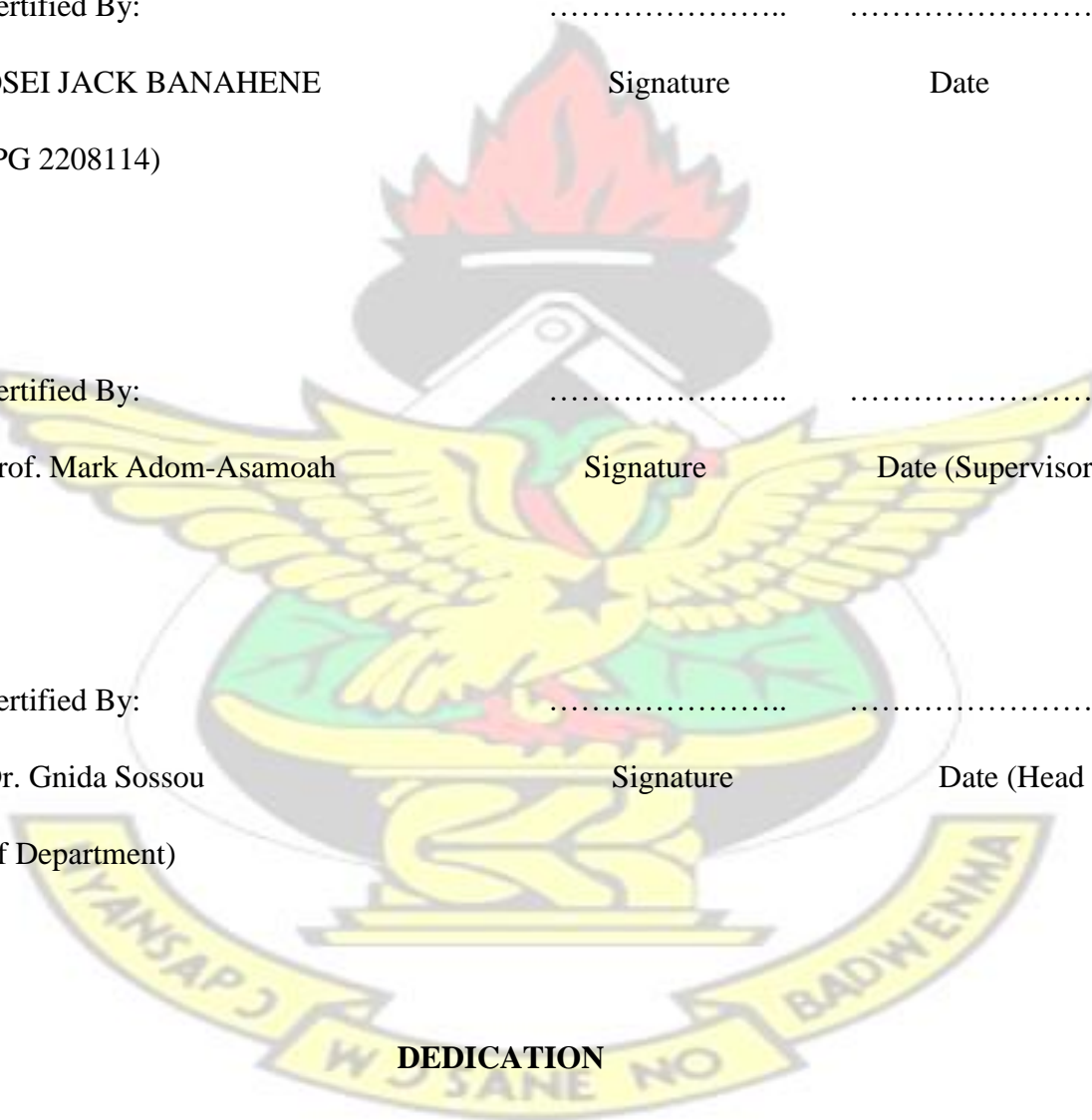
Certified By: .....

Dr. Gnida Sossou

Signature

Date (Head

of Department)



This work is dedicated to Jill Osei Banahene and the entire Osei Family.

# KNUST



## **ACKNOWLEDGEMENT**

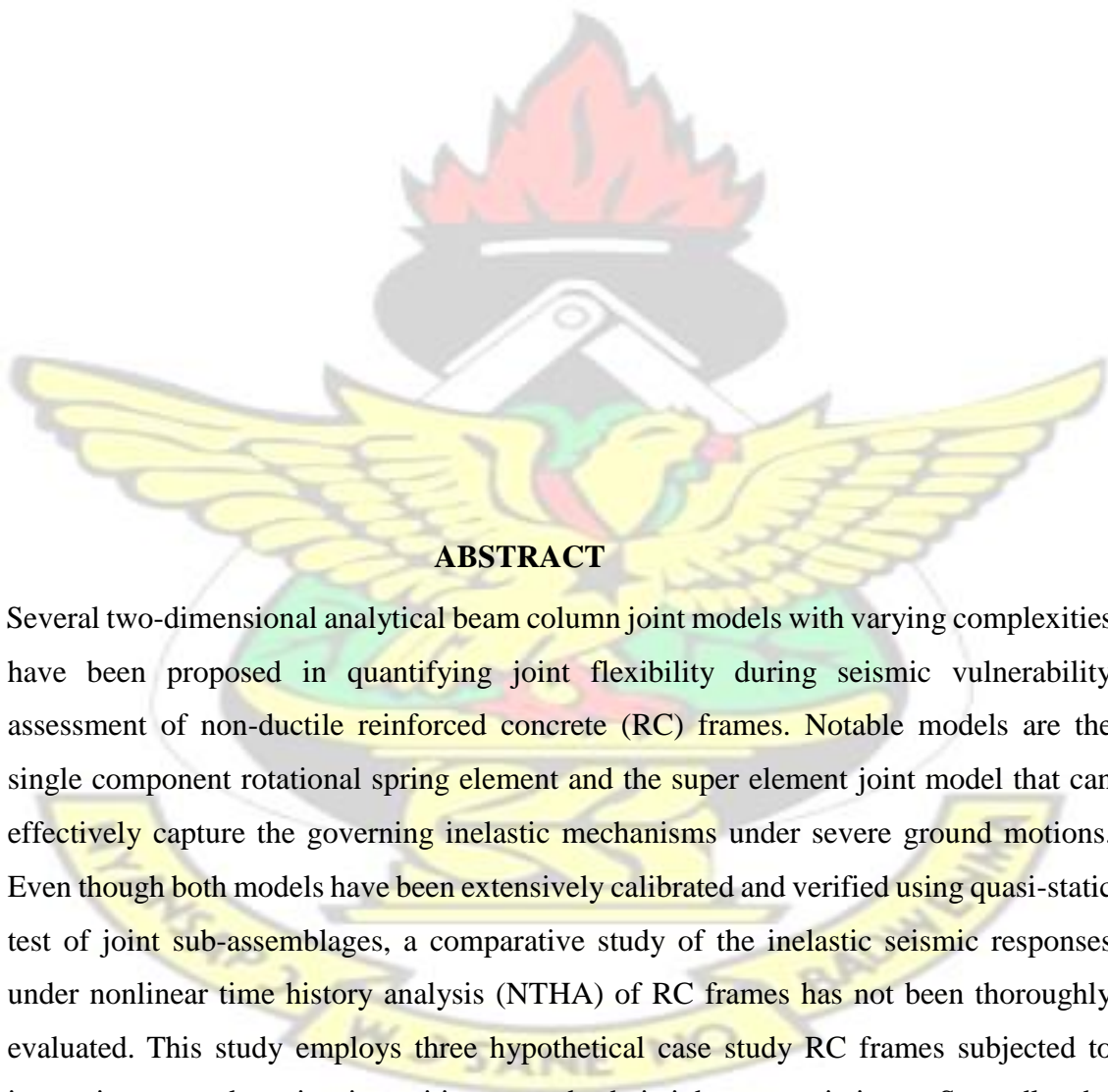
I would like to express my deep appreciation to my supervisor, Professor Mark AdomAsamoah, for his encouragement and constant support during all these years and for granting me the opportunity to work under his supervision. Many thanks are due Professor Reginald DesRoches and Dr. Jong-Su Jeon for generously sharing with me experimental results of shake table test which was used in this study and providing helpful feedback.

Thanks are also due students, staff and faculty who in one way or the other helped shape my career path. A special thanks to Amanda and Daniel Peprah for allowing me to run

most of my simulations on their computers. They played a big role in my productivity throughout the years of demanding studies.

Finally, I am very grateful to my parents and siblings for all the sacrifices and the unbelievable support given me. May the Good Lord Bless them.

# KNUST



## **ABSTRACT**

Several two-dimensional analytical beam column joint models with varying complexities have been proposed in quantifying joint flexibility during seismic vulnerability assessment of non-ductile reinforced concrete (RC) frames. Notable models are the single component rotational spring element and the super element joint model that can effectively capture the governing inelastic mechanisms under severe ground motions. Even though both models have been extensively calibrated and verified using quasi-static test of joint sub-assemblages, a comparative study of the inelastic seismic responses under nonlinear time history analysis (NTHA) of RC frames has not been thoroughly evaluated. This study employs three hypothetical case study RC frames subjected to increasing ground motion intensities to study their inherent variations. Secondly, the issue of super-element joint models, causing numerical divergence in non-linear time history analysis of reinforced concrete frames, is investigated. The rigid joint assumption and a single rotational spring model are implemented for comparison. Reinforced concrete joint sub-assemblages and a one-third scaled frame have been employed for

model validation. Results indicate that the super element joint model overestimates the transient drift ratio at the first storey and becomes highly unconservative by under-predicting the drift ratios at the roof level when compared to the single-component model and the conventional rigid joint assumption. In addition, between these storey levels, a decline in the drift ratios is observed as the storey level increased. However, from this limited study, there is no consistent evidence to suggest that care should be taken in selecting either a single or multi component joint model for seismic risk assessment of buildings when a global demand measure, such as maximum inter-storey drift, is employed in the seismic assessment framework. Probabilistic seismic demand analysis also indicates that super-element joint model may be less vulnerable relative to the single-component joint model. Furthermore, the shift in fragility function may lie in between the rigid joint and single-component joint modelling schemes, implying non-divergence.

## TABLE OF CONTENT

DECLARATION .....	II
DEDICATION .....	III
ACKNOWLEDGEMENT .....	IV
ABSTRACT .....	V
LIST OF TABLES .....	VIII
LIST OF FIGURES .....	
IX	CHAPTER 1: INTRODUCTION
.....	1
1.1 Background .....	1
1.2 Problem Statement .....	5
1.3 Aim of Research .....	6

1.4 Manuscript Organization .....	7
<b>CHAPTER 2: LITERATURE REVIEW .....</b>	<b>8</b>
2.1 Introduction .....	8
2.2 Performance Based Earthquake Engineering Framework .....	8
2.2.1 Hazard Analysis .....	9
2.2.2 Structural Analysis .....	12
2.2.3 Damage Analysis .....	20
2.2.4 Loss Analysis .....	23
2.3 Analytical Representation of Component Behaviour .....	26
2.3.1 OPENSEES Conceptual Framework .....	26
2.3.2 Component Deteriorating Hysteretic Models .....	28
2.3.3 Joint Shear Strength Models .....	35
2.3.3.2 Joint Component Modelling Schemes .....	45
2.4 Summary .....	51
<b>CHAPTER 3: METHODOLOGY AND CONCEPTUAL FRAMEWORK .....</b>	<b>53</b>
3.1 Introduction .....	53
3.2 Analytical Modelling of Structural Component .....	54
3.3 RC Joint Sub-assemblages for Validation .....	56
3.5 Conceptual Framework for Assessing Variation in Dynamic Responses .....	60
3.5.1 Analysis .....	62
3.6 Fragility Assessment Framework of a Case Study RC Frame .....	65
<b>CHAPTER 4: RESULTS AND DISCUSSIONS .....</b>	<b>68</b>
4.1 Introduction .....	68
4.2 Comparison of joint modelling schemes for RC joint sub-assemblages .....	68
4.2.1 Interior Joint .....	68
4.2.1 Exterior joint .....	69
4.2.3 Knee Joint .....	71
4.3 One third scaled prototype RC Frame .....	72
4.4 Evaluation of Dynamic response .....	74
4.4.1 First Storey .....	76
4.4.2 Roof Level .....	78
4.4.3 General Case .....	80

4.5 Seismic Vulnerability Assessment .....	81
4.5.1 Probabilistic seismic demand model .....	81
4.5.2 Fragility Functions .....	83
4.6 Summary of Findings .....	87
CHAPTER 5: CONCLUSIONS AND RECOMMENDATIONS .....	89
5.1 Conclusions .....	89
5.2 Recommendations for Future Research .....	91
6. REFERENCES .....	92

## LIST OF TABLES

<b>Table</b>	<b>Page</b>
Table 3.1. Statistical properties of parameters for Latin-hyper cube experimental design. .....	66
Table 4.1. Ratio of mean and standard deviation of the normalized drift responses at the first floor level .....	76
Table 4.2. Ratio of mean and standard deviation of the means of Z at the first floor level .....	77
Table 4.3. Ratio of mean and standard deviation of the normalized drift responses at the roof floor level .....	79
Table 4.4. Ratio of mean and standard deviation of the means of Z at the roof floor level .....	79
Table 4.5. Ratio of mean and standard deviation of the normalized drift responses.....	80
Table 4.6. Ratio of mean and standard deviation of the means of Z. ....	81

## LIST OF FIGURES ..... VII

Fig. 1.1. Partial Building Collapse due to failure of beam-column joints in the Izmit, Turkey earthquake of August 17,1999, (b) close-up of third-level joint, (c) close-up of second-level joint, (Courtesy of NISEE, University of California, Berkeley).....	2
Fig. 1.2. Typical sub-standard construction details, (adopted from Hassan, 2011) .....	3
Fig. 2.1. Hazard curve at Van Nuys, California, USA (adapted from Baker, 2005).....	10

Fig. 2.2. Typical de-aggregation results at Van Nuys, California, USA (adapted from Baker , 2005) .....	11
Fig. 2.3. Cloud analysis (adopted from Baker, 2005).....	15
Fig. 2.4. Incremental dynamic analysis (adopted from Vamvatsikos, 2011) .....	18
Fig. 2.5. Single stripe analysis (Baker, 2005).....	19
Fig. 2.6. Multi stripe analysis (adopted from Baker, 2005).....	19
Fig. 2.8. Power law functional approximation of a ground motion hazard curve. (adopted from Jalayer , 2003).....	23
Fig. 2.9: Typical drift hazard curve (adopted from Baker , 2005) .....	24
Fig. 2.10. Typical example of mean repair cost-intensity measure relationship .....	26
Fig. 2.11. Schematic illustration of PBEE.....	26
Fig. 2.12. <i>Opensees</i> conceptual framework.....	28
Fig. 2.13. Clough and Johnstone (1965) hysteretic model .....	29
Fig. 2.14: Takeda (1970) hysteretic model.....	30
Fig. 2.15. Song and Pincheira (2000) hysteretic model.....	30
Fig. 2.16. Ibarra-Medina-Krawinkler hysteretic model.....	31
Fig. 2.17. Modified Ibarra-Medina-Krawinkler hysteretic model.....	32
Fig. 2.18. Cyclic force displacement relationship of the YSPDs generated using the BWBN material model (adopted from Hossain <i>et al.</i> , 2013).....	33
Fig. 2.19. Shear force-deformation behaviour of Leborgne (2012) degrading hysteretic model.....	35
Fig. 2.20: Pinching4 material model (Lowe and Altoontash , 2003).....	36
Fig. 2.21. Schematic diagram of Ortiz (1993) joint shear strength model (adopted from Park and Mosalam, 2012).....	39
Fig. 2.22. Schematic diagram of Vollum (,1998) joint shear strength model (adopted from Park and Mosalam , 2012) .....	40
Fig. 2.23. Schematic diagram of Hwang and Lee (1999) joint shear strength mechanisms (adopted from Hassan , 2011) .....	40
Fig. 2.24. Relative contribution of shear transfer mechanisms to joint shear strength proposed by Hwang and Lee (1999), adopted from Hassan (2011).....	41
Fig. 2.25. Schematic diagram of Park and Mosalam (2012) joint shear strength model. ....	42
Fig. 2.26. Alath and Kunnath (1995) schematic representation of joint region .....	47
Fig. 2.27. Lowe and Altoontash (2003) schematic representation of joint region.....	49
Fig. 2.28. Altoontash (2004) schematic representation of joint region .....	51
Fig. 3.1. Joint modelling techniques and constitutive material models.....	56

Fig. 3.2. Selected RC joint sub-assemblages for validation of modelling schemes .....	59
Fig. 3.3. One-third scaled frame (Bracci <i>et al.</i> ,1995).....	59
Fig. 3.4. 1952 Taft (N021E) accelerogram to a peak ground acceleration of 0.2g .....	60
Fig. 3.5. Target Response Spectrum for various classes of record sets.....	61
Fig. 3.6: Geometry of hypothetical RC frames .....	61
Fig. 3.7. Case study RC frame for fragility assessment .....	66
Fig. 4.1. Base shear –drift responses for interior joint sub-assemblages.....	69
Fig. 4.2. Base shear –drift responses for exterior joint sub-assemblages.....	71
Fig. 4.3. Base shear –drift responses for exterior joint sub-assemblages.....	72
Fig. 4.4. Roof displacement response history for various joint models .....	73
Fig. 4.5. Peak in-time drift profile for the three RC frames .....	76
Fig 4.6. Probabilistic demand model analysis of RC frame with different joint modelling schemes .....	82
Fig. 4.7: Analytical fragility functions for various joint modelling schemes.....	85
Fig. 4.8: Relative shift in limit state probability between joint model .....	86

**Figure**

**Page**



## CHAPTER 1: INTRODUCTION

### 1.1 Background

In the present wake of performance-based earthquake engineering (PBEE), the assessment of the vulnerability of a structural system to withstand seismic forces has been addressed by employing probabilistic models to quantify the level of uncertainties associated with the estimation of the seismic demand imposed on a structure given an intensity of ground shaking (Liel *et al.*, 2009). Reliable quantification of the seismic performance of existing reinforced concrete buildings has been one of the major challenges within the earthquake engineering research community. The performancebased earthquake engineering (PBEE) methodology, since its inception, has provided engineers with a systemic way to incorporate and propagate uncertainties relating to, for instance, the estimation of seismic responses of structures subjected to severe ground shaking. The process culminates in a probabilistic framework for seismic assessment. This developed probabilistic framework decouples the risk assessment problem into four key areas; hazard, structural, damage and loss analysis. The final output may be the conditional mean annual frequency of repair cost exceeding a specified percentage of the total replacement cost of a specific structural system given the intensity of the ground motion (Liel *et al.*, 2009). Usually, a global scalar parameter, with a prescribed probability distribution, is used to interface the various stages of the assessment framework. In order to systematically quantify the degree of uncertainties, such as modelling of structural elements and record to record variability in selected ground motions, past researches have assumed the conditional distributions of the parameters in the PBEE methodology to be markovian dependent (Baker and Cornell, 2003). This assumption allows, for instance, to estimate the probability of exceedance

of the structural response quantity (structural analysis), given a parameter describing the intensity of ground shaking (hazard analysis), without necessarily requiring knowledge of pertinent information such as the distribution of magnitudes and source-to-site distances during the probabilistic seismic hazard analysis (PSHA) as well as the ground motion attenuation model used. Hence, one can analytically estimate the fragility of the structural system without necessarily requiring certain site specific information.

In order to reduce the dispersion in the modelling uncertainties associated with structural components, past researches have emphasized the importance of modelling the behaviour of beam-column connections in a bid to predict the seismic demand efficiently (Park, 2010). This is due to the fact that recent earthquakes have shown that older type non ductile reinforced concrete buildings are very vulnerable and do sustain significant damage under seismic action (see Fig. 1.1). Existing earthquake reconnaissance surveys (Moehle and Mahin, 1991; Sezen *et al.*, 2002) have stressed that non-ductile detailing of structural components should not be tolerated in highly seismic zones.



Fig. 1.1. Partial Building Collapse due to failure of beam-column joints in the Izmit, Turkey earthquake of August 17,1999, (b) close-up of third-level joint, (c) close-up of second-level joint, (Courtesy of NISEE, University of California, Berkeley)

In low to moderate seismic zones, where the capacity design philosophy is usually ignored, vulnerability assessment of existing older type reinforced concrete structures designed before the introduction of modern seismic codes, must concentrate on RC joint details. The major deficiencies that are typical of such buildings include the absence of transverse hoops, insufficient anchorage of beam reinforcement, splicing longitudinal reinforcement and short embedment length of bottom beam reinforcement within the joints (see Fig. 1.2).

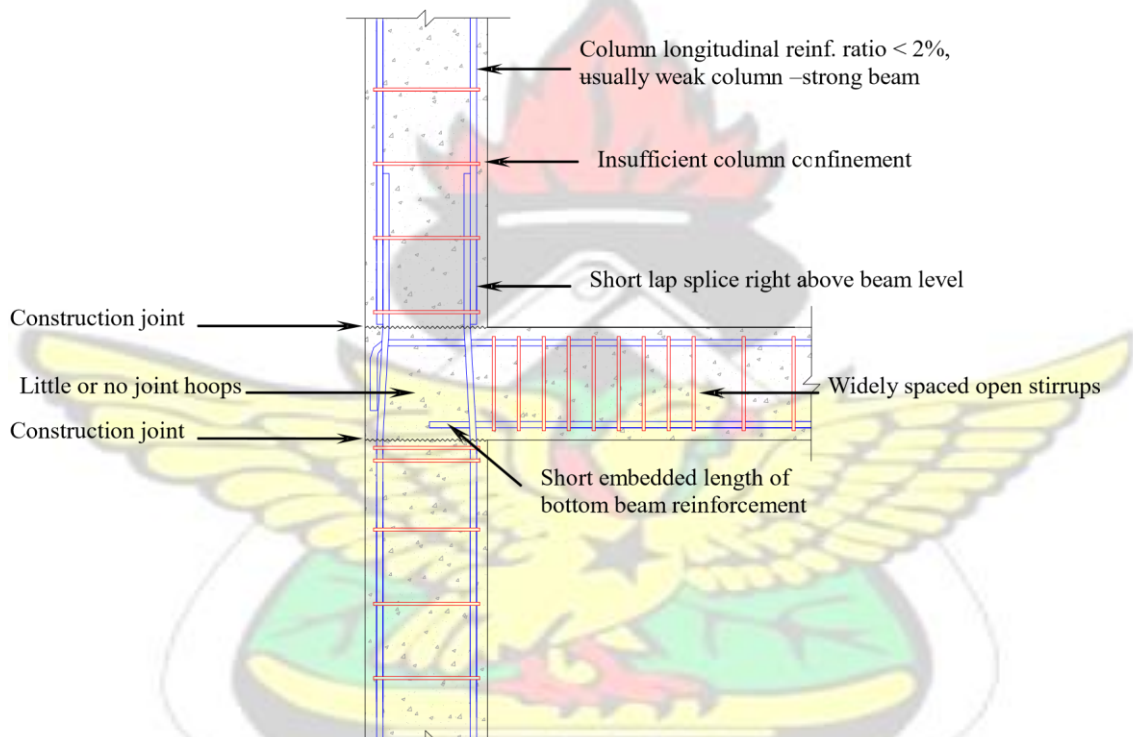


Fig. 1.2. Typical sub-standard construction details, (adopted from Hassan, 2011)

Of these deficiencies, the absence of transverse reinforcement within the joint has been found to be the major contributor to the formation of inelastic mechanisms that can significantly increase the inter storey drift ratio. An implication to this phenomenon will be to develop high fidelity analytical models that can capture these joint inelastic mechanisms to help understand the seismic behaviour of these older -type frames for

effective risk mitigation strategies. Also, these joints do not have the ability to dissipate more energy due to their limited shear capacities. They may, therefore, fail when subjected to high shearing stress from the lateral forces generated by earthquakes. If these lateral forces are high enough to induce bond deterioration between the reinforcing steel and the surrounding concrete, anchorage failure, leading to bar pullout, is observed. Moehle and Mahin (1991) noted that beam-column joints of reinforced concrete (RC) buildings, typical of the pre 1970 regime, have exhibited significant strength and stiffness deterioration during earthquakes and may lead to the global collapse of the structural system. Hence, in such frames, the development of shear resisting mechanisms (strut and truss mechanisms), to induce ductile failure under dynamic loading are not present (Hoffmann *et al.*, 1992).

In view of this, researchers (Celik and Ellingwood, 2008; Park and Mosalam, 2012; Jeon *et al.*, 2015) have proposed joint shear strength models that can be used to predict the behaviour of joints under seismic excitation. Most of these models have been validated and calibrated to satisfy specific RC joint configurations and types. Currently, some researchers have employed statistical methods, such as Bayesian analysis and multivariate linear regression analysis, to predict the joint shear strength of a wide range of beam-column connections using a single predictive equation. By employing this unified predictive equation, the risk assessment of non-ductile RC frames that include joint flexibility can be performed with ease, relatively. Intuitively, by quantifying joint contribution in the modelling process, we gain more knowledge into the behaviour of RC frames as well as reducing the aleatorical uncertainties in the probabilistic risk assessment framework.

## **1.2 Problem Statement**

To incorporate joint flexibility in nonlinear seismic analysis, most researches have quantified the deformations due to shear and pull-out by proposing joint shear stress-strain envelope responses and bond strength-slip models for appropriate definition of the joint region; rotational springs, bar-slip springs and link elements (Hassan, 2011; Birely *et al.*, 2012; Jeon, 2013; Shafaie *et al.*, 2014; Borghini *et al.*, 2016). One major simplification has been to explicitly model the joint response by providing a single rotational spring to simulate all the underlying inelastic mechanisms. This approach, with the introduction of rigid links that span the joint dimensions, has been widely used to numerically simulate joint flexibility. This is because, with the appropriate description of the joint constitutive law, it is able to yield a fairly strong correlation of the highly pinched behaviour of tested RC joint sub-assemblies under quasi-static loading (Theiss, 2005; Celik, 2007; Hassan, 2011). Concerns have been raised as to it being inappropriate to capture joint kinematics (Theiss, 2005; Celik, 2007; Hassan, 2011). Hence, by adopting a super element model that allows transparency in assessing the individual contributions of the major inelastic mechanisms, the joint kinematics can be accounted (Youssef and Ghoborah, 2001; Lowes and Altoontash, 2003; Chao-Lie and Bing, 2015; Zhang *et al.*, 2016).

Even though this approach has been extensively validated by experimental responses of quasi statically tested RC sub-assemblies, researchers have noted that the use of multi-spring joint models (super element), for quantifying joint response in nonlinear time history analysis of RC frame simulation, may cause numerical divergence; as such, the approach of using a single rotational spring element is preferred (Park and Mosalam, 2012). Mitra and Lowes (2007) noted that this numerical instability in the global solution algorithm may be attributed to the fact that the bar-slip springs possessing a strain softening behaviour, characterized by having a negative tangent stiffness after

reaching their ultimate capacities, results in having negative eigenvalues. Significant modification has been made to the parent model to address this issue, which was validated using an extensive dataset of quasi-statically loaded sub-assemblages. More so, the number of one dimensional constitutive models required to define the monotonic backbone curve and hysteretic rules make it demanding as opposed to the single-element model. Therefore, studies relating the use of the super-element model in nonlinear simulation of RC frames have been given little attention.

### **1.3 Aim of Research**

The aim of this study was to explore the impact and differences in seismic demands when the explicit representation of the joint region is implemented by either a single or a multi-component model, under nonlinear time history analysis.

The specific objectives were:

- To validate the usage of the super element joint modelling scheme for assessing seismic performance.
- To explore the relative contributions of joint flexibility in the estimation of the inelastic seismic response of gravity loading RC frames, when the rigid, single or super element joint modelling schemes are implemented in computer simulations.
- To assess the inherent variations of the various joint models in estimated analytical fragility functions

### **1.4 Manuscript Organization**

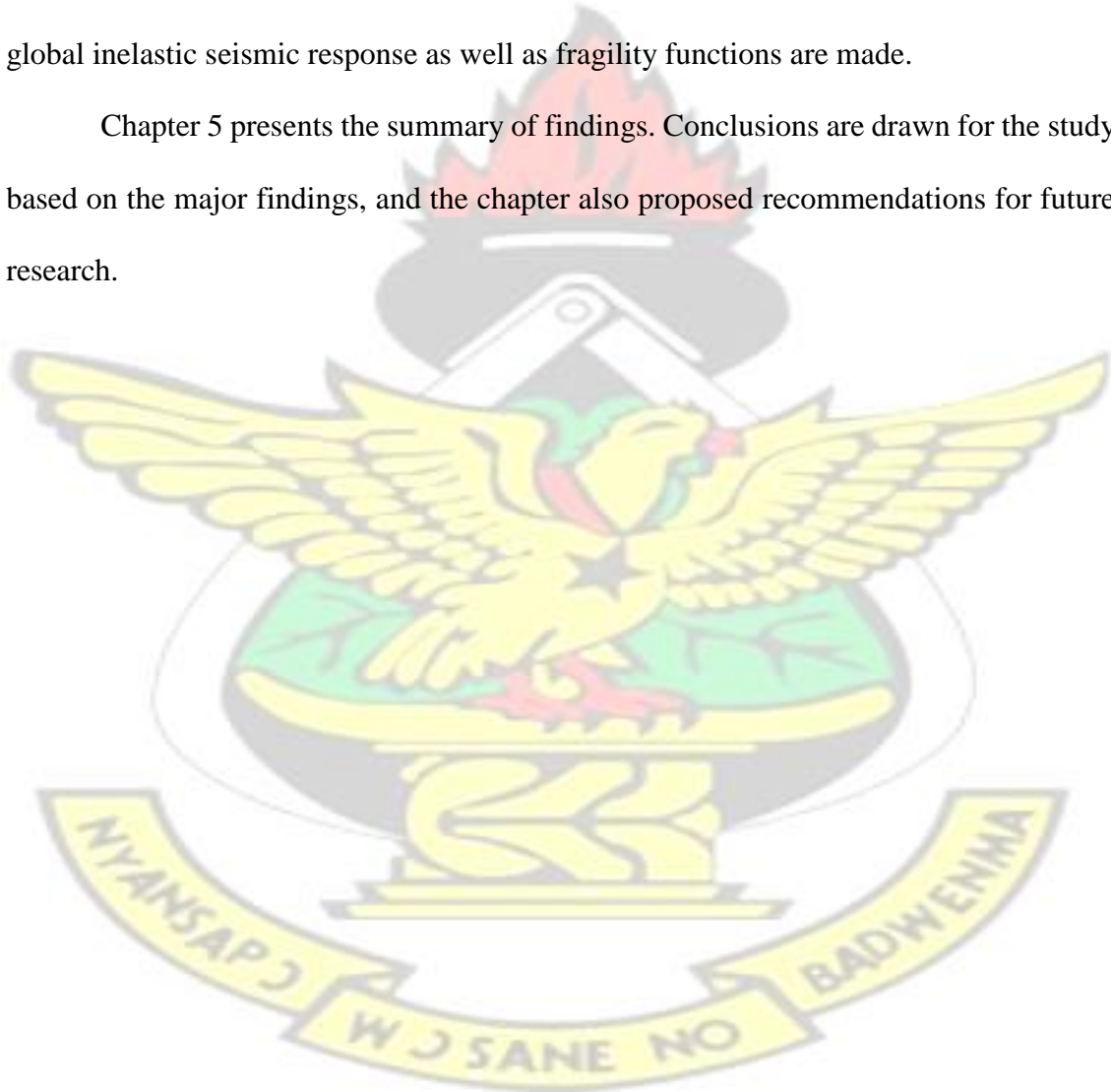
This research document is organized in five chapters. Chapter 2 presents a literature review on the application of the performance based earthquake engineering framework,

laying much emphasized on methods and analytical modelling approaches that are used to collaborate the various stages of assessment.

Chapter 3 details out the analytical modelling of structural components, describes the conceptual framework for assessment and the estimation methods used to generate the fragility curves for various joint modelling schemes.

Chapter 4 presents results of validation of the numerical simulation of the various joint modelling schemes under study. Discussions on the impact and variation of the global inelastic seismic response as well as fragility functions are made.

Chapter 5 presents the summary of findings. Conclusions are drawn for the study based on the major findings, and the chapter also proposed recommendations for future research.



## **CHAPTER 2: LITERATURE REVIEW**

### **2.1 Introduction**

This chapter provides a review of pertinent literature on the assessment of seismic performance of structures that rely on probabilistic methods for propagating the major source of uncertainties arising from analytical representation of component behaviour and variability in seismic responses from future seismic events. It provides a systematic walk through the application of the performance based earthquake engineering framework, laying much emphasis on methods and analytical modelling approaches that are used to collaborate the various stages of assessment.

## **2.2 Performance-Based Earthquake Engineering Framework**

Earthquakes, which are rare and extreme events, are highly stochastic in nature and, as such, in assessing the seismic performance of structural systems, a probabilistic framework that is able to propagate all the various forms of uncertainties is warranted. The performance-based methodology, since its inception, has allowed practicing engineers, to make reliable quantitative assessment of economic and financial losses that future uncertain seismic events may pose. In order to perform a holistic probabilistic risk assessment, a collaborative effort from multiple research disciplines such as seismology, geotechnical engineering, structural dynamics and soil dynamics is required (Chandler and Lam, 2001). Extensive research effort (Cornell and Krawinkler, 2000; Moehle and Deierlein, 2004) has been spent over the years to make this complex framework worthwhile for practical use. The thematic stages of the assessment framework involves sequentially performing a hazard analysis, structural analysis, damage analysis and finally a loss analysis as discussed below.

### **2.2.1 Hazard Analysis**

Hazard analysis begins with the determination of the distribution of the levels of ground excitation that future seismic events may generate at a particular building site. This is done through probabilistic seismic hazard analysis (PSHA) which aggregates all sources

of uncertainties in seismic characteristics of future earthquakes. PSHA primarily involves the identification of seismically active faults that may pose damaging effects to structures, characterizing their distribution of magnitude (through rates of occurrences) that they generate and the distribution of how far these faults are from the sites of interest (source-to-site distances). Once this information becomes available, Equation (2.1) can then be used to compute the mean annual rate of exceeding an intensity measure (IM), conditional on the fundamental period of the structure located at the site of interest.

$$\lambda(IM \geq x) = \sum_{i=1}^{n_{sources}} \lambda(M_i) \sum_{j=1}^{n_M} \sum_{k=1}^{n_R} P(IM \geq x | m_j, r_k) P(M_i = m_j) P(R_i = r_k) \quad (2.1)$$

Where  $\lambda(IM \geq x)$  is the mean annual rate of exceeding at intensity measure,  $x$ ;  $\lambda(M_i)$  is the rate of occurrence for magnitude  $i$ , which can be computed using —*GutenbergRichter recurrence law*”;  $P(IM \geq x | m_j, r_k)$  is the conditional probability of exceedance of the intensity measure given a specific magnitude,  $m_j$ , and source-to –site distance,  $r_k$  (this requires using a ground motion prediction equation to compute the related mean and standard deviation of the density function needed for computation of probabilities);  $P(M_i = m_j)$  is the probability of magnitude  $m_j$  occurring at the fault;

$P(R_i = r_k)$  reflects the likelihood of source-to-site distance being  $r_k$ . From this computation, a ground motion hazard curve that relates the intensity measure to the mean annual rate of exceeding a particular hazard level is developed (see Fig. 2.1).

Since this approach (PSHA) aggregates the relative contribution of each seismically active fault in finding the mean rate of exceedance, the hazard curve does not explicitly give any information on which magnitudes or faults are more likely to cause the exceedance of specific ground motion intensity. Hence, an extension of PSHA, known

as *de-aggregation*, can be used to answer the question of —which seismic events can lead to exceeding a particular intensity measure?— and is computed using Equation (2.2) or (2.3).

$$P(M = m | IM = x) = \frac{(IM = x, M = m)}{\sum_{i=1}^{n_{sources}} P(IM = x | m_i, r_k) P(M_i = m) P(R_i = r_k)} \quad (2.2)$$

$$P(M = m | IM = x) = \frac{\sum_{i=1}^{n_{sources}} P(M_i = m) P(IM = x | m_i, r_k) P(R_i = r_k)}{\sum_{j=1}^{n_{sources}} \sum_{k=1}^{n_M} P(M_j = m_j) P(IM = x | m_j, r_k) P(R_j = r_k)} \quad (2.3)$$

A comprehensive PSHA would require the generation of the basic output, that is, the hazard curve (see Fig. 2.1) and de-aggregation results as seen in Fig. 2.2

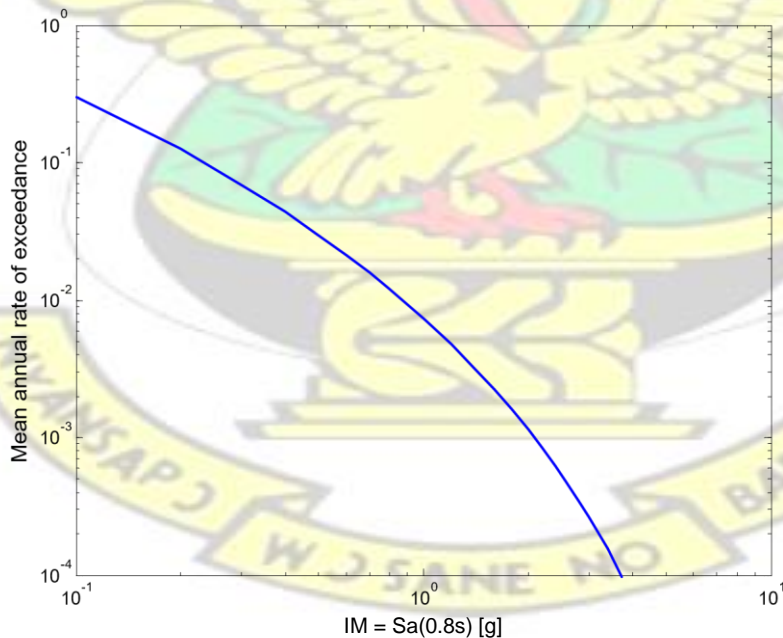


Fig. 2.1. Hazard curve at Van Nuys, California, USA (adapted from Baker, 2005).

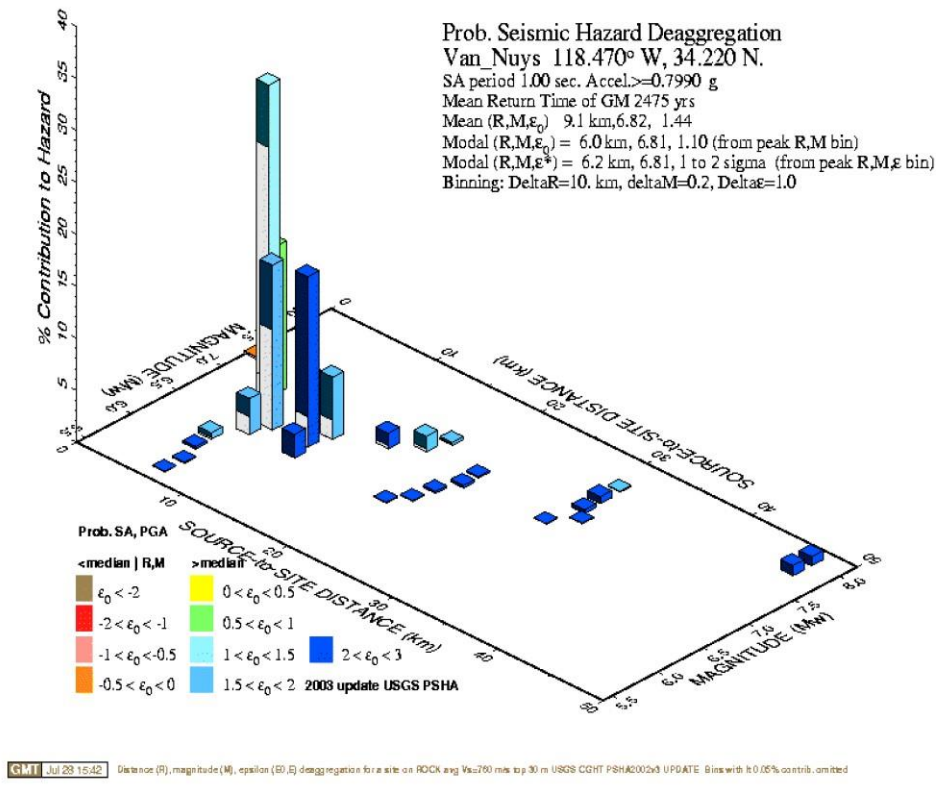


Fig. 2.2. Typical de-aggregation results at Van Nuys, California, USA (adapted from Baker, 2005).

An intensity measure (IM) that is sufficient enough to convey the extent of hazard posed by future earthquakes is usually recommended. If for one reason or another this scalar parameter is insufficient, other researchers have advocated the use of a vector of variables to quantify the degree of ground shaking (Baker and Cornell, 2006; Bazzurro, 1998). Typical intensity measures used are the spectral inelastic displacement, spectral velocity, 5% damped first mode spectral acceleration or peak ground acceleration. Targeted seismic performance objectives such as immediate occupancy, collapse prevention and life safety (FEMA, 2003) can be used to select a desired hazard level (mean annual frequency of exceedance, e.g., 2% in 50 years return period) to obtain the corresponding distribution of intensity measure for which the structure is expected to resist.

### 2.2.2 Structural Analysis

The output of the ground motion hazard analysis serves as input for the next stage of assessment which involves structural analysis. Utilizing appropriate representation of structural component through macro finite element models that capture all the major modes of cyclic deterioration and material nonlinearities either through lumped plasticity (Liel, 2008; Lignos, 2008; Laura *et al.*, 2016) or distributed inelastic (Celik, 2008; Mosalam, 2012) formulations, the distribution of structural responses can be quantitatively assessed through well-known structural analysis methods such as nonlinear static pushover or non-linear time history analysis. At this stage, a Markovian dependent assumption is made to allow for ease of propagation of uncertainties from the previous stage, thereby making the framework modular in scope. This implies that the analyst does not necessarily need to have prior knowledge of the distribution of magnitudes and site associated active faults that were involved in the PSHA, and that all the hazard information posed by the earthquake under consideration, is lumped and carried by the selected intensity measure. Once this assumption is deemed to be valid, a suite of earthquake accelerograms is carefully selected from a database of historical records or synthetically simulated and validated schemes, for reasons best known to the analyst. The framework requires defining an engineering demand parameter (EDP) which relates well with the extent of damage to describe the structural response. Typical EDPs used by researchers include floor accelerations (Medina, 2002) for mainly defining non-structural inelastic component deformation and inter-storey drift (Haselton *et al.*, 2011; Jeon, 2015) for damage of structural components.

#### (a) Demand-Capacity Estimation Methods

Advancement in computing power over the years has seen the transition from linear static, nonlinear static, linear dynamic and presently nonlinear dynamic procedures for

assessing the seismic performance of structures. The nonlinear static method that is fairly used for practical purposes is reviewed as well as estimation methods that are employed in relating the IM to the EDP through the lens of rigorous nonlinear time history analysis is evaluated.

(b) Non-linear Static Pushover Analysis

With this method, a global assessment of the performance of a structural system is performed by monotonic application of a lateral force distribution along the height of the building. Either a displacement or load control is applied to the tip of the roof to a predetermined drift ratio or up onto collapse of the system (Armelle, 2006; Mirko *et al.*, 2014). The target roof drift ratio depicts the performance objective, that is, the hazard level for which the structure is intended to meet. The final outcome for this analytical method is the base shear – roof drift relationship. For collapse prediction, the drift at which base shear reduces to zero upon reaching its peak may be used as a metric. Equation (2.4) shows ASCE recommended lateral force distribution as a function of the storey height and total building weight.

$$W_i = \frac{w_i h_i}{\sum_{j=1}^n w_j h_j} W \quad (2.4)$$

Where  $W_i$  is the applied lateral force at floor  $i$ ;  $w_i$  and  $w_j$  are the seismic weights at floor  $i$  and  $j$ ;  $h_i$  and  $h_j$  are the corresponding height above ground level;  $k$  is the exponential term that depends on the period of the structure (1 if fundamental period  $< 0.5$  sec, 2 if

fundamental period  $> 2.5$ secs and linear interpolation on 1 to 2 if fundamental period lies in the range of 0.5-2.5 secs) and  $W$  is the total considered seismic weight.

Krawinkler and Zareian (2007) pointed out that the method does not explicitly admit deterioration of hysteretic components and that the focus is mainly reaching the target drift ratio, where inelastic force and deformation demands are evaluated for seismic performance assessment. Furthermore, researchers such as Denis (2014); Villaverde, (2007) have emphasized that the method fails to detect appropriate location of plastic hinge zones for very ductile structural systems and may also under-estimate the storey drift at collapse. These limitations have been attributed to the fact that pushover analysis excludes the seismic variant of earthquakes events such as duration and frequency composition as well as contribution of higher modes effect due to period elongation. Hence, current state of the art requires using nonlinear dynamic methods for assessing seismic performance.

#### (c) Non-linear time history analysis

The method alleviates the major short comings of the nonlinear static procedures. By employing this analytical tool, researchers have proposed various ways in which the ground motion intensity measure (IM) can be related to the structural response, that is, the engineering demand parameter (EDP).

In one approach, an arbitrarily large suite of ground motions is selected from a catalogue of historical records, such as PEER strong ground motion database, with preferably large variation in duration and frequency content. Others have recommended the usage of synthetic time-series that were developed either using stochastic or physics based ideological frameworks (Rezaeian, 2010; Yamamoto, 2011). This normally comes into play when there are not enough records that are representative of the location under

study (low to moderate seismicity zones). Through non-linear time history analysis, the EDP, typically the maximum inter storey drift ratio, from each realization of ground motion is obtained after post processing of results. Under the assumption that the theoretical distribution of the IMs and EDPs are lognormal (Shome, 1999; Baker and Cornell, 2003; Jeon, 2015), conventional linear regression is performed in this log-transformed space. A scatter plot of the EDP-IM relationships normally shows roughly bound elliptically region (see Fig. 2.3), and as such it is popularly known as the *cloud analysis* or more technically a probabilistic seismic demand analysis (PSDA).

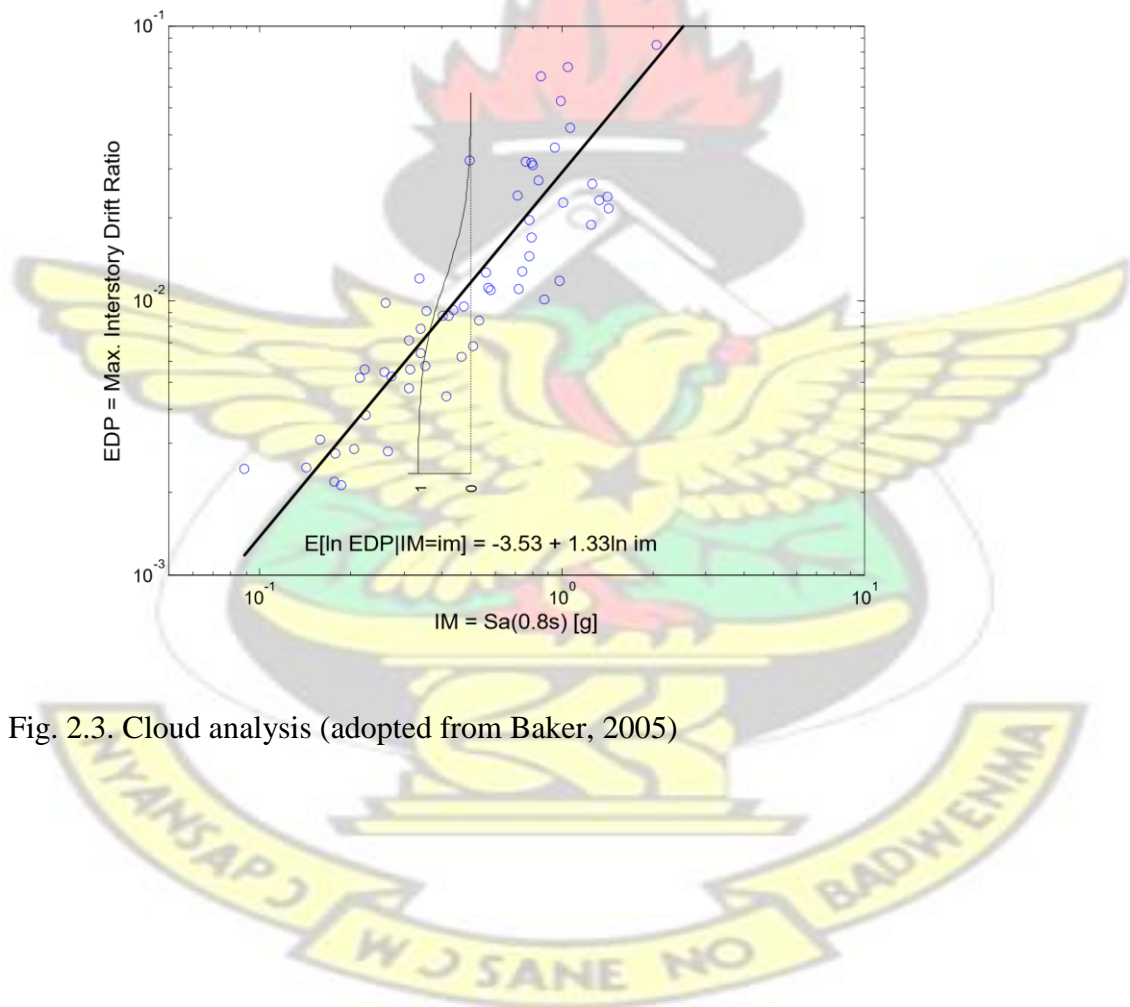


Fig. 2.3. Cloud analysis (adopted from Baker, 2005)

The final outcome of this method will be a closed functional form of the conditional mean EDP given IM as seen in Equation (2.5) and a constant variance (homoscedascity ) in Equation (2.6).

$$E[\ln EDP | IM = im] = \hat{a} + \hat{b} \ln im + e \quad (2.5)$$

$$Var[e] = \sqrt{\frac{\sum_{i=1}^n (\ln edp_i - \hat{a} - \hat{b} \ln im_i)^2}{n - 2}} \quad (2.6)$$

where  $\hat{a}$  and  $\hat{b}$  are slope and intercept values respectively, from the linear regression analysis;  $e$  is the zero mean residual error;  $E(.)$  is the mean function;  $Var(e)$  is the variance. The assumption of constant variance across the range of IMs should be treated with caution since a much larger dispersion of inelastic deformation is normally observed at higher IMs (see Fig. 2.6). Hence other researches have suggested the use of piecewise linear window fitting other than the conventional closed form solution (Mackie and Stojadinovic, 2003).

In assessing the collapse capacity of structural systems with which very severe ground motions are required for non-linear time history analysis, the current state-of-the-art requires using *incremental dynamic analysis* (IDA) to provide a thorough understanding of the distribution of seismic demand, given a range of intensity levels. Demand metrics could be the maximum inter-storey drift, roof drift, stability index (Mehanny and Deirelin, 2000), Park- Ang Index (Park and Ang, 1985) whilst typical intensity measures can be scalar entities such as first mode spectral acceleration (Haselton, 2007), spectral velocity (Jeon, 2015), inelastic spectral displacement (Tothong and Cornell, 2008), earthquake power index (Ridell, 2007), Arias intensity (Arias, 1970) or vector representations such as epsilon and spectral acceleration (Baker

and Cornell, 2006). In this methodological framework, the acceleration time series of carefully selected suite of ground motion are incrementally scaled up or down till the targeted performance limit state is reached. The outcome is a series of curves that is used to explicitly characterize the record-to-record variability of the IM-EDP relationship (see Fig. 2.4). The intensity measure, IM, at which for a very small increase, will cause a pronounced increase in the EDP, that is, where the IDA curve flattens, is defined as the collapse point. Collapse is defined as the instant at which the structure is unable to sustain gravity loads due to loss of lateral resistance with which it is unable to find a new equilibrium configuration in the presence of seismic effects. This parametric estimation method offers a great deal of understanding of the implications of extreme events on the seismic performance and the variations in the structural responses at increasing intensity levels. One unusual chaotic behaviour, is a phenomenon for which the IDA curves flattens (collapse) at a particular intensity level, only to regain strength at a higher intensity. This is known as structural resurrection, and Vamvatsikos and Cornell (2002) proposed rules to overcome this challenge in the estimation of the dynamic capacity. Also, by scaling to high intensity measure, the frequency composition of the ground motion is unchanged, and as such, realistic representation of future severe seismic events may be flawed.

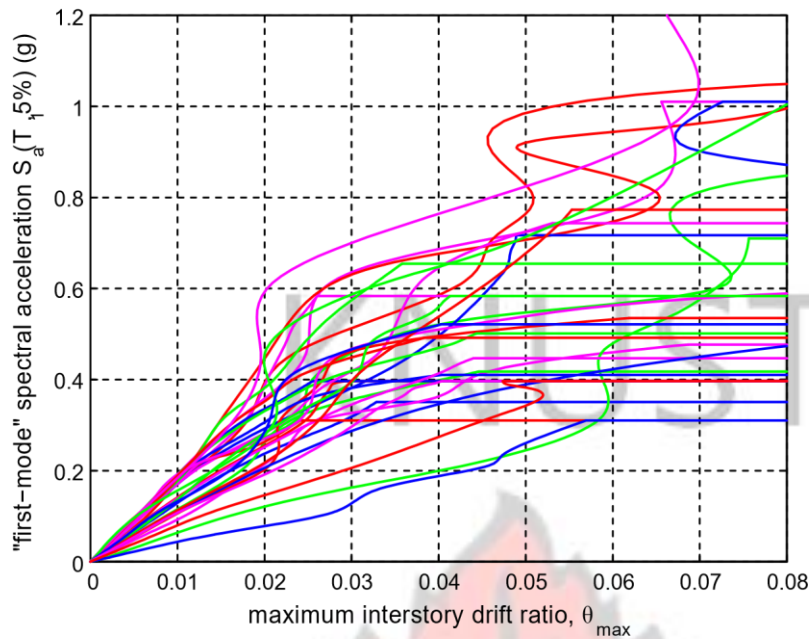


Fig. 2.4. Incremental dynamic analysis (adopted from Vamvatsikos, 2011)

In other approaches where the distribution of the EDPs at a specific hazard level (intensity measure) is of importance, the suite of selected accelerograms are scaled to this target intensity and nonlinear time history analysis performed (see Fig. 2.5). This is known as the *single stripe analysis*, and if it is repeated at other hazard levels with the assumption of independent time histories, then we have the *multiple strip analysis* (MSA) as shown in Fig. 2.6. If the independence assumption is relaxed, that is employing the same records at multiple hazard levels, then the estimation method may coincide with incremental dynamic analysis.

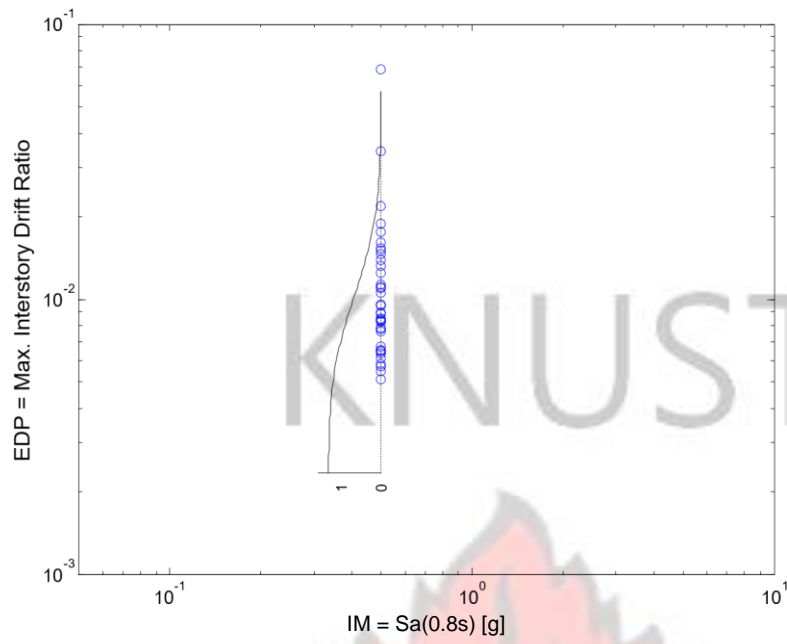


Fig. 2.5. Single stripe analysis (Baker, 2005)

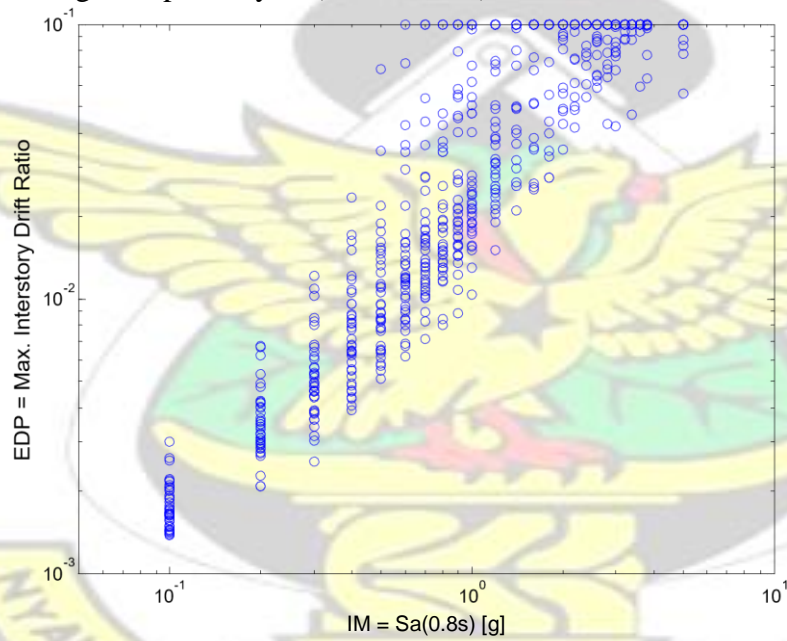


Fig. 2.6. Multi stripe analysis (adopted from Baker, 2005)

### 2.2.3 Damage Analysis

Qualitative damage measures (DM) is used to describe the degree at which structural damage will be allowed to be exceeded. These discrete damage limit states are typically mapped to the conditional distribution of the EDPs, preferably in the same dimensional unit. A typical example is the slight, moderate, extensive and complete limit states with median drift values of 0.5%, 0.8%, 2.0% and 5.0% respectively as prescribed in HAZUS-MH (FEMA, 2003). In other seismic risk mitigation documents such as FEMA 273/356, performance functions such as immediate occupancy (at 1% drift demand), life safety (at 2% drift demand) and collapse prevention (at 4% drift demand) are stipulated. At this stage of the damage analysis, fragility functions which provides the conditional probability of the structural system or component, exceeding a damage limit state (denoted here as the value of DM) given a site specific intensity measure is sought. Therefore the use of a conditional complementary cumulative lognormal distribution function as shown in Equation (2.7) is used to derive an analytical fragility function when employing cloud analysis.

$$P[D \leq C | IM = im] = 1 - \frac{\exp\left\{-\frac{[\ln C - (a\hat{c} + b \ln im)]^2}{2(\sigma_{D|im}^2 + \sigma_c^2 + \sigma_M^2)}\right\}}{\sigma_{D|im} \sigma_c \sigma_M} \quad (2.7)$$

where  $C$  and  $D$  are the limit state capacity and seismic demand respectively,  $IM$  is the intensity measure,  $\Phi$  is the standard Gaussian cumulative distribution function;  $a\hat{c}$  and  $b$ , are regression coefficients from regression analysis and  $\sigma_{D|im}$ ,  $\sigma_c$  and  $\sigma_M$ , represents the dispersion in the demand model, limit state capacity and modelling uncertainties respectively. However for incremental dynamic analysis, its formulation requires rather

finding the distribution of intensity measures given a particular performance function as seen in Equation (2.8) to (2.10).

$$P[IM_{cap} \leq im | EDP = y] = \frac{1}{\sigma_{im} \sqrt{2\pi}} \exp\left[-\frac{(\ln im - \mu_{im})^2}{2\sigma_{im}^2}\right] \quad (2.8)$$

$$\int_{im_1}^{im_2} \frac{1}{\sigma_{im} \sqrt{2\pi}} \exp\left[-\frac{(\ln im - \mu_{im})^2}{2\sigma_{im}^2}\right] \ln im \, d(\ln im) \quad (2.9)$$

$$\int_{im_1}^{im_2} \frac{1}{\sigma_{im} \sqrt{2\pi}} \exp\left[-\frac{(\ln im - \mu_{im})^2}{2\sigma_{im}^2}\right] \ln im \, d(\ln im) \quad (2.10)$$

where  $im_i$  is the intensity measure associated with predefined limit state  $y$ , (eg. Onset of collapse) ;  $\mu$  and  $\beta_{im}$  are the expected value and standard deviation of the Gaussian distribution function respectively.

If information about the ground motion hazard becomes available through a hazard curve as shown in Fig. 2.1, the mean annual frequency of exceeding that particular limit state can be computed by numerical integration as in Equation (2.11) and schematically in Fig. 2.7.

$$\lambda_{EDP}(y) = \int P[IM_{cap} \leq im | EDP = y] \cdot d\lambda_{IM}(im) \quad (2.11)$$

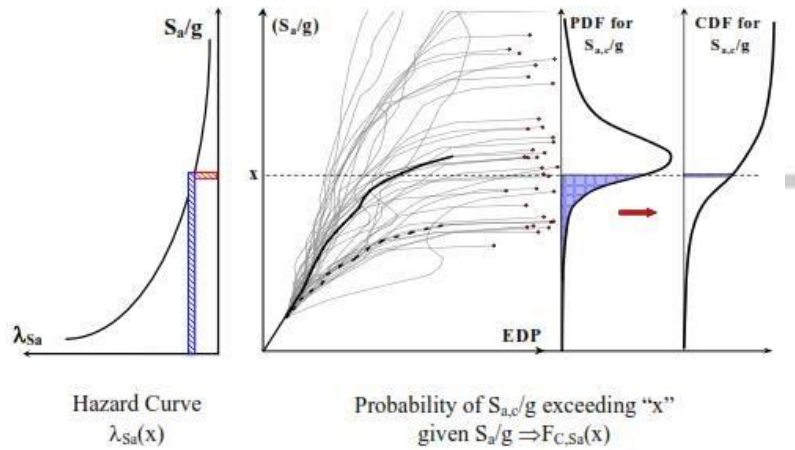
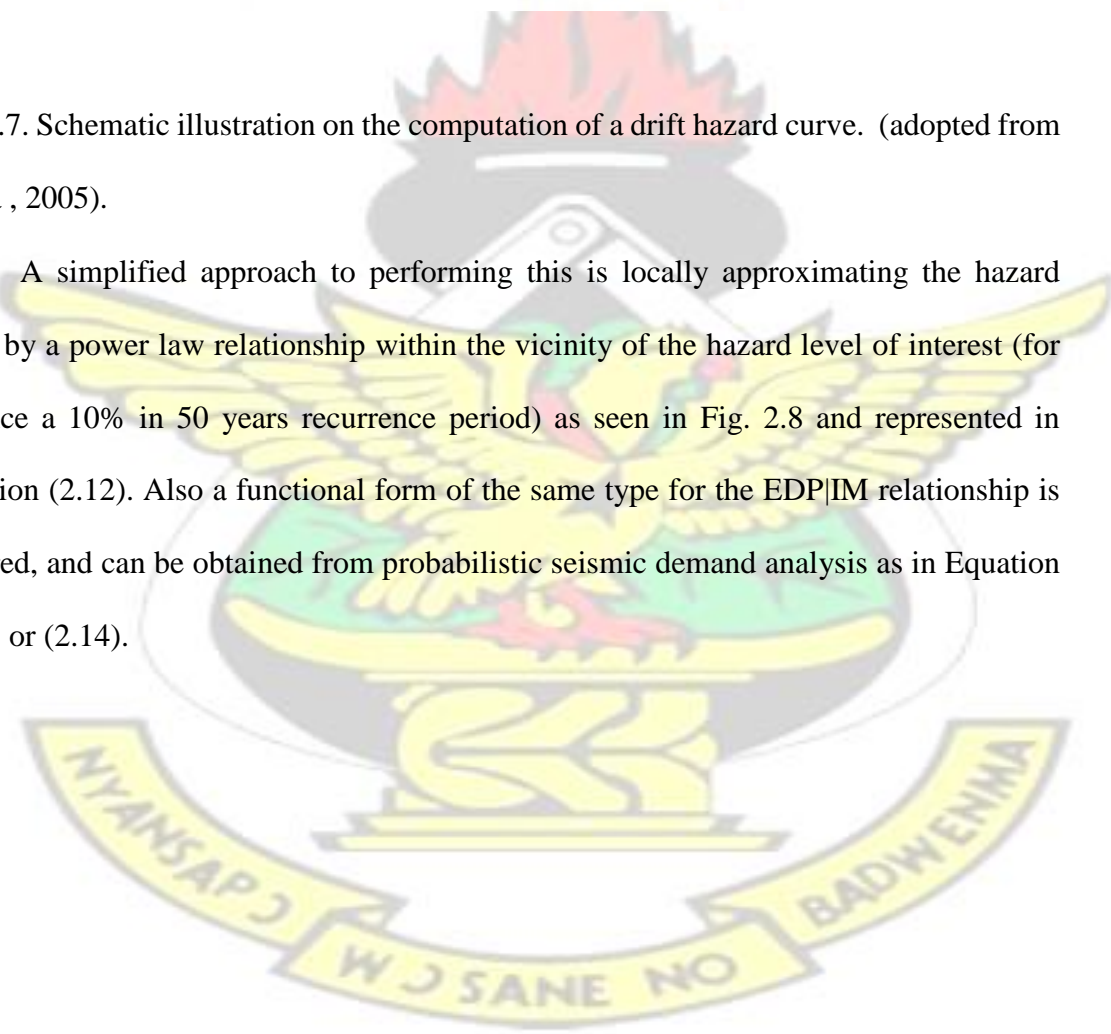


Fig. 2.7. Schematic illustration on the computation of a drift hazard curve. (adopted from Ibarra , 2005).

A simplified approach to performing this is locally approximating the hazard curve by a power law relationship within the vicinity of the hazard level of interest (for instance a 10% in 50 years recurrence period) as seen in Fig. 2.8 and represented in Equation (2.12). Also a functional form of the same type for the EDP|IM relationship is required, and can be obtained from probabilistic seismic demand analysis as in Equation (2.13) or (2.14).



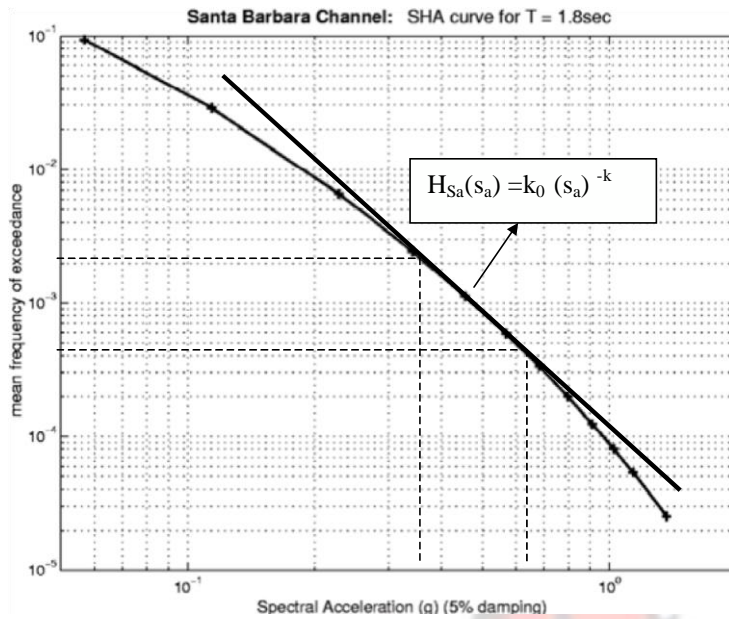


Fig. 2.8. Power law functional approximation of a ground motion hazard curve. (adopted from Jalayer , 2003)

$$\square_{IM}(x) \square k_0 x^{\square k} \quad (2.12)$$

$$E[\ln EDP | IM \square im] \square a \square b \ln im \quad (2.13)$$

$$EDP_{IM}(im) \square a(im)^b \quad (2.14)$$

where  $a \square \exp(\hat{a})$  and  $b \square \exp(\hat{b})$

Substituting the inverse function of Equation (2.14) into Equation (2.12) gives the mean rate of exceedance at an intensity measure (IM) that corresponds to the drift level,  $y$ , as shown in Equation (2.15).

$$\square_{IM}(IM_y) \square k_0 [y/a]^b \quad (2.15)$$

This can then be substituted into Equation (2.11) and after evaluating the integral, a final function form for computing the drift hazard curve is given by Equation (2.17) and is shown in Fig. 2.9.

$$\lambda_{EDP}(y) = \lambda_{IM}(IM_y) \cdot \exp\left[-\frac{1}{k} \left(\frac{y}{a}\right)^b\right] \cdot \lambda_{im} \cdot \lambda_2 \cdot \lambda_1 \quad (2.16)$$

$$\lambda_{EDP}(y) = k_o \left[\frac{y}{a}\right]^b \cdot \exp\left[-\frac{1}{k} \left(\frac{y}{a}\right)^b\right] \cdot \lambda_{im} \cdot \lambda_2 \cdot \lambda_1 \quad (2.17)$$

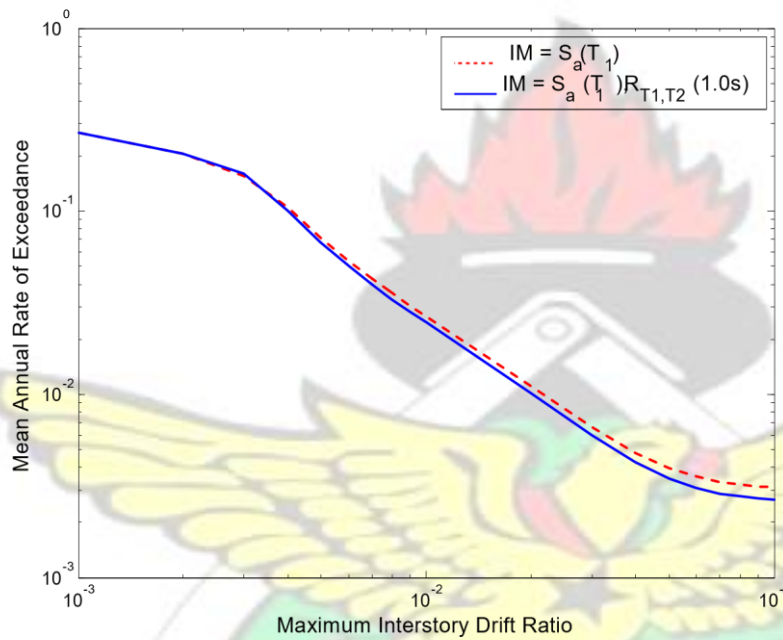


Fig. 2.9: Typical drift hazard curve (adopted from Baker , 2005)

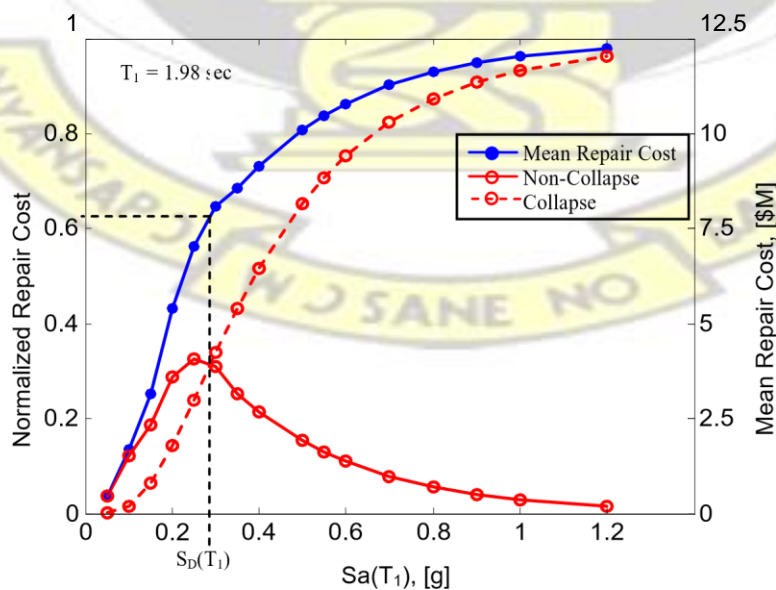
#### 2.2.4 Loss Analysis

The final stage of the framework is relating the computed mean annual frequency of the damage measure to decision variables that give an insight to the repair costs, fatalities or business interruption at a given intensity measure. The output may be the conditional mean annual frequency of repair cost exceeding a specified percentage of the total replacement cost of a specific structural system given the intensity of the ground motion (Liel *et al.*, 2009). This information becomes imperative for risk management decisions

serving as a direct measure of building seismic performance upon which appropriate extent of seismic upgrading of non-conforming building through retrofiting strategies is based. Notable studies on seismic loss estimation that have adopted the probabilistic performance-based earthquake engineering framework (Porter *et al.*, 2002; Aslani, 2005; Baker and Cornell, 2007; Mitrani-Reiser, 2007; Liel, 2008) have decomposed the expected value (mean) of the total repair cost resulting from damages to all structural or non-structural components given an intensity measure, as a function of discrete damage states, such as collapse and non-collapse damage states as given by Equation 2.18.

$$E[TC | IM] = E[TC | C, IM] \cdot P[C | IM] + E[TC | NC, IM] \cdot [1 - P[C | IM]] \quad (2.18)$$

where  $TC$  is the total repair cost;  $C$  denotes collapse and  $NC$  denoted non-collapse;  $P[C | IM]$  is the collapse fragility function;  $[1 - P[C | IM]]$  is the complement of the collapse fragility function which can be computed from the summation of all noncollapse limit state considered;  $E[TC | IM]$ ,  $E[TC | C, IM]$ ,  $E[TC | NC, IM]$  are the expected values of the repair cost needed given an intensity measure and are subjectively related to the damaged sustained. Following this framework, a relationship between the intensity measure and a normalized form of the total repair cost (repair cost divided by total replacement cost) can be developed as shown in Fig. 2.10.





backbone curves have generally been employed with hysteretic rules that can capture the degradation in strength and stiffness. This section provides a brief discussion of the architectural framework of the nonlinear finite element platform adopted, *OpenSees* (McKenna , 2010), and provides a review of notable deteriorating hysteretic models that have been proposed in literature and made available using this open source simulation tool.

### 2.3.1 OPENSEES Conceptual Framework

*OpenSees* is a nonlinear finite element platform that is used for performance based earthquake engineering simulation of structural and geotechnical systems. This is an open source code developed by the Pacific Earthquake Engineering Research (PEER) Centre and allows for development of entities of the major objects without any restriction whatsoever (see Fig. 2.12). It has been used by most researchers for performing collapse vulnerability assessment of structures due to its rich database of hysteretic component material models with degrading effect. The software architectural framework is written in the object-oriented programming language C++ and divided into four major objects. The executable is an extension of scripting language known as Tcl, which serves as an interpreter. The —model builder| object constructs entities such as nodes, constitutive material model, elements, load patterns, time series, constraints etc. These entities are then added to the domain object which holds the state of the analytical model at a particular time step. The analysis object, contains general solution algorithms, equation solvers, static and transient integrators etc., and is used to move the state of the model to the next time step before relayed back to the domain object for storage. The recorder object then allows one to assess structural response quantities that are of interest and monitors user defined parameters in the model during analysis. This could be

displacement time history at a node or sectional stress-strain relationship at an integration point.

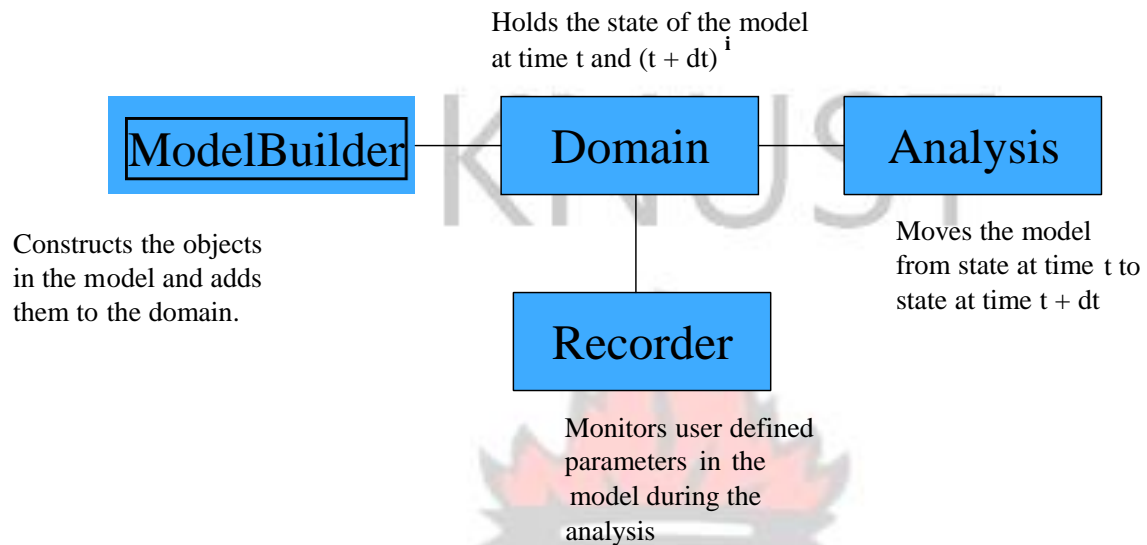


Fig. 2.12. *Opensees* conceptual framework

### 2.3.2 Component Deteriorating Hysteretic Models

Clough and Johnstone (1965) developed a hysteretic bilinear elastic-plastic loaddeformation relationship for characterizing the behaviour of structural components. This model primarily allowed for the degrading in stiffness of the reloading branch based on previously observed maximum displacement in the direction of loading (point B in Fig. 2.13). Hence it is normally referred to as a peak-oriented hysteretic model. Since its introduction, a couple of developed hysteretic model have been based on this formulation (Nielson and Imbeault, 1970; Anagnostopulos, 1972; Iwan, 1973). Recently, Sucuoglu and Erberik (2004) incorporated an energy based hysteretic rule to account for strength

degradation as well as seven damage rules to mimic asymmetric behaviour of tested structural components.

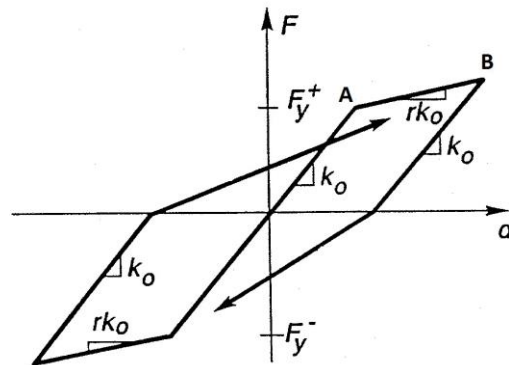


Fig. 2.13. Clough and Johnstone (1965) hysteretic model

The Clough model was a bilinear approximation to a tri-linear non-deteriorating hysteretic model developed by Hisada (1962). Takeda (1970) suggested a tri-linear deteriorating hysteretic model to be used for simulating the cyclic behaviour of reinforced concrete components (see Fig. 2.14). An initial portion of this piece-wise linear backbone curve represented an un-cracked concrete section. The other portions were able to represent typical primary modes of deterioration such as, a peak-oriented unloading stiffness degradation and stiffness degradation at flexural cracking and yielding. Otani and Sozen (1972) noted that a major difference between this model, that can be made bilinear by excluding the un-cracked concrete portion, and the basic Clough model, is the additional hysteretic rules for inner cyclic loops.

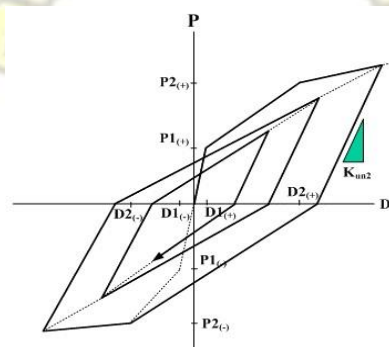


Fig. 2.14: Takeda (1970) hysteretic model

Song and Pincheira (2000) proposed a deformation dependent cyclic deteriorating hysteretic model that could capture the pinching phenomenon of structural component as well as unloading stiffness and accelerated reloading stiffness degradation upon reaching their ultimate strength. Unloading stiffness degradation only initiates when the RC member reaches its yield point,  $F_y$ , while strength decay occurs after reaching the predefined peak strength,  $F_u$ , (see Fig. 2.15). This implies that in-cyclic strength degradation becomes absent with the portion of the response envelope up to the ultimate strength and its corresponding deformation limit. Also, upon reaching their ultimate strength, explicit simulation of post-capping cyclic strength deterioration is excluded, unless procedures developed by Pincheira *et al.* (1999) for in-cyclic strength deterioration are employed to allow for the softening behaviour. Lastly, in the strain softening branch, a target mirror point corresponding to where unloading began, is used to quantify the maximum attainable strength for subsequent cyclic excursions

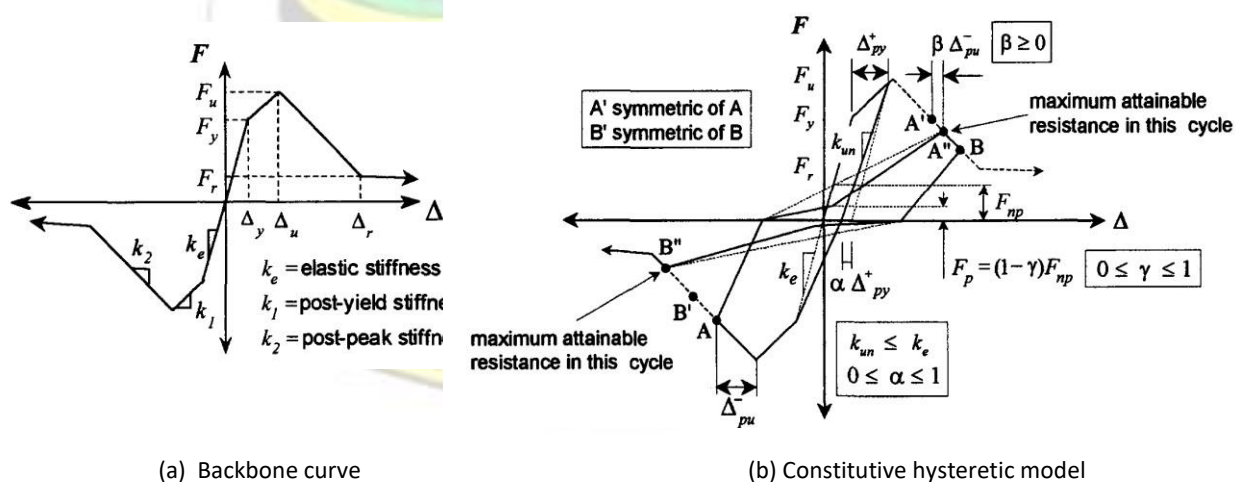


Fig. 2.15. Song and Pincheira (2000) hysteretic model

Ibarra *et al.* (2005) proposed three piecewise linear hysteretic models, that account for primarily four modes of cyclic deterioration; bilinear, peak-oriented and pinching models. These models were evaluated and calibrated to experimental test specimen of steel, reinforced concrete and wood. The four modes of deterioration, that is, basic strength degradation in the pre-capping strain hardening branch; strength degradation of the post-capping strain softening branch; accelerated reloading stiffness deterioration and unloading stiffness deterioration, employ an energy based damage index, developed by Rahnema and Krawinkler (1993), to quantify the rate of cyclic deterioration under cyclic load reversals (see Fig. 2.16). This index assumes that the structural component possesses a limiting energy dissipation capacity, which after every excursion of cyclic loading, reduces in capacity and modifies the preceding stiffness. An exponential term is also used to account for the accelerated cyclic stiffness deterioration as observed in experimental studies during reloading. Even though the developed model relates well with the behaviour of structural components, it does not explicitly account for cyclic isotropic hardening that steel specimen possesses as well as its associated bauschinger effect.

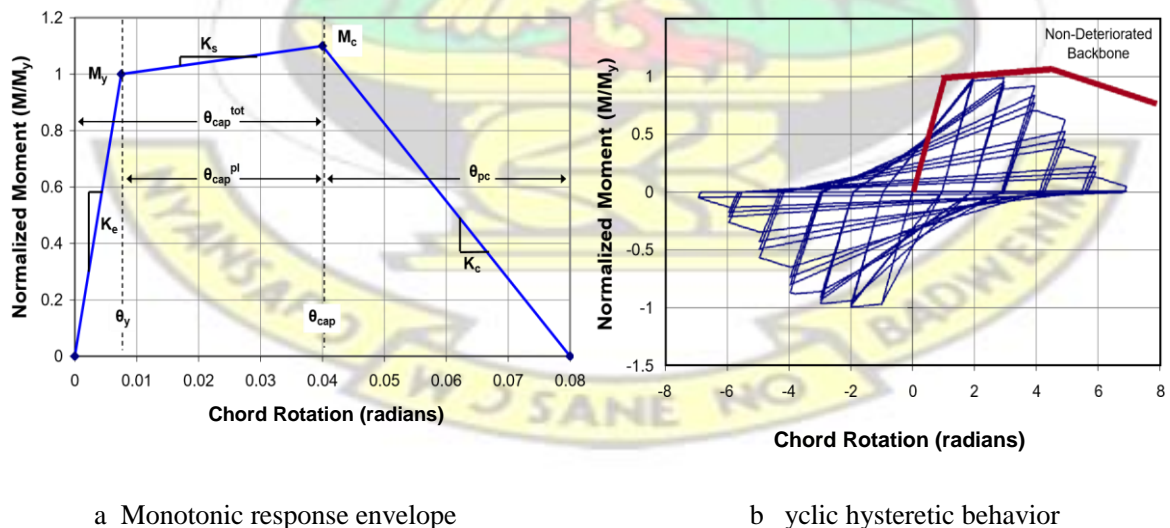


Fig. 2.16. Ibarra-Medina-Krawinkler hysteretic model

Lignos and Krawinkler (2012) made significant modification to the parent model, motivated from observed responses of brittle failure of steel connections and ductile tearing of steel components under very large inelastic deformations. They included an additional branch to the original monotonic backbone curve to account for complete strength loss due to these phenomena (see Fig. 2.17). They also noted that for composite structural components, such as a W-section steel beam and a reinforced concrete slab, the rate of cyclic degradation may be slower in the loading path that induced compressive stresses in concrete, as compared to compressive action of the beam bottom flange in the opposing direction. The definition of an additional scalar parameter was employed to account for this asymmetric behaviour of composite structural components. All these modifications were incorporated in the originally proposed three hysteretic model; bilinear, peak-oriented and pinching models.

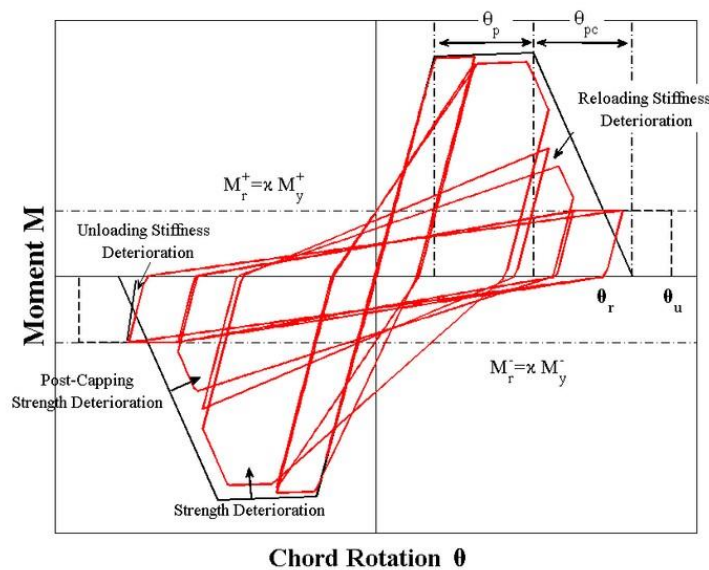


Fig. 2.17. Modified Ibarra-Medina-Krawinkler hysteretic model

Bouc-Wen-Baber-Noori deteriorating hysteretic model is an aggregated extension of a non-deteriorating curvilinear hysteretic model developed by Bouc (1975) for random vibration analysis of single degree of freedom systems. Wen and Baber provided

hysteretic rules based on amount of hysteretic energy dissipated to simulate strength and stiffness degradation, and applied it to the solution of multi degree of freedom systems. Baber and Noori (1985), while maintaining compatibility with the previous modifications, extended it to admit pinching effect of structural systems. The final form is the well-known Bouc-Wen-Baber-Noori (BWBN) hysteretic model. Recently, Chao-Lie *et al.* (2016) employed this model to define the one-dimensional constitutive law of a joint panel zone component with fairly good accuracy. Hossain *et al.* (2013) also used it to define the degrading hysteretic behaviour of yield shear panel devices when conducting a probabilistic performance evaluation of its appropriateness (see Fig. 2.18). However, Lignos and Krawinkler (2008) noted that the model requires 13 parameters for implementation, which does not have a direct relationship with typical design parameters, hence making it complex. More so Thyagarajan and Iwan (1990) pointed out that it intuitively violates basic principles when a relatively small post-yield stiffness is applied; thus experiences an unexpected pronounced drift capacity.

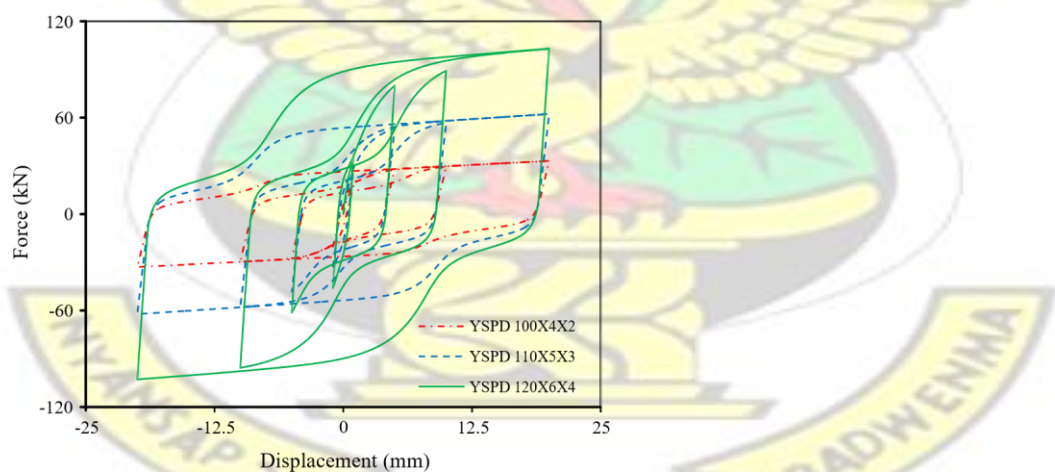


Fig. 2.18. Cyclic force displacement relationship of the YSPDs generated using the BWBN material model (adopted from Hossain *et al.*, 2013).

Continuum micro finite element models have been employed in capturing the shear degrading behaviour of RC columns (Kaneko *et al.*, 2001; Ozbolt *et al.*, 2001; Shing

& Spencer, 2001). However due to they being computationally expensive in implementation and calibration, macro element models through the use of one dimensional shear spring (Liel *et al.*, 2009; Pincheira *et al.*, 1999; Lee and Elnashai , 2001; Sezen and Chowdhury ,2009) are typically used for nonlinear time history analysis of large multi degree of freedom structural systems. Leborgne (2012) sought to improve upon previous existing analytical models (Elwood, 2005) for simulating the full nonlinear response of shear-critical RC columns. This model, (see Fig. 2.19), utilizes both a predefined strength and deformation capacity to trigger the onset of shear failure from which the constitutive behaviour, a zero-length shear spring is altered to capture strength and stiffness degradation as well as pinching effect. At the onset of shear failure, the model was made to compensate for the loss in deformation in flexural members that are in series with shear spring; a limitation of previous works (Elwood, 2005). Also, a couple of damage accumulation algorithms were implemented based on energy, displacement and cyclic formulations. The modelling parameters were calibrated using a database of 34 tested RC columns to serve as a simplified risk assessment tool for degrading behaviour of column due to shear failure.

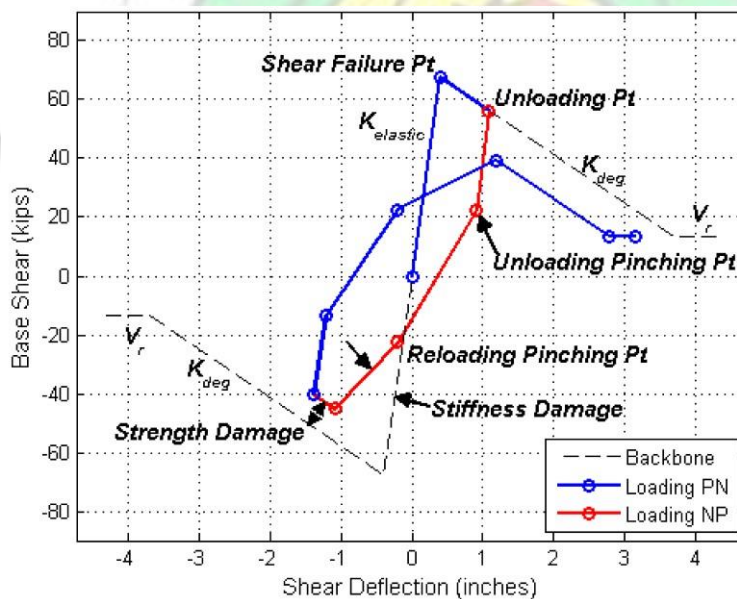


Fig. 2.19. Shear force-deformation behaviour of Leborgne (2012) degrading hysteretic model.

Lowes and Altoontash (2003) developed a one dimensional deformation-based constitutive hysteretic model to capture all the major inelastic mechanisms of RC joint under quasi static loading. It employed a multi-linear response envelope and a tri-linear unload-reload path that utilizes 34 parameters to characterize joint shear and bond slip behaviour as well as hysteretic damage. Three modes of cyclic deterioration were captured, that is, unloading stiffness degradation, reloading stiffness degradation and strength degradation, by adopting the Park and Ang (1985) damage index. This material was also implemented in *Opensees* as —Pinching4 materialll (see Fig. 2.20), and has been widely used for simulating the shear and bond slip deformation of non-seismically detailed joint with great accuracy (Thiess, 2005; Celik and Ellingwood , 2008; Jeon *et al.*, 2012).

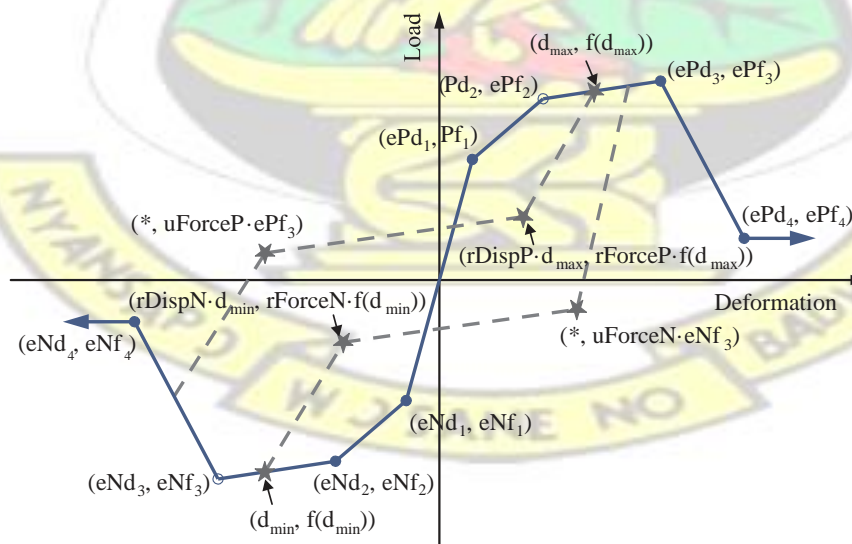


Fig. 2.20: Pinching4 material model (Lowes and Altoontash , 2003)

### 2.3.3 Joint Shear Strength Models

#### (a) Analytical joint shear strength models

Recent earthquakes have shown that older type non-ductile reinforced concrete buildings are very vulnerable and do sustain significant damage under seismic action. Beam-column joints of these buildings are deemed to have detailing deficiencies that can impose significant strength and stiffness loss and as such contribute to their global collapse (Moehle *et al.*, 1991). The joint region of these buildings is believed not to be adequately confined and lacks the capacity design method, a concept that most seismic codes have emphasized (Park *et al.*, 1995). The major deficiencies that are typical of such buildings include the absence of transverse hoops, insufficient anchorage of beam reinforcement, splicing longitudinal reinforcement and short embedment length of bottom beam reinforcement within the joints. Hence in such frames, the development of shear resisting mechanisms (strut and truss mechanisms) to induce ductile failure under dynamic loading are not present (Hoffmann *et al.*, 1992). Under seismic action, the primary inelastic mechanisms that govern joint response are bond slip and shear deformation (Celik and Ellingwood, 2008). These mechanisms are characterized by cracking of concrete, crushing of confined and unconfined concrete, closing of concrete cracks under load-reversal, shearing across concrete crack surfaces, yielding of reinforcing steel and damage to bond-zone concrete (Mitra, 2007). They also exhibit poor hysteretic properties and as such joints should not be seen as a major source of energy dissipation (Paulay *et al.*, 1978).

For appropriate utilization of the truss mechanism, adequate bond strength is required, initially through bearing of longitudinal reinforcement of framing beams and columns and, if present, transverse hoops, in order to sustain the force gradient across joint due to moment reversals. Due to short embedment length of the beam's bottom

longitudinal reinforcement in the joint core of older type non-seismically designed RC frames, the bond strength required to prevent joint anchorage failure before the full moment capacities of adjoining members are reached, is reduced. Current seismic codes, such as FEMA 356 (2000), recommend that the yield strength of the reinforcing steel within the plastic hinge zone of the structural system be reduced by a factor approximately equal to the ratio of provided embedment length to required development length. Bar-slip springs are typically used to represent anchorage failure, where properties are defined with an appropriate bond-slip model or calibrated to experimental results. Depending on the stress state of anchored reinforcing bars, researchers have either used piecewise constant bilinear or tri-linear bond strength models to estimate the resulting slip (Lowe and Altonash, 2003; Hassan, 2011; Park and Mosalam, 2012).

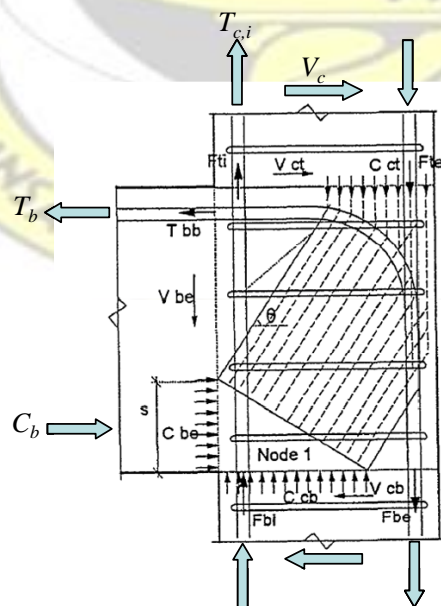
In all cases, should the shear capacity and bond strength be exceeded before yielding of longitudinal reinforcement of beam and column, joint failure may occur which does not allow for the full flexural capacities of the framing elements to be utilized. The joint then serves as the weak link which can cause excessive drift responses in the global system. Kien *et al.* (2012) noted that the joint shear demand may be a much more significant metric for assessing the seismic performance of RC beamcolumn connections, rather than the limiting requirement of column-beam flexural capacity ratios per current seismic code provisions. Hence, quantification of the shear strength of joint in vulnerability assessment has been a major subject of study in recent times.

Notable design parameters that have been used to quantify the shear capacity of RC joints include compressive strength of concrete, joint transverse reinforcement ratio, column axial load, joint aspect ratio, confinement factor and longitudinal reinforcement ratio. Researchers have assessed the shear capacities of RC joints by using either analytical or empirical methods. Various approaches to estimating the joint shear strength using typical design parameters are discussed.

## (b) Strut and tie models

Strut and tie models have evolved as one of the most useful design methods for shear critical components. It reduces the complex state of stress within structural member to an appropriate truss member consisting of compression struts, tensile ties and nodes that intersect struts and ties. In order to estimate the strength of a structural member, empirical observations of the strength of the component need to be combined with an appropriate truss mechanism for formulation of a strut and tie strength model. Strut and tie models were developed analytically to satisfy primarily equilibrium, constitutive and compatibility stress conditions within the joint core. They require the implementation of iterative algorithms that satisfy the underpinning conditions to estimate joint strength. These softening concrete models have been calibrated and verified using a limited experimental database of RC joint sub-assemblages, and as such are normally appropriate for a specified type of joint configuration such as unconfined exterior joints.

Ortiz (1993) developed a strut and tie model with a single diagonal strut to estimate the joint shear strength of unconfined and confined exterior beam-column joints (see Fig. 2.21).



$$T_{c,e}$$

Fig. 2.21. Schematic diagram of Ortiz (1993) joint shear strength model (adopted from Park and Mosalam, 2012).

Iteratively, it requires estimation of the strut depth, which was formulated to relate the optimal strut angle and neutral axis depth that maintains force equilibrium from the applied loading. The cracked concrete compressive strength suggested by the CEB model code (1990) was employed to relate the strut depth and column width with the joint shear capacity.

Vollum (1998) adopted a slightly different approach to predicting this joint shear capacity. An equilibrium condition for joint shear failure was set, as top diagonal strut stresses reach the cracked concrete strength (Fig 2.22). A limiting calibrated multiplicative coefficient for the strut depth of 0.4 was recommended. He suggested that accounting for the effect of column axial load may underestimate the joint shear strength at low to moderate axial loads which may not relate well to observed experimental failure loads.

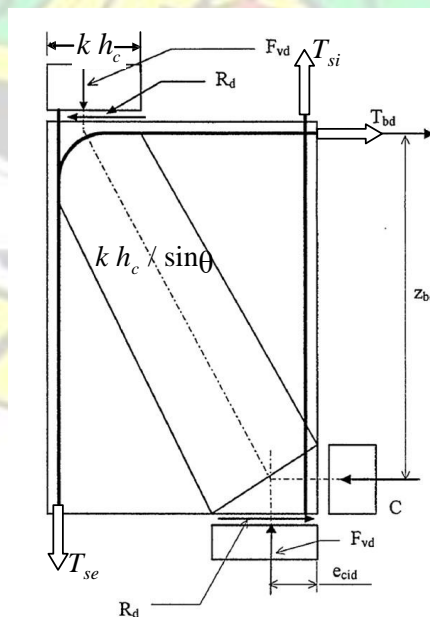


Fig. 2.22. Schematic diagram of Vollum (1998) joint shear strength model (adopted from Park and Mosalam, 2012).

Hwang and Lee (1999) proposed a joint shear strength model for cracked concrete that is capable of admitting three force transfer mechanisms; diagonal, horizontal and vertical strut mechanisms (see Fig. 2.23 and Fig 2.24). With a fixed strut angle depending on the joint aspect ratio, that is, ratio of distance between top and bottom beam reinforcing bars to distance between column longitudinal bars, and a softening concrete model proposed by Belarbi and Hsu (1995), they developed an iterative algorithm to satisfy three basic mechanical principles; stress equilibrium, constitutive relations and strain compatibility. They claimed that computed shear strength from this model were in good agreement with experimental test of exterior beam-column joints.

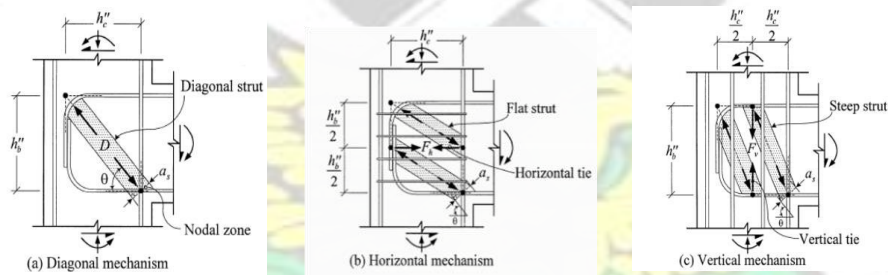


Fig. 2.23. Schematic diagram of Hwang and Lee (1999) joint shear strength mechanisms (adopted from Hassan, 2011).

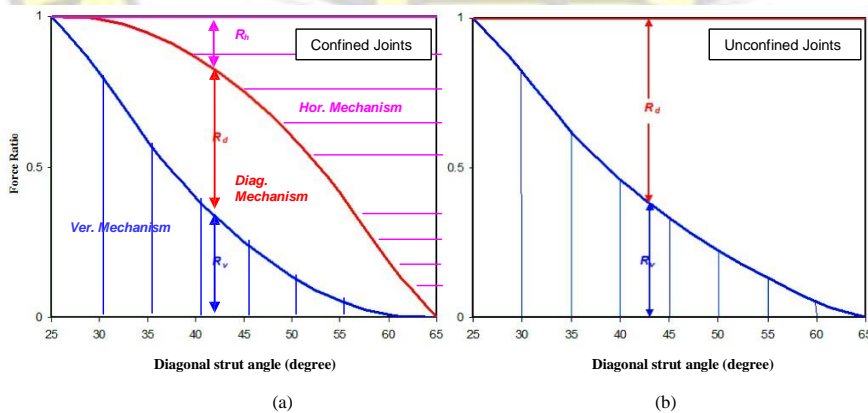


Fig. 2.24. Relative contribution of shear transfer mechanisms to joint shear strength proposed by Hwang and Lee (1999), adopted from Hassan (2011).

Wong (2005) utilized the softened concrete model, modified compression field theory (MCFT), satisfying a similar stress and strain compatibility condition as suggested by Hwang and Lee (1999), to predict the shear strength of confined exterior beam-column joints. An extensive numerical iterative algorithm is required to obtain estimate of joint shear strength since it allows for modifying the principal strut angle if equilibrium conditions are not satisfied. Hence, it is more popularly known as the —Modified Rotating-Angle-Softened-Truss-Modell.

Park and Mosalam (2013) proposed a semi-empirical and an analytical joint shear strength models for unreinforced exterior beam-column joints (see Fig. 2.25). The primary shear resisting mechanism utilizes an inclined strut that requires two influential parameters, that is, the beam reinforcement index and joint aspect ratio to develop the calibrated predictive equations. The analytical model admits bond deterioration effect by utilizing a second inclined strut, from which the fractional contribution for shear capacity may be significant for unreinforced exterior joint with joint shear failure mode. The relative contributions from these struts were developed by employing the softened concrete constitutive model as suggested by Vollum (1998) with a tri-linear stress-strain for reinforcing steel and a bi-uniform bond strength model proposed by Lehman and Moehle (2000). From the database of 57 unreinforced exterior joints, the proposed model approximated the experimental shear strength with a normalized mean of 0.98 and coefficient of variation of 0.15.

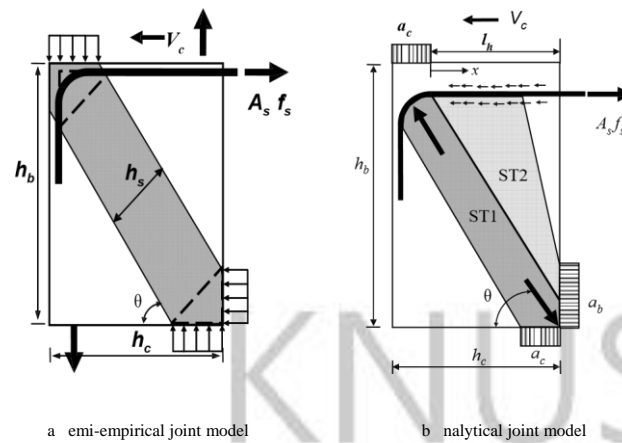


Fig. 2.25. Schematic diagram of Park and Mosalam (2012) joint shear strength model.

### (c) Empirical models

These approaches to quantifying joint shear strength requires a database of experimental test results from which well-established statistical tools, such as conventional linear regression or Bayesian methods, is used to relate selected design parameters that are generally independent. Influential parameters such as beam and column longitudinal reinforcement ratio, transverse reinforcement ratio, anchorage type, extent of out-of-plane confinement, joint aspect ratio, compressive strength etc. Notable researches conducted from such approaches are discussed.

Taylor (1974) suggested a limiting joint shear capacity by using the joint aspect ratio and compressive strength as the underlying design parameters. This calibrated empirical model is based on similar approach for estimating the shear strength of deep beams, which utilizes shear-span to depth ratio as a predictor. Analogous to this is the joint aspect ratio, which was defined as the ratio of the effective depth of column to the internal lever arm of the beam reinforcement. He neglected the reduction in ultimate shear capacity that would have resulted from the contribution of the column shear as seen in Equation (2.20).

$$V_j = b_c d_c v_c \left( \frac{z_b}{d_c} \right)^{0.4289} \left( \frac{z_b}{d_c} \right)^{-0.61} \quad (2.20)$$

where,  $b_c$  is the width of column;  $d_c$  is the effective column depth;  $z_b$  is the distance between the top and bottom beam reinforcement;  $V_j$  is the ultimate joint shear strength and  $v_c$  is the nominal concrete shear stress adopted from CP 110 (1972) which depends on the compressive strength.

Bakir and Boduroglu (1994) assembled a database of monotonically loaded exterior joint, from which they independently assessed the influence of beam reinforcement ratio, beam anchorage type and joint aspect ratio. This model was able to quantify the additional strength gain when horizontal transverse ties are situated within the joint panel zone. They also observed a significant reduction in the ultimate joint shear capacity when the joint aspect ratio is increased as seen by the negative exponential term for this in the unified predictive Equation (2.21) below.

$$V_j = 0.71 \left( \frac{A_{sb}}{b_b d_b} \right)^{0.4289} \left( \frac{h_{bc}}{h_b} \right)^{-0.61} \left( \frac{A_{sv}}{2 b_b h_c} \right) \sqrt{f_c} \left( \frac{A_{sv}}{b_b h_c} \right) f_{yv} \quad (2.21)$$

Where,  $V_j$  is the ultimate joint shear capacity;  $\beta$  is the beam anchorage detail type (1.0 for a 90° standard hook bend);  $\gamma$  is 1.37 and 1.0 for diagonal transverse joint reinforcement and unconfined joint, respectively);  $A_{sb}$  is the area of beam reinforcement in the tension zone;  $b_b$  is the width of beam;  $d_b$  is the effective depth of beam;  $h_b$  is the height of beam;  $h_c$  is the out-of-plane column depth;  $A_{sv}$  is the total area of joint transverse reinforcement;  $f_{yv}$  is the yield strength of transverse reinforcement.

Kim and Lafave (2009) also assembled a database of 341 tested specimens of various RC joint types and out-of-plane configurations to assess the joint shear behaviour

from seismic effect. They proposed a unified joint shear stress-strain predictive equation by employing the Bayesian parameter estimation method. The effect of 10 influential parameters were sought from which 6 of them proved to be statistically significant as well as maintained a high degree of reliability with results from test specimens. Equation (2.22) presents this joint shear strength model.

$$V_j = 1.01^{0.981} TB^{1.2} b^e e^{0.679} BI^{0.136} JP^{1.33} f_c^{0.764} b_j h_c \quad (2.22)$$

where,  $V_j$  is the joint shear capacity;  $TB$  is the out-of-plane geometry for confining members, 1.0 and 1.2 for sub-assemblages with 0 to 1 and 2 transverse beams respectively;  $e$  is the joint eccentricity;  $b_c$  is the column width;  $JI$  is the joint transverse reinforcement index (defined as the ratio of the product of joint transverse reinforcement ratio and its yield strength to the compressive strength of concrete);  $BI$  is the beam reinforcement index (defined as the ratio of the product of the beam reinforcement ratio and its bar yield strength to the compressive strength of concrete);  $JP$  describes the in-plane geometry (1.0 for interior connections, 0.75 for exterior connections and 0.5 for knee joints);  $f_c$  is the concrete compressive strength;  $b_j$  is the joint width and  $h_c$  is the depth of column.

Jeon (2015) also developed an empirical joint shear strength model using a multivariate linear regression approach on 261 and 454 non-ductile and ductile RC beam-column joint sub-assemblages respectively. He adopted 6 and 10 predictor variables of Kim and LaFave (2009), which were log-transformed to assess the joint shear strength of the selected databases of sub-assemblages (non-ductile and ductile, respectively). The proposed ultimate joint shear strength equations yielded an R-squared value of 0.858 for

non- ductile and 0.913 ductile experimental databases. Equations (2.23) and (2.24) show the proposed joint model.

$$V_{j(non\text{-}ductile)} = 0.586TB^{0.774}BI^{0.495}JP^{1.25}f_c^{0.941} b_j h_c \quad (2.23)$$

$$V_{j(ductile)} = 1.113JI \left[ \frac{e}{0.078 + 1} \right]^{0.28} b^{0.125} b_c TB^{1.103}BI^{0.342}JP^{1.509}f_c^{0.796} b_j h_c \quad (2.24)$$

where,  $V_j$  is the ultimate joint shear capacity;  $TB$  is the out-of-plane geometry for confining members, 1.0 and 1.2 for sub-assemblages with 0 to 1 and 2 transverse beams, respectively;  $e$  is the joint eccentricity;  $b_c$  is the column width;  $b_b$  is the beam width;  $JI$  is the joint transverse reinforcement index (defined as the ratio of the product of joint transverse reinforcement ratio and its yield strength to the compressive strength of concrete);  $BI$  is the beam reinforcement index (defined as the ratio of the product of beam reinforcement ratio and its bar yield strength to the compressive strength of concrete);  $JP$  describes the in-plane geometry (1.0 for interior connections, 0.75 for exterior connections and 0.5 for knee joints );  $f_c$  is the concrete compressive strength;  $b_j$  is the joint width and  $h_c$  is the depth of column.

#### (b) Joint Component Modelling Schemes

Researchers have attempted to simulate the inelastic joint mechanisms by providing analytical models that can be easily incorporated into computer simulations of RC frames. The behaviour of the joint region under seismic forces is now more popularly simulated by use of single component models (rotational spring) whose constitutive relations can easily be calibrated experimentally or defined analytically.

Otani (1974) and Anderson and Townsend (1977) presented some of the earliest works regarding the introduction of discrete inelastic beam-column joint action into the seismic behaviour of reinforced concrete frames. They calibrated plastic-hinge zones of beam-column elements to simulate the joint shear behaviour as well as the inelastic responses under flexure.

Others (Hoffmann *et al.*, 1992; Kunnath *et al.*, 1995) have also proposed analytical modelling schemes that account for joint flexibility by reducing the moment capacities of the beams and columns framing into the joint to levels that will induce joint shear failure and anchorage failure. These models were unable to explicitly quantify the deformations that are representative of joint panel zone and as such cannot account for the kinematics in the joint.

In providing a better understanding to the response of beam-column joints by subjecting reinforced concrete sub-assemblages to reverse quasi-static loading, researchers have tried to reduce the modelling uncertainties by introducing rotational springs that could characterize the inelastic mechanism in the finite region of the beam column joint (El-Metwally and Chen 1988; Alath and Kunnath, 1995; Deng *et al.*, 2000).

To account for the flexural rigidity in the joint panel zone model, Alath and Kunnath (1995) included rigid links that span the joint region (see Fig. 2.26). It requires the joint region be connected by two nodes of length zero, each independently connecting the rigid links of adjoining beams and columns. The two translation degrees of freedom for each node are then being slaved by the other duplicate node, thereby allowing for only relative rotation between framing beam and column line elements. A one dimensional shear stress-strain response envelope is then required to describe the joint behaviour under seismic loading. This modelling approach has been widely used to validate experimental responses of beam-column sub-assemblages and reinforced concrete scaled frames that

have been subjected dynamic loading from shake table tests (Jeon *et al.*, 2012; Hassan, 2011).

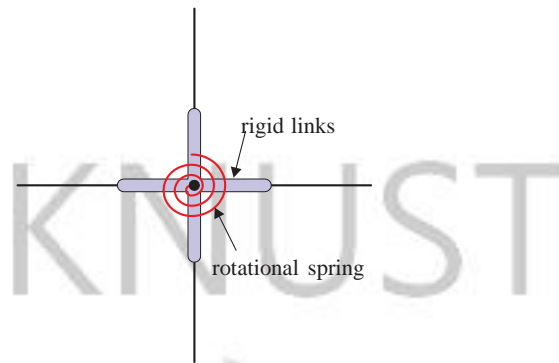


Fig. 2.26. Alath and Kunnath (1995) schematic representation of joint region.

Theiss (2005) used this joint modelling scheme to assess the impact of joint response on a case study reinforced concrete frame. It was concluded that the inclusion of the joint model in nonlinear time history analysis can significantly impact the maximum interstorey drift demand levels. Celik and Ellingwood (2008) having assessed the performance of four computer simulation joint modelling schemes, concluded that the rotational spring with rigid end zones approach of characterizing joint behaviour, produced the best correlation between the simulated base shear-drift response with the experimental response. The study further proposed a constitutive relation that can be used to implement the joint model, and later used it to generate fragility functions as part of the seismic risk assessment of RC frames in regions of low to moderate seismicity. Park (2010) sequentially performed both nonlinear static and dynamic analysis on two prototype RC building and concluded that for unreinforced joints in which the shear mode of failure precedes beam reinforcement yielding, the inclusion of joint flexibility (rotational spring model) is considerable and essential for simulating seismic responses. Hassan (2011) in his assessment of seismic vulnerability of unreinforced RC joints compared the approach of localizing all the inelastic mechanisms in one single rotational

spring to one that decouples the shear and bond deformation by providing two springs. It was observed that both approaches were able to predict the maximum shear strength of tested sub-assemblages at the same drift amplitude, with a marginal variation in the estimation of the post peak drift capacities.

The rotational spring with rigid links being able to capture fairly the hysteretic response RC joint subassemblies, he emphasized that the rigid joint assumption of modelling shear failure dominated RC frames in nonlinear analysis is generally incorrect. Using a rotational spring element to define the finite joint region, these shear strength models was used to develop a constitutive relation for the envelope curve, which was tested on three hypothetical RC frames in order to explore the degree of flexibility unreinforced joints imposed in generating fragility functions. The RC frames showed an increase in maximum inter-storey drift caused by joint rotation, propagating as the spectral acceleration increases. This proves the relevance of modelling beam-column joints in earthquake simulation and vulnerability assessment of non-seismically designed reinforced concrete buildings that possessed unreinforced beam-column joints.

One disadvantage of its implementation is that, by slaving the translation degrees of freedom, the relative horizontal deformation between the upper and lower column elements then becomes absent, and as such joint kinematics cannot be fully accounted for. Hence, there is a genuine concern with the use of a single component beam-column joint (rotational spring) element to adequately simulate the different inelastic failure mechanism expected. Therefore, the need to develop joint models that can explicitly capture more realistic inelastic mechanisms (anchorage, shear and interface shear transfer deformations) by adopting a multi-component joint element formulation to simulate more realistic behaviour of beam column joints is warranted.

A joint modelling scheme that possesses transparency in characterizing each individual mechanism is greatly sorted. Lowes and Altontash (2003) proposed a classical super-element model that consists of thirteen zero-length springs each defined by a one-dimensional constitutive model to simulate three inelastic mechanisms (see Fig. 2.27).

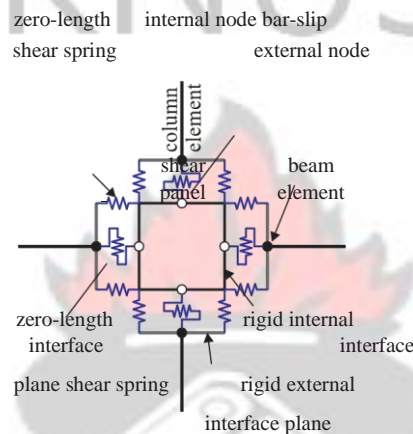


Fig. 2.27. Lowes and Altoontash (2003) schematic representation of joint region.

The parent model consisted of eight bar-slip springs located at the perimeter of the joint. Mitra and Lowes (2007) later made some modifications in the element definition of the parent model and proposed a framework for the calibration of the joint shear panel component as well as the bar-slip springs. Mitra (2007) suggested that moving them to the centroid of compression and tension zones of beam and column, could yield better predictions of joint response. All these modifications have evolved with the prime aim of providing a good fit of the observed response of beam-column joint sub-assemblages that are usually subjected to quasi-static reverse cyclic loading tested in the laboratory. The bar-slip springs enable the quantification of strength and stiffness loss due to pullout of adjoining beam and column longitudinal reinforcement. In order to simulate shear-failure mechanism, a central shear panel zone connected by four internal nodes is properly calibrated to account for the relative rotation of framing members. Also, interface shear

springs that are located at the perimeter of the joint panel zone is used to simulate shear flexibility and loss of shear strength at transfer of seismic forces due to opening of diagonal cracks during the loading history. They adopted the modified compression field theory (Vecchio and Collins, 1986) to define the joint shear strength, and a highly pinched hysteresis model to account for the cyclic strength and stiffness degradation under seismic action. By utilizing this two dimensional thirteen component super-element joint modelling scheme, we can independently quantify the impact of each inelastic mechanism, as well as appropriately capture joint kinematic, a disadvantage of single-component joint modelling approach. Even though this approach has been extensively validated by experimental responses of quasi statically tested RC sub-assemblies, researchers have noted that the use of multi-spring joint models (super element), for quantifying joint response in nonlinear time history analysis of RC frame simulation may cause numerical divergence; as such the approach of using a single rotational spring element is preferred (Park and Mosalam, 2012). Mitra and Lowes (2007) noted that this numerical instability in the global solution algorithm may be attributed to the fact that the bar-slip springs possessing a strain softening behaviour, characterized by having a negative tangent stiffness after reaching their ultimate capacities, results in having negative eigenvalues.

Altootaash (2004) developed a simplified version of this super element model, by employing four beam-column interface zero-length rotational springs to represent bar-slip deformation and a joint shear rotational spring for shear deformation of the panel zone (see Fig. 2.28).

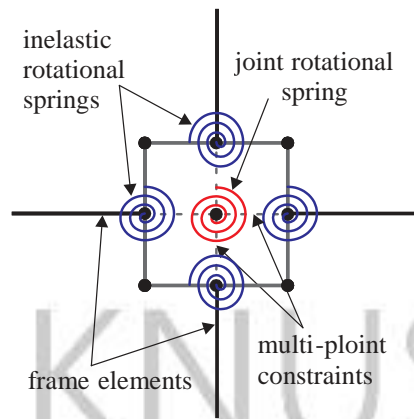


Fig. 2.28. Altoontash (2004) schematic representation of joint region

He maintained the one-dimensional hysteretic model used by Lowes and Altoontash (2003) to describe shear panel zone component, and noted that validation of calibration parameters for unconfined joint should be emphasized since the modified compression field theory (MCFT) may underestimate the ultimate shear strength of such joints. A fibre section moment curvature analysis was also employed to derive the envelope response of independent member end rotation of the interface shear springs. A couple of researchers have employed the joint model scheme to simulate the inelastic behaviour of joint under high shearing forces and the deteriorating hysteretic nature of reinforced concrete beams and columns. Haselton (2007) provided calibration procedures for quantifying the independent moment-rotation relationship for a database of 255 tested reinforced concrete column specimen. By using the deteriorating hysteretic model proposed by Ibarra and Krawinkler (2005) to describe the constitutive behaviour of the interface rotational springs, they assessed the collapse vulnerability of modern codeconforming RC frames, assuming that the joint shear panel is rigidly elastic. Liel (2009) also employed a similar approach but incorporating joint shear distortion by adopting ASCE/SEI 41-06 joint shear strength Equation. Their numerical modelling approach was based on concentrated

plasticity finite element formulation other than the fibre section macro model with distributed inelasticity, a preferred option for seismic collapse risk assessment.

## 2.4 Summary

State-of-art seismic risk assessment strategies, such as the performance based earthquake engineering framework, has allowed engineers, to systematically quantify and propagate all sources of uncertainties resulting from conceptual representation of structural component behaviour and variability of seismically related parameters such as frequency composition. However, for older type non-seismically designed RC frames, appropriate representation of joint behaviour is imperative. This is because earthquake reconnaissance surveys (Moehle and Mahin ,1991; Sezen *et al.*, 2000) have stressed that the joint region undergoes significant stiffness and strength deterioration and may lead to global collapse of structures. Even though modelling schemes such as the single component rotational spring model may be appropriate for describing joint behaviour, intuitively, the usage of multi spring model that allows for transparency in the various deformation mechanisms as well as capturing joint kinematic may also be preferred. As discussed, an evaluation of its appropriateness for performing non-linear time history analysis is lacking, and as such, the main objective of this study in subsequent chapters, is to assess the impact of its implementation on global dynamic response quantities and fragility computations.

# KNUST

## CHAPTER 3: METHODOLOGY AND CONCEPTUAL FRAMEWORK

### 3.1 Introduction

The appropriateness and reliability of the thirteen element beam column joint model (Lowe and Altoontash, 2003) under nonlinear time history analysis of RC frames has not been given much great attention. This has been attributed to the fact that multicomponent joint models have the possibility of causing numerical divergence during frame analysis (Park, 2010). More so, there is the perception that modelling demands in terms of calibration of each spring element can be computationally expensive, and may not assure accuracy of the analysis. The evaluation of this joint model through nonlinear time history analysis was the main focus of this study. The implicit assumption of rigidity at beam-column joint and the explicit representation of the joint region using a single zero-length

rotational spring was used for comparative assessment. An initial step was to validate and evaluate the joint models considered. This was achieved by employing base shear –drift responses of quasi static loaded reinforced concrete beamcolumn joint sub-assemblages and the displacement time history of a prototype shake table test of a 1/3 scaled RC gravity designed frame . Nonlinear time history analysis was then performed on three hypothetical case study RC frames to test the appropriateness of the super element joint modelling and finally analytical fragility functions are developed to study the impact of joint flexibility on seismic responses as well as evaluating the variations in seismic performance when uncertainties in ground motion and modelling techniques are incorporated.

This chapter details out the analytical modelling of structural components, describes the conceptual framework for assessment and the estimation methods used to generate the fragility curves for various joint modelling schemes.

### **3.2 Analytical Modelling of Structural Component**

The nonlinear open source platform, OpenSees (McKenna, 2010), was employed in numerical simulation of the responses of structural components. The beams and columns were modelled using line elements that can account for both material and geometric nonlinearities. The “*nonlinear beamColumn element*”, based on a distributed inelasticity formulation, along with fibre element modelling of the various component that make up the element cross-section, i.e , confined, unconfined and reinforcing steel, was used to represent the beams and columns component behaviour. The concrete properties were modelled using the “*Concrete02*” material object that assumes zero tensile strength. In order to account for the marginal increase in compressive strength due to confinement, the model of Mander *et al.* (1988) was employed. The reinforcing steel was modelled using the “*steel02*” material object that uses a bilinear response envelope and Menegotto-

Pinto (1973) hysteretic curves to describe the cyclic behaviour as well as accounting for the Bauschinger effect.

The schematic representation of the joint region as described by Alath and Kunnath (1995), was modelled using a zero length rotational spring with rigid links across the joint region (see Fig. 3.1a). This was implemented by defining two nodes at the same location, thus of length zero, each independently connecting the rigid links of adjoining beams and columns. The two translation degrees of freedom for each node were then being slaved by the other duplicate node, thereby allowing for only relative rotation between framing beam and column line elements. A one dimensional shear stress-strain response envelope was then required to describe the joint behaviour under seismic loading. For the super-element joint modelling representation, the

“*beamColumnJoint*” element implemented in *OpenSees* by Altootaash (2004) was employed. It requires 34 modelling parameters to describe the one dimensional monotonic and hysteretic behaviour of the thirteen spring components (see Fig. 3.1b). The “*Pinching4*” material model was used to simulate the behaviour of the shear panel zone of zero length rotational spring of the scissors and super element model, respectively. This uniaxial material model approximates the element shear stress-strain response by using a quad-linear envelope and a tri-linear unload-reload path to control the hysteretic damage (see Fig. 3.1d). An appropriate joint shear strength model is required to define the one dimensional constitutive model to describe the envelope response. Jeon (2013) used an extensive database of 261 quasi statically loaded subassemblages, and proposed a joint shear strength model that depends on typical design parameters such as the compressive strength, the joint confinement factor, number of transverse beams and beam reinforcement index. This model was adopted to estimate the maximum joint strength. For the remaining key points on the backbone, the suggestions made by Anderson *et al.* (2008) were utilized (see Fig. 3.1c). In order to account for bond slip, a reduction in the

moment capacities of the beams framing into the joint or using recommendations provided by FEMA 356 (2000) to modify the strength of the longitudinal reinforcement steel located in the plastic hinge zone of the adjoining beams and column can be adopted. A strength reduction factor of 0.5 on the moment capacity of the beam framing into the joint was selected in order to simulate anchorage failure mechanism. The interface shear transfer failure mechanism was modelled assuming elastic and stiff shear spring elements (Mitra and Lowes, 2007).

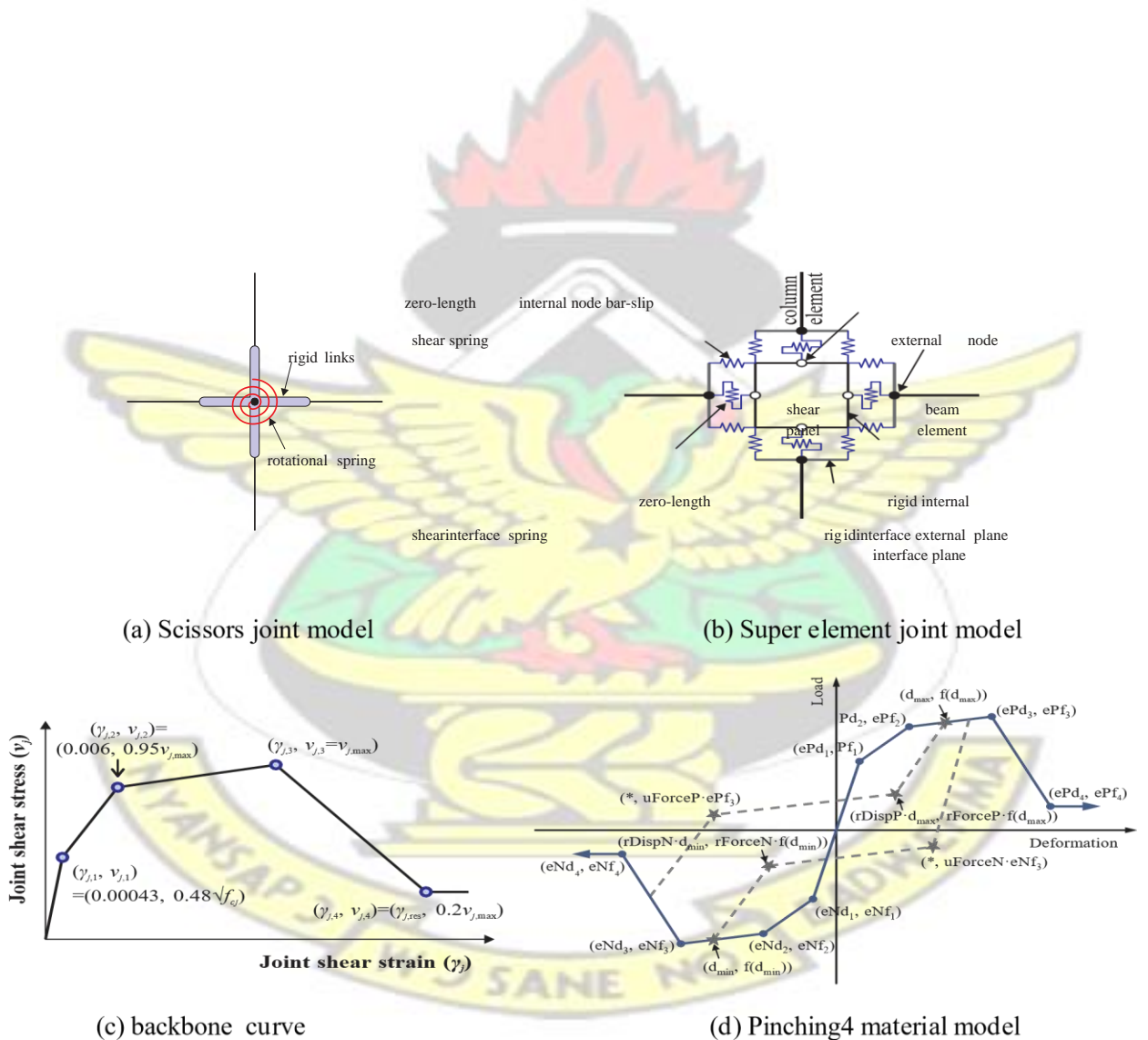


Fig. 3.1. Joint modelling techniques and constitutive material models.

### 3.3 RC Joint Sub-assemblages for Validation

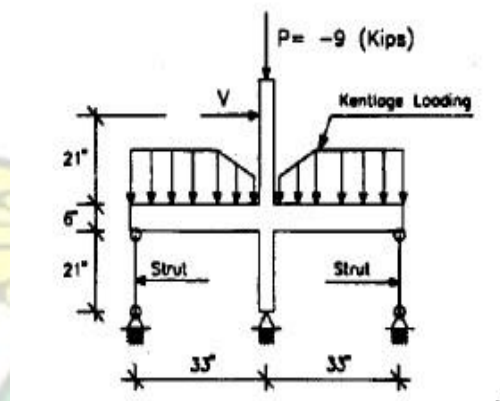
For nonlinear vulnerability assessment of non-ductile RC frames, accurate prediction of seismic responses that account for joint flexibility requires the validation of the onedimensional load –deformation response used for the various types of joint configuration. Three experimental tested RC sub-assemblages of interior (Bracci *et al.*, 1994), exterior (Pantelidis *et al.*, 2002) and knee joints (Pampanin *et al.*, 2000) under quasi-static reverse cyclic loading are used to evaluate the representation of both explicit joint models (scissors and super-element joint model) and implicit approach (rigid joint model).

Aycardi *et al.* (1994), in predicting the nonlinear behaviour of a 1/3 scaled gravity loaded designed RC frame, initially assessed the behaviour of structural components, that is, columns and RC sub-assemblages by subjecting them to quasistatic reverse cyclic loading at increasing drift amplitudes of  $\pm 0.25, \pm 0.50, \pm 0.75, \pm 1.00, \pm 2.00, \pm 3.00, \pm 4.00$  and  $\pm 5.00$  percent. Typical substandard reinforcing details investigated were lap splices located at potential plastic hinge zones, inadequate joint transverse reinforcement and discontinuous bottom beam reinforcement in the joint. The interior joint sub-assemblage (see Fig. 3.2a), which exhibited a strong column-weak beam failure mechanism is selected in validating the modelling approach for both single component and super element model.

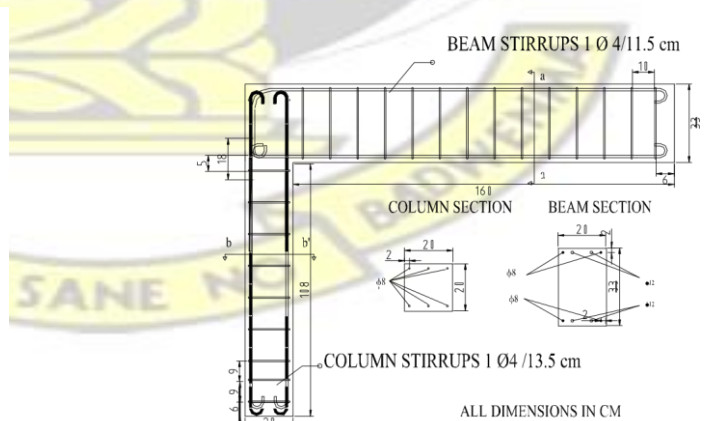
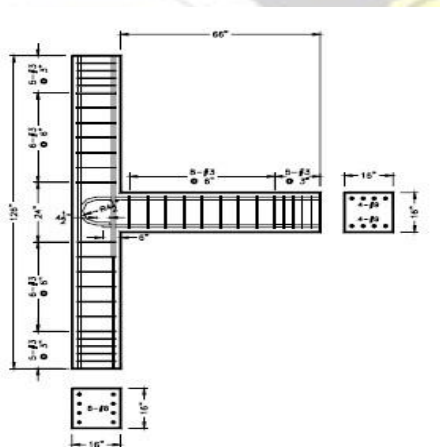
Pantelidis *et al.* (2002) assessed the impact of column axial load and joint embedment length in exterior joint with substandard details. In evaluating the seismic performance of such joint details, the longitudinal reinforcement was increased, so that a shear failure mode can be exhibited in order to quantify the seismic performance of shear-dominated exterior joints. Two levels of axial compressive loads (10% and 25%) as well

as three extent of embedment length in the joints were studied. The experimental validation of test unit 1, having an axial compressive load of 10% with a 6 inches embedment length of bottom bars is selected as seen in Fig. 3.2b.

Pampanin *et al.* (2000) in assessing the vulnerability of beam-column joints, tested six two-third scaled beam-column joint sub-assemblages with smoothed reinforcing bars and lack of joint transverse reinforcement. The designs of the specimens were based on allowable stress philosophy and as such emphasis for ductile behaviour at both local and global levels, a capacity design principle, were absent. The exterior knee joint typology from this investigation was selected in validating the joint modelling scheme (see Fig. 3.2c).



Interior R joint sub assemblage  
ycardi et al 1994



Exterior R joint sub assemblage Knee R joint sub assemblage Pantelidis et al 2002  
Pampanin et al 2000

Fig. 3.2. Selected RC joint sub-assemblages for validation of modelling schemes

### 3.4 Scaled Model RC Frame for Validation

In evaluating the seismic adequacy of low rise reinforced concrete buildings, Bracci *et al.* (1992) tested a 1/3 scaled RC frame with non-seismic detailing provisions of ACI318-39 (see Fig. 3.3). The three-storey three-bay frame was intended to represent an interior frame of an office building. Three main levels of ground motion intensities were assessed to quantify the seismic performance of the case study frame.

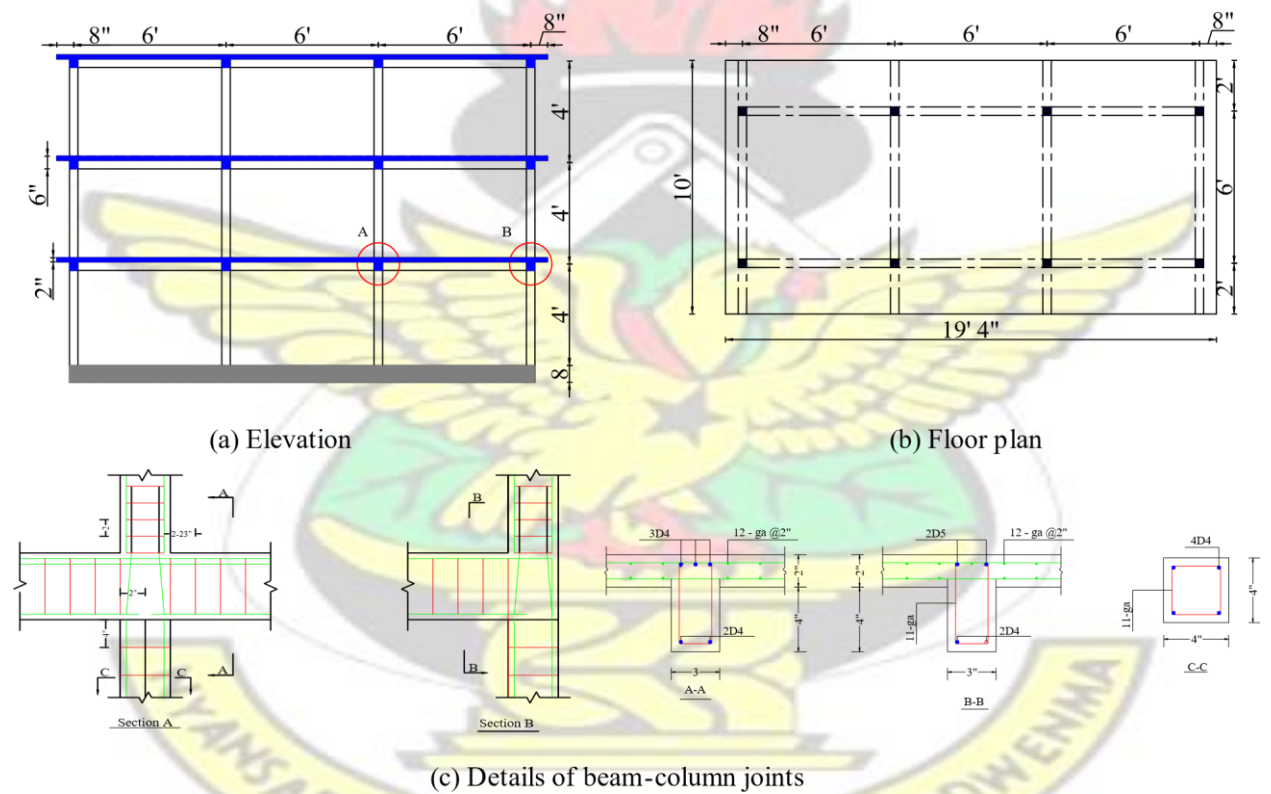


Fig. 3.3. One-third scaled frame (Bracci *et al.*, 1995)

The horizontal component of the 1952 Taft earthquake, N021E, was selected because it is able to produce high levels of base motion for a wide range of building

frequencies. Fig. 3.4 shows the scaled accelerogram with peak ground acceleration 0.2g, serving as the excitation for the 1/3 scaled analytical models under study.

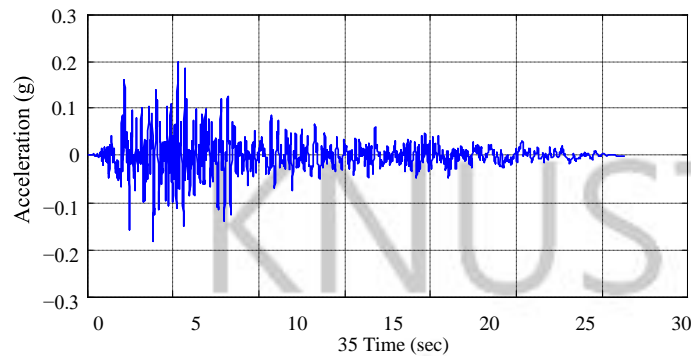


Fig. 3.4. 1952 Taft (N021E) accelerogram to a peak ground acceleration of 0.2g

### 3.5 Conceptual Framework for Assessing Variation in Dynamic Responses

The following provides a framework for assessing the variations in the seismic demand of two explicit joint models in nonlinear time history analysis of RC frames. The null hypothesis is given as that, inclusion of different joint models in frame analysis does not matter in the estimation of nonlinear seismic demand, quantified here by using the interstorey drift ratio. Three different hypothetical RC frames (see Fig. 3.6), which are conditioned on their natural vibrational periods are subjected to nonlinear time history analysis at various classes of ground motion intensities to gain knowledge into whether and under what conditions this assumption of equivalence holds. The classes of records index, R-1, R-2 and R-3 consist of 10 historical ground motions with magnitude ranging from; 5-5.5 to represent low intensities, 5.5-6.5 to represent moderate intensities, 6.5-7.5 to represent high intensities, respectively with all having a maximum source to site distance of 50km ( see Fig. 3.5). These records have been matched to the PEER NGA West2 Spectrum with strike-slip fault type and magnitude conditioned on the mid-point on the selected in each class. Only one component of the horizontal motion for each record was selected for nonlinear time history analysis.

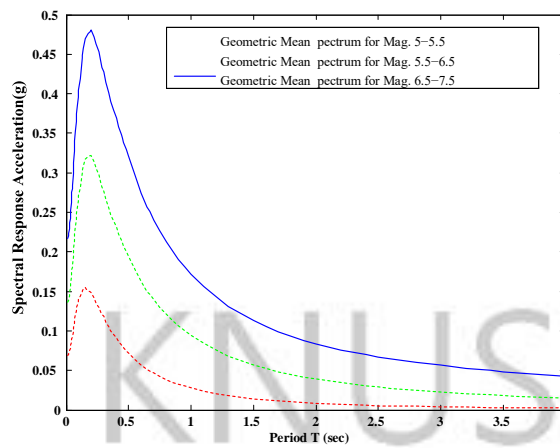


Fig. 3.5. Target Response Spectrum for various classes of record sets.

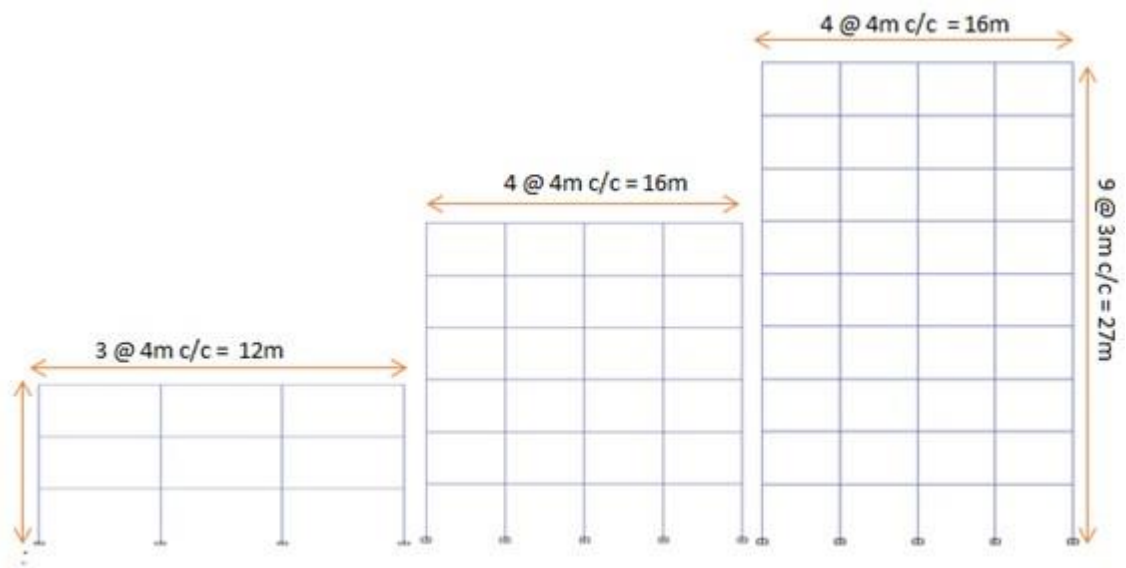


Fig. 3.6: Geometry of hypothetical RC frames.

The implicit assumption of RC joints maintaining their orthogonality (hence rigidly connected) is referred to here as *rigid joint model* and can be viewed as the control group with the explicit joint models categorised as the treatment groups. The three different joint models were incorporated into each of the three hypothetical RC frames, thus producing nine case study RC frames. Each of these frames was subjected to the three classes of records to yield twenty seven combinations and finally 270 runs of nonlinear dynamic analysis. The rigid joint model served as the baseline model from

which relative ratios of the inter-storey drift ratio for each joint element formulation was then computed from a record set given a particular prototype RC frame. The mean of these ratios in each record set was then computed alongside the sample standard deviation. A two sided hypothesis test was then performed on each joint model type with a particular record set. Finally results were pooled together to address the issue of whether it matters in the selection of a joint model scheme in estimating structural demand under dynamic loading.

### 3.5.1 Analysis

A structural response quantity that is closely related to its degree of damage is required to assess the vulnerability of buildings to seismic action. The inter-storey drift ratio has been one of the most widely used damage indices for assessing the seismic performance of RC frame components and is used here as the engineering demand parameter (Sozen, 1981). Each of the considered hypothetical RC frames that incorporate the three joint models has been analysed by running the three classes of record sets. The post processing phase consists of obtaining,  $IDR_{if|j,k,l}$ , which represents the peak interstorey drift at a particular storey  $f$ , for record  $i$ , belonging to a particular class of record  $j$ , for RC frame  $k$ , with joint model,  $l$ . These responses were monitored at critical floor levels in order to address the hypothesis that the structural demand is equal irrespective of the joint model used. The peak in time drift ratio at the first, roof and at any storey level was used in this study. To test this equivalency statistically, a two phase process was adopted.

In the first phase, the inter-storey drift ratio for the joint models in the treatment group (scissor and super-element joint models) was normalized by using the demand from the rigid joint model (control group) to investigate the degree to which it underestimates or overestimate the responses from the conventional approach. This parameter is given as;

$$\frac{IDR_{ex(i)}}{IDR_{im}} \quad (3.1)$$

where  $IDR_{im}$ , is defined in here exclusively as the drift due to implicit modelling (rigid joint model), while  $IDR_{ex(i)}$ , is the drift due to explicit modelling;  $i$  is 1 for scissor model and 2 for super element model.

In the second phase, a ratio of the estimated means of the normalized quantity,  $\alpha$ , in a particular class of record set, for the scissors and super-element joint model, was then defined as  $Z$ ;

$$Z = \frac{N_1}{N_2} \quad (3.2)$$

where  $N_1$  and  $N_2$ , is defined as the mean of the normalized drift responses of the scissors and super element joint model respectively within a particular record set. This quantity is desirable, because it can be used to address the issue of the conditions under which assumption of equivalence in explicit representation of joint by single or multi component holds.

A two sided hypothesis test was made on the null,  $H_o$ , defined as

*$H_o$ : the mean of the normalized responses are equal*

The theoretical lognormal probability density function is typically used to describe the distribution of drift responses in vulnerability assessment, (Shome,1999; Iervolino, 2004). In the generation of fragility functions for lightly reinforced beam-column joints, Piyali and Bing (2014) showed how consistent and efficient this probability model can be used to fit an empirical cumulative distribution of observed responses. Under this assumption of log-normality in the peak drift responses with an unknown standard

deviation, the test statistic computed is required to follow a student-t distribution, (Rice, 2007). This test statistic is calculated as;

$$t = \frac{\ln(N_1) - \ln(N_2) - \ln(Z)}{B_{1-2}} \quad (3.3)$$

where  $B_{1-2}$  is the standard error of  $Z$ , and can be estimated as;

$$B_{1-2} = S_p \sqrt{\frac{1}{n_1} + \frac{1}{n_2}} \quad (3.4)$$

$$S_p = \sqrt{\frac{(n_1 - 1)s_1^2 + (n_2 - 1)s_2^2}{n_1 + n_2 - 2}} \quad (3.5)$$

where  $s_1$ ,  $s_2$ , are the standard deviation of the natural logarithms of  $\alpha$  in the scissors and super-element joint models;  $S_p$  is the pooled sample standard deviation of the logarithms of  $\alpha$ ;  $n_1$  and  $n_2$  are the number of records in each record set. The number of degrees of freedom for the student-t distribution is given as  $(n_1 + n_2 - 2)$ . Typical values used in here are 18, 58 and 178 depending on the chosen pair of normalized responses being compared.

Two statistical significance levels of 5% and 10% were adopted in the present study in order to determine whether to accept the hypothesis that the mean of the normalized drift responses from the scissors and super-element joint model are the same. This value corresponds to the probability of making a type 1 error; thus rejecting the null hypothesis when it is in fact true. Given a two-sided test, with the selected level of significance under a student-t distribution with 18 degrees of freedom, the region of acceptance will correspond to  $\pm 2.101$  and  $\pm 1.734$  standard error,  $B_{1-2}$ , away from the mean, which is centered at zero. For the 58 degrees of freedom under a student-t

distribution, these quantiles corresponded to  $\pm 1.67$  and  $\pm 2.002$  standard deviations away from the expected mean of the sampling distribution. A Gaussian distribution was assumed in the case of 178 degrees of freedom, and the corresponding test statistic at 5% and 10% significance level was  $\pm 1.64$  and  $\pm 1.96$ , respectively.

From Equation (3.3), the test statistic,  $t$ , is computed and compared to the ranges of acceptance under a given significance level in order to test the hypothesis that the responses from the two joint models investigated are equal under a particular record set.

### 3.6 Fragility Assessment Framework of a Case Study RC Frame

Fragility functions provides the conditional probability of the structural system or component, exceeding a damage limit state, for instance immediate occupancy limit state (FEMA, 2003), given a site specific intensity measure is sought. The three storey three bay RC frame (see Fig. 3.7), which was employed in the assessment of the variations of the dynamic response quantities, is used to generate analytical fragility curves.

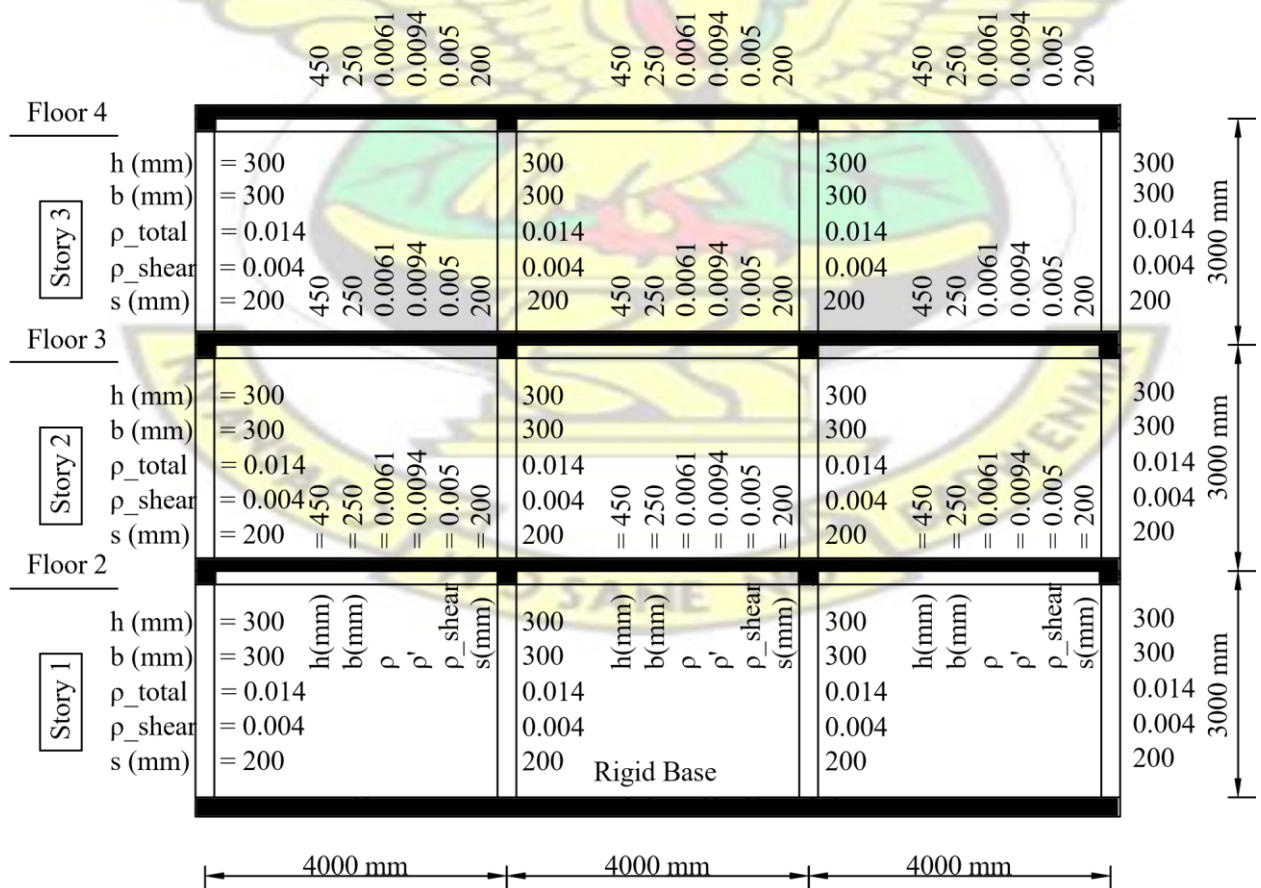


Fig. 3.7. Case study RC frame for fragility assessment.

Adopting the terms of the Pacific Earthquake Engineering Research (PEER) Centre, the scalar intensity measure (IM) used in computation of the seismic reliability was the 5% damped spectral acceleration at the first modal period of the building. The engineering demand parameter also adopted is the maximum inter-storey drift ratio (MIDR) because it is closely related to the degree of damage sustained by structural components under earthquake excitation. The stochastic time-series simulation model developed by Yayamoto (2011) was employed for obtaining a large sample of synthetic accelerograms. This model which uses the wavelet packet transform that easily modulates the time and frequency characteristics of the ground motion is selected because it has been validated for a wide range of magnitude, structure specific modal periods, shear wave velocities, etc. A cumulative sample of 180 synthetic records were generated depending widely on the range of magnitudes, that is, 6 to 8, with a 30m depth shear wave velocity of 400cm/s. From this a Latin hypercube experimental design, that models the variation in the compressive strength of concrete, tensile yield strength of steel and damping ratio, were constructed which each realization mapped to a random sample of the ground motion for nonlinear time history analysis. The statistical properties of these random variables are shown in Table 3.1.

Table 3.1. Statistical properties of parameters for Latin-hyper cube experimental design.

Parameter	Probability Distribution	Mean	Coefficient of variation
Compressive Strength	Normal	27.6MPa	0.176
Steel yield strength	Lognormal	460MPa	0.08
Damping Ratio	Lognormal	0.05	0.6

The conventional *cloud analysis* was selected because a closed form solution can be established easily in order to access the probability of exceeding a prescribed limit state (Baker and Cornell, 2006). However, an underlining assumption of constant variance (homoscedascity) across the range of ground motion intensity may be invalid when frame are excited into the highly non-linear ranges. This stems from the fact that RC structure with deteriorating hysteretic load-deformation responses possesses an inherent strain softening phenomenon after reaching their ultimate capacities (Liel, 2008), hence increasing the extent of inelasticity. Baker and Cornell (2006) noted for drift response above the 10% and with a first mode elastic spectral acceleration of 2.5, generally signifies global dynamic instability. Using these recommendations, the seismic responses from the non-linear time history analysis were processed to exclude such results in order to develop a well-defined closed form solution.



#### **CHAPTER 4: RESULTS AND DISCUSSIONS**

## 4.1 Introduction

This chapter presents the results for (1) the joint modelling scheme validation at quasi static reverse cyclic test of RC joint sub-assemblages and shake table test of a 1/3 scaled gravity designed RC frame, (2) the evaluation of the equivalence in dynamic responses for various joint models using three hypothetical RC frames subjected to various levels of ground motion intensity and (3) assessment of their variations in analytical fragility functions that gives the probability of exceeding a performance limit state given an intensity measure. Each section is concluded with a comprehensive discussion of the major findings from the study.

## 4.2 Comparison of joint modelling schemes for RC joint sub-assemblages

### 4.2.1 Interior Joint

Fig. 4.1 shows the plots for the base shear and lateral drift ratio for the interior subassemblage of the various joint models. The tested sub-assemblage was able to sustain a maximum horizontal load of 1.65kips at drift amplitude of 2%. Both explicit models (scissors and super element joint models) and rigid joint model were appropriate in capturing the pinching effect resulting from accelerated stiffness deterioration at unloading. However, the implementation of the rigid joint assumption, showed symmetric load-deformation behaviour in both loading directions, as opposed to the experimental observation having a reduced shear capacity due to anchorage failure in one of the loading directions. One consequence of this would be a much larger energy dissipation capacity that deviated from observed experimental responses. This thereby provides enough evidence as to the importance of including joint flexibility when quantifying seismic performance in vulnerability studies of non-ductile RC frames. Even though the explicit joint model were able to account for the effect of anchorage failure, the scissors joint

model showed a much lower dissipation capacity as compared to the super element model that fairly represented the hysteretic responses of the tested specimen.

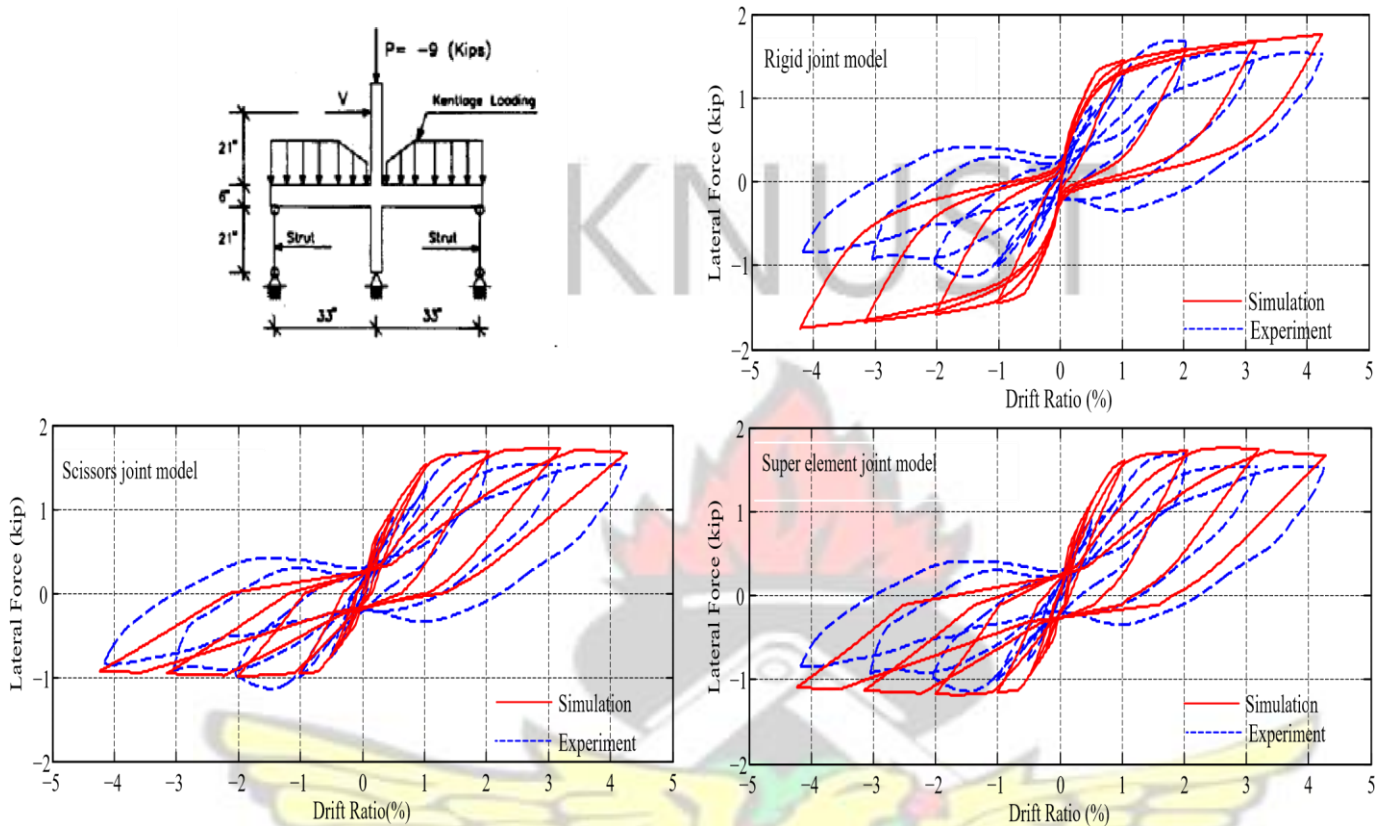
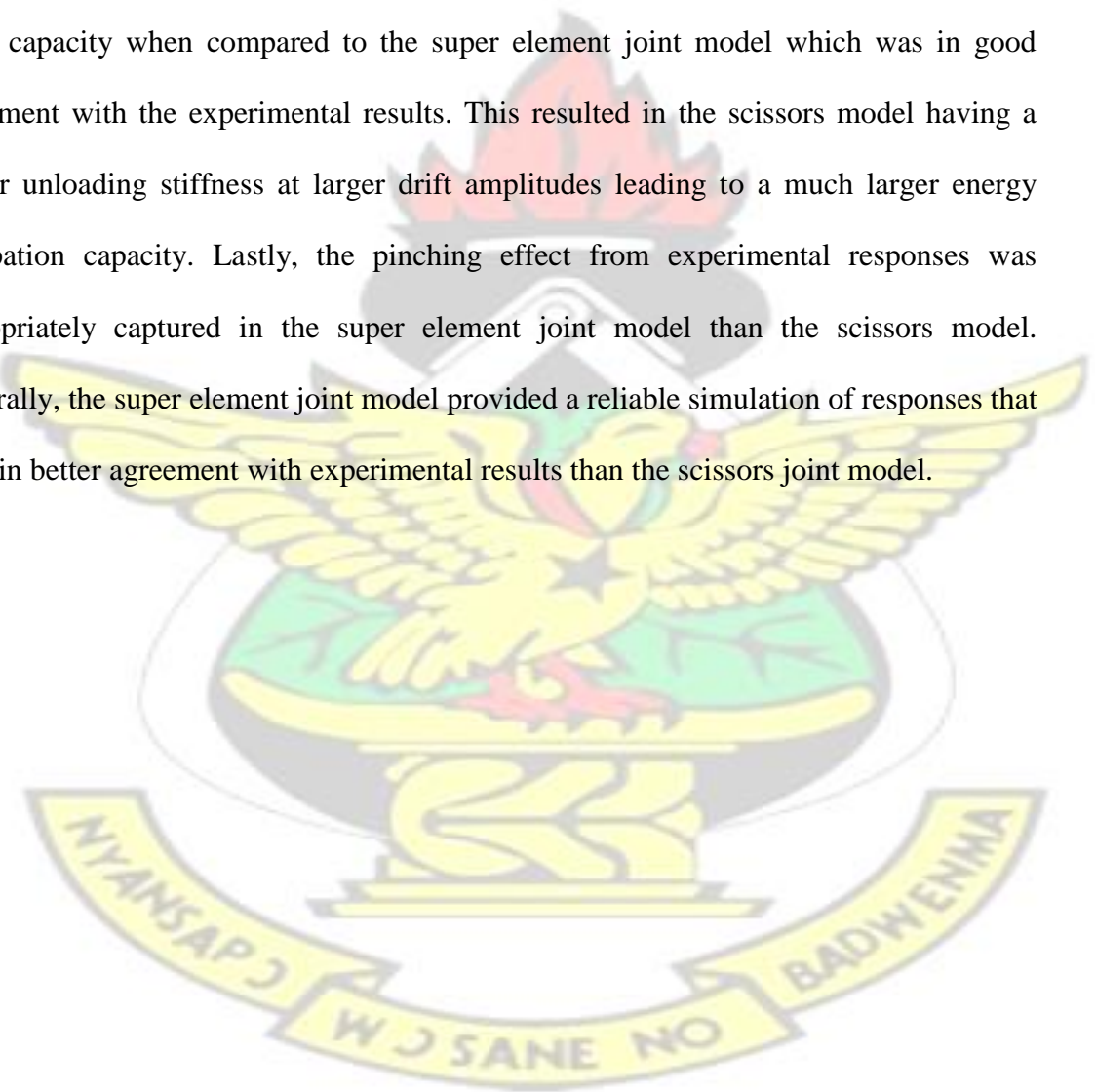


Fig. 4.1. Base shear –drift responses for interior joint sub-assemblages

#### 4.2.1 Exterior joint

The simulation of the base shear –drift responses of the exterior joint under the assumption of fully fixed end connections, showed a very large deviation from experimental responses in terms of ultimate shear strength, post peak shear strength envelope and cyclic degradation in strength and stiffness (see Fig. 4.2). Also, the predicted amount of hysteretic energy dissipated in the rigid joint model was significantly above the experimental responses which possessed highly pinched hysteretic cyclic loops. This trend in load-deformation behaviour of RC joint under quasi static loading emphasizes and affirms the need for incorporating joint flexibility in computer simulation of RC frames with expected shear dominant joint failure modes. For the explicit joint models

under study, the employed constitutive joint shear strength model, monotonic backbone curve and component degradation model were adequate enough to give an appropriate representation of observed responses, that is, the joint shear capacity and reduction in shear capacity due to anchorage failure in one of the loading directions. However, there were marginal difference in predicting the initial stiffness, strength and stiffness degradation and cyclic hysteretic paths for loading and unloading. The scissors joint model underestimates the accelerated loss of lateral resistance upon reaching the peak shear capacity when compared to the super element joint model which was in good agreement with the experimental results. This resulted in the scissors model having a higher unloading stiffness at larger drift amplitudes leading to a much larger energy dissipation capacity. Lastly, the pinching effect from experimental responses was appropriately captured in the super element joint model than the scissors model. Generally, the super element joint model provided a reliable simulation of responses that were in better agreement with experimental results than the scissors joint model.



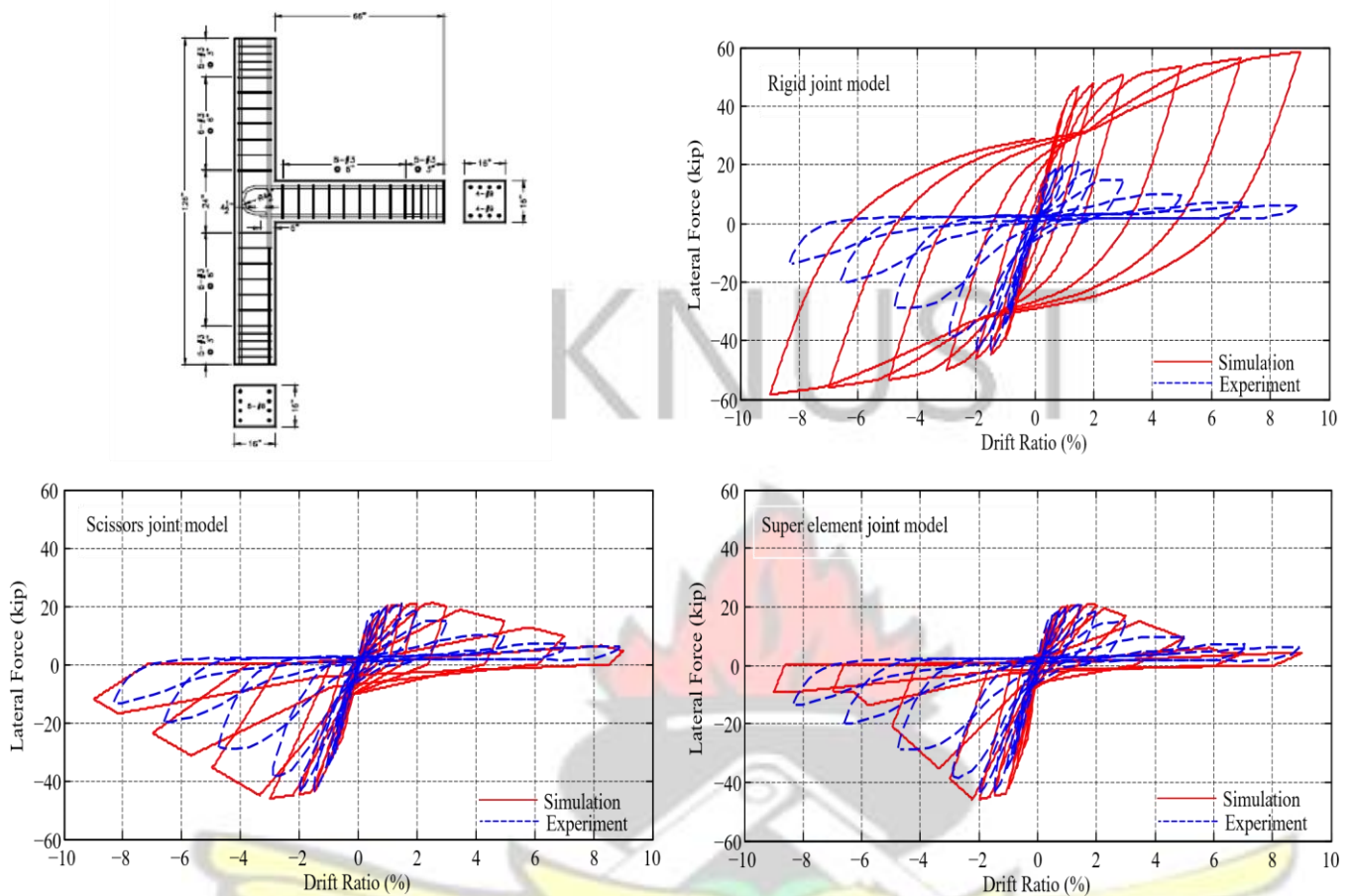


Fig. 4.2. Base shear –drift responses for exterior joint sub-assemblages

#### 4.2.3 Knee Joint

Fig. 4.3 shows the simulated load-drift relationship of the knee joint from Pampanin (2002) for the various joint modelling schemes. The reported failure mechanism was primarily controlled by flexural, concentrating at the column interface and bar pull-out that resulted in the pinching behaviour of lateral force –drift response. This signifies a beam yielding preceding joint shear failure mode, hence, the rigid joint model even though overestimated the shear capacity, was not that significant as in the case of the simulated responses of exterior joint of Pantelidis (2002) as previously discussed. Both explicit joint models were adequate enough to characterize the envelope of experimental responses in terms of shear capacity. However, they possessed a significantly reduced initial stiffness at loading and unloading, thereby reducing the expected amount of

hysteretic energy dissipated from experimental observations. Comparatively, the super element joint model gave better predictions in terms of simulated backbone curves as well as cyclic responses.

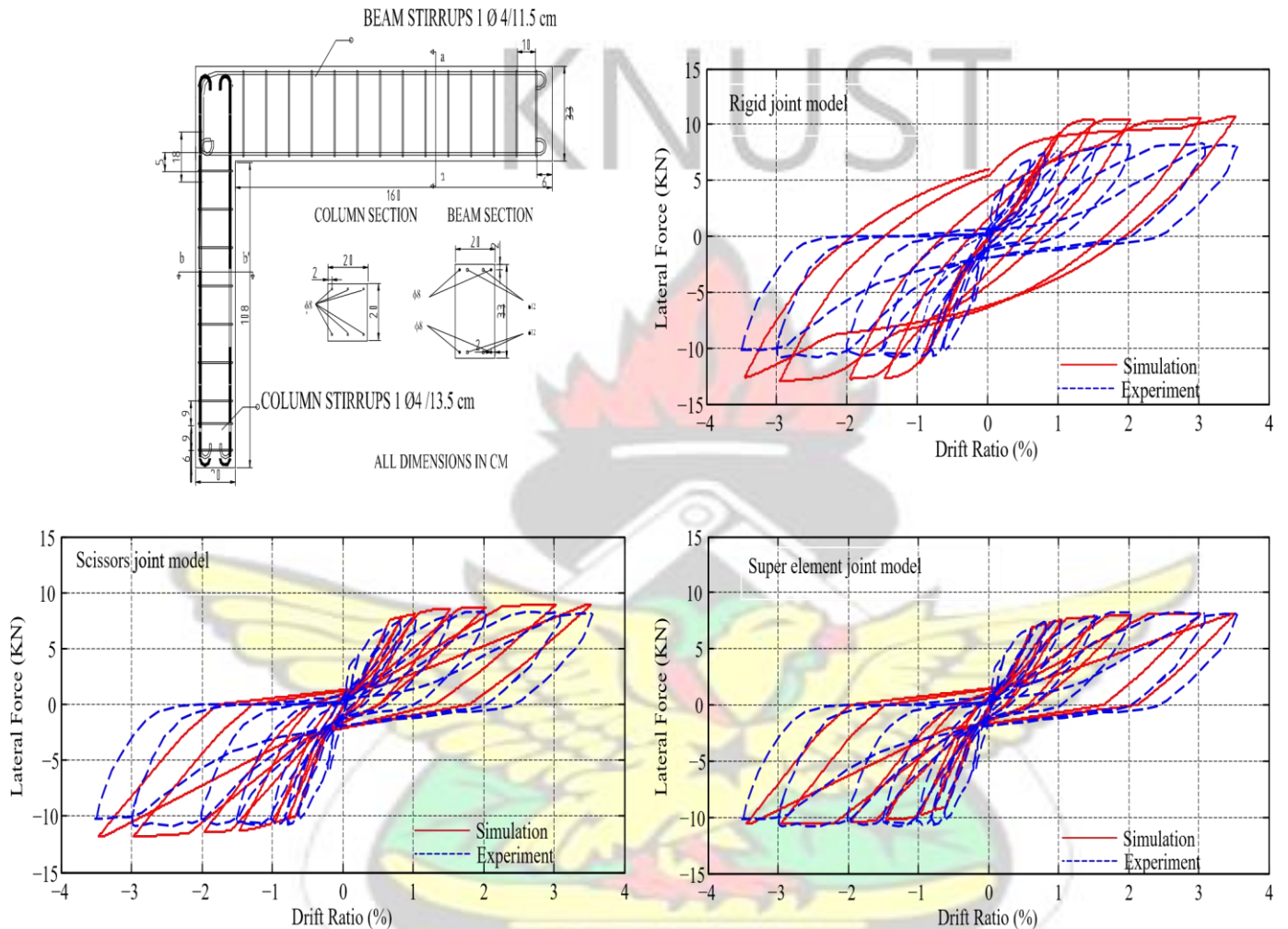


Fig. 4.3. Base shear –drift responses for exterior joint sub-assemblages

### 4.3 One third scaled prototype RC Frame

Fig. 4.4, illustrates how the various modelling schemes were able to match the roof displacement response history of a shake table test of a 1/3 scaled gravity designed RC frame that was subjected to the 1952 Taft N021E accelerogram with a peak ground acceleration of 0.2g. In all cases, the simulated responses closely matched the displacement history adequately. This may be attributed to the fact that tested interior sub-assemblages showed little joint shear distortion with a beam yielding before shear failure

mechanism. Comparatively, the super element joint model gave the closest prediction of the observed maximum displacement. The scissors joint model gave the highest maximum displacement at duration of about 4.27secs which subsequently resulted in higher permanent deformations in the time range of 25-30 seconds due to a reduced residual strength for lateral resistance.

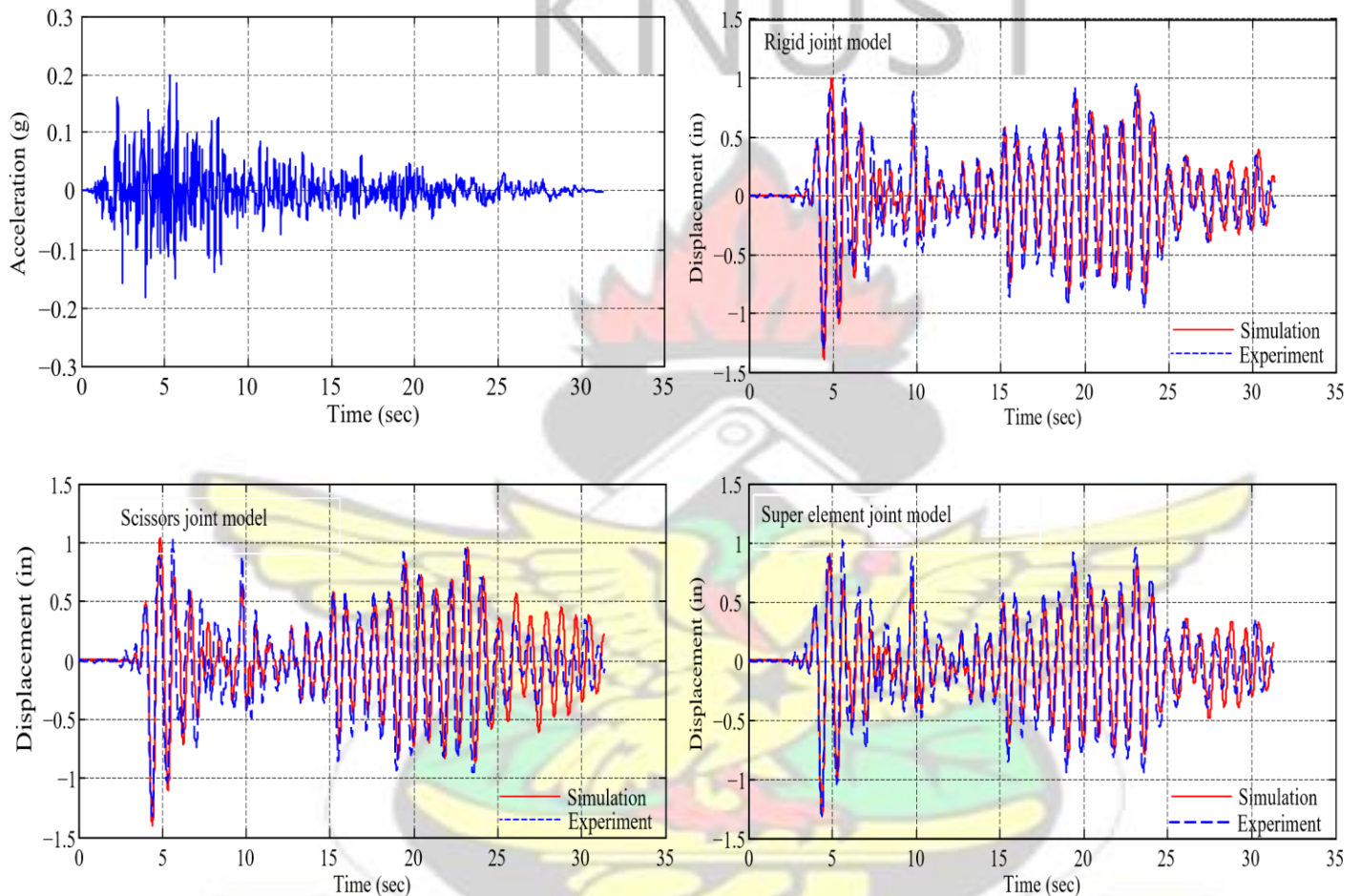
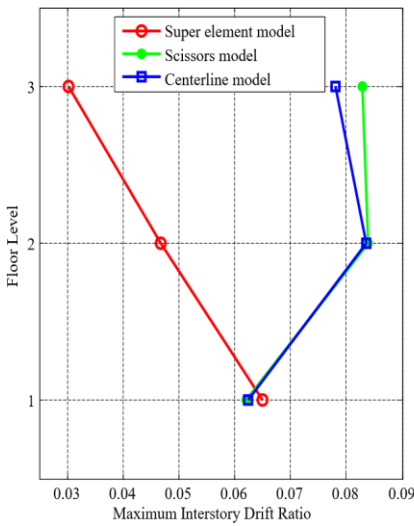


Fig. 4.4. Roof displacement response history for various joint models

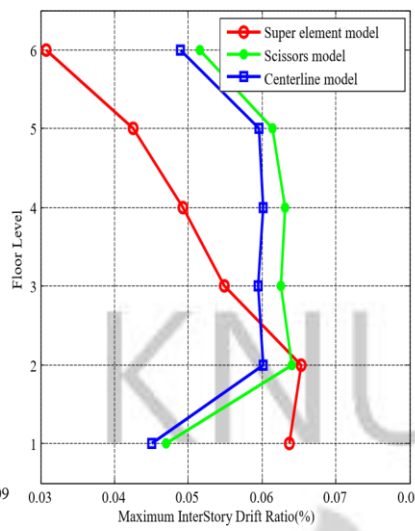
#### 4.4 Evaluation of Dynamic response

The joint modelling schemes have been verified for quasi-static reverse cyclic tests of RC joint sub-assemblages and a tested 1/3 scaled prototype RC frame. A comparative assessment of the inelastic seismic responses under nonlinear time history analysis (NTHA) of RC frames is evaluated using the conceptual framework developed in Chapter 3 - Section 3.5, to test the hypothesis of equivalence in a global response quantity; specifically the drift ratio at first and roof. In addition to this, the variations in maximum inter storey drift ratio along all floors is assessed since this is a preferred engineering demand parameter used to relate the intensity measure and damage sustained under the probabilistic performance-based earthquake engineering framework. This study employs three hypothetical case study RC frames subjected to increasing ground motion intensities to study their inherent variations.

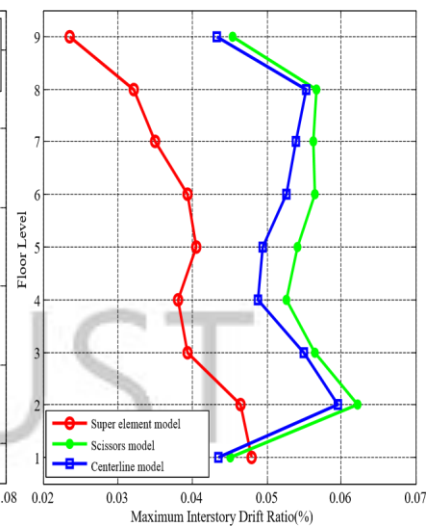
In a preliminary attempt to investigate the impact of the inclusion of the joint models in RC frame simulation, and also the extent to which it overestimates or underestimates the peak in-time drift ratios, the averages of the storey-specific peak drift in each class of record (R-1, R2 and R-3) for a particular building configuration was computed. Fig. 4.5 summarizes the profile of this quantity along the frame height. Significant differences in the mean of the peak drift ratios were observed at the first and roof level, and as such, results presented lay much emphasis on their seismic demand. One other observation was that, whilst the path of drift ratio for the rigid joint model and the scissors joint model seem to follow the same line, the super element joint model exhibited a decline in the drift ratio from the second storey, which propagates monotonically to the roof level.



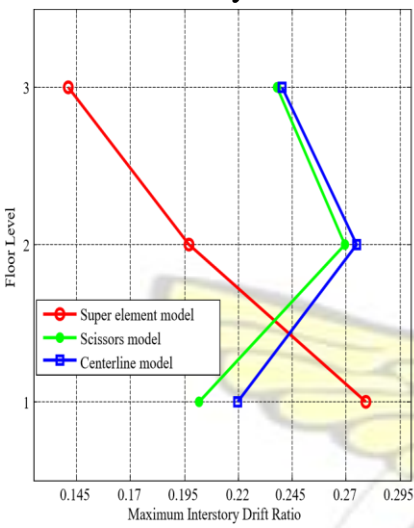
a 3- tore - R1



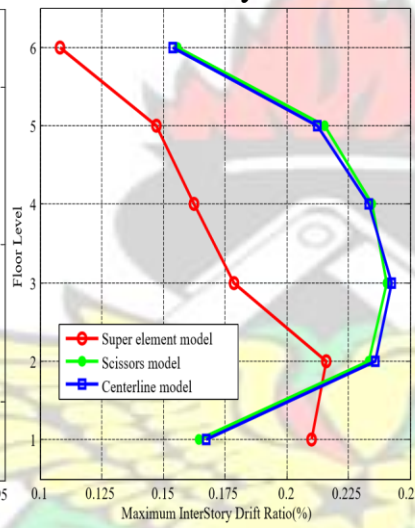
b 6- tore - R1



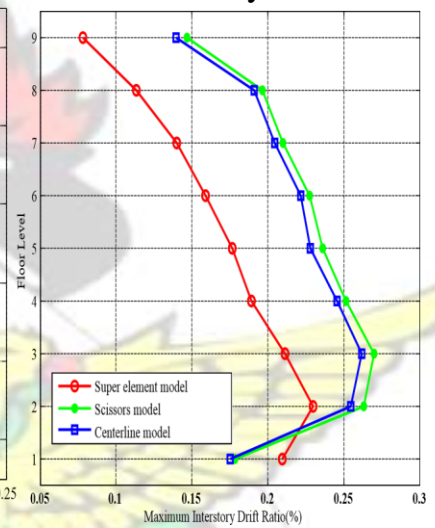
c 9- tore - R1



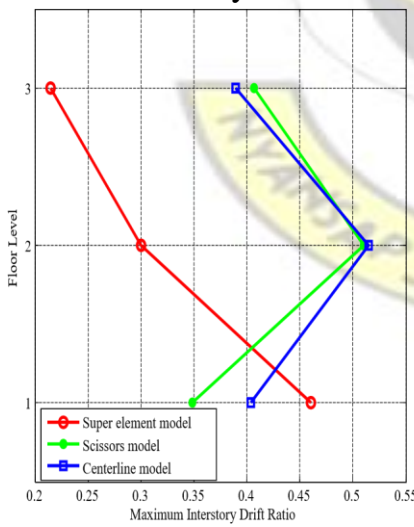
a 3- tore - R2



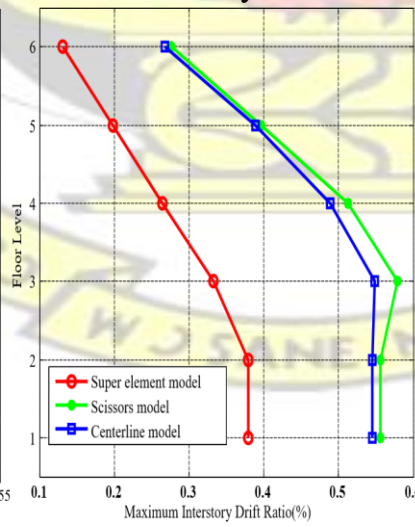
b 6- tore - R2



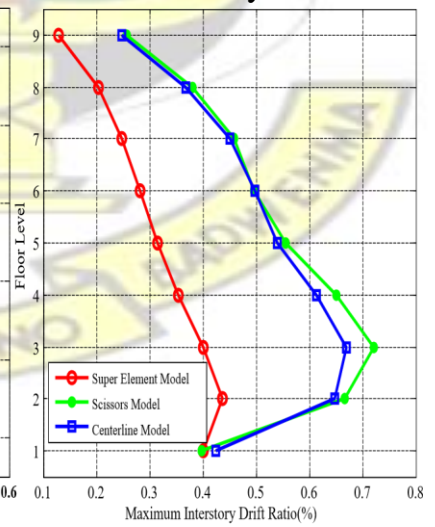
c 9- tore - R2



a 3- tore - R3



b 6- tore - R3



c 9- tore - R3

Fig. 4.5. Peak in-time drift profile for the three RC frames.

Tables 4.1 and 4.2 are used to provide summaries of the mean and standard deviation of the normalized responses of the scissors and super element joint models as discussed in Chapter 3-Section 3.5.1. Considering the duality between hypothesis testing and the establishing of confidence intervals, these quantities were used to assess the degree to which the joint models deviate from the rigid joint model. The results are pooled for each hypothetical RC frame given a class of record set, and are shown in the last row and column of each table.

Table 4.1. Ratio of mean and standard deviation of the normalized drift responses at the first floor level

			CM-R1	CM-R2	CM-R3	CM-P
Three Storey	SM	Mean	1.00	0.93	0.93	0.95
		SD	0.12	0.20	0.33	0.22
	SEM	Mean	1.11	1.44	1.22	1.26
		SD	0.15	0.23	0.33	0.24
Six Storey	SM	Mean	1.04	0.98	1.02	1.02
		SD	0.12	0.14	0.23	0.27
	SEM	Mean	1.44	1.21	0.65	1.10
		SD	0.14**	0.19	0.31	0.25
Nine Storey	SM	Mean	1.08	1.02	0.96	1.02
		SD	0.14	0.19	0.16	0.25
	SEM	Mean	1.17	1.33	0.98	1.16
		SD	0.13	0.18	0.22	0.25
Pooled	SM	Mean	1.04	0.98	0.97	1.00
		SD	0.08	0.11	0.15	0.14
	SEM	Mean	1.24	1.33	0.95	1.17
		SD	0.09**	0.16*	0.17	0.14

\*CM-R1: Rigid joint model for record set 1; CM-R2: Rigid joint model for record set 2 ; CM-R3: Rigid joint model for record set 3; CM-P: Rigid joint model for pooled record set; SM: Scissors model; SEM: Super element model; SD: Standard deviation ; \*\* and \* signify the rejection of the null hypothesis at 5% and 10% significance levels respectively.

Table 4.2. Ratio of mean and standard deviation of the means of Z at the first floor level

			SM-R1	SM-R2	SM-R3	SM-P
Three Storey	SEM	Mean	1.10	1.54	1.35	1.33
		SD	0.15	0.22*	0.32	0.23
Six Storey	SEM	Mean	1.38	1.24	0.64	1.09
		SD	0.14	0.19	0.31	0.25
Nine Storey	SEM	Mean	1.09	1.30	1.00	1.13
		SD	0.11	0.18	0.21	0.24
Pooled	SEM	Mean	1.19	1.36	1.00	1.18
		SD	0.08*	0.16*	0.17	0.14

\*SM-R1: Scissors model for record set 1; SM-R2: Scissors model for record set 2 ; SM-R3: Scissors model for record set 3; SM-P: Scissors model for pooled record set; SEM: Super element model; SD: Standard deviation ; \*\* and \* signify the rejection of the null hypothesis at 5% and 10% significance levels respectively.

#### 4.4.1 First Storey

In 30 of the 32 cases of mean normalized drift responses in Table 4.1, the hypothesis that the equality of the seismic demand of RC frames that includes joint models, can be accepted at the 95% confidence level when compared to the rigid joint model. In order to assess the degree of equivalence at the explicit joint model level, the ratio of the normalized drift responses as discussed was used. Table 4.2 shows its distribution for the range of RC frames and record set considered. None of the cases investigated resulted in rejecting the null hypothesis at the 5% significance level. However in 3 out of 16 cases, the equivalency of the estimates of the peak drift ratios for the scissors and super element joint model may be rejected at the 10% significance level. Also, the observed mean of the normalized drift ratio in Tables 4.1 and 4.2 is distributed on either side of unity. For the normalized scissors-rigid joint model comparison, their mean ranges from 1.08 to as low as 0.93, whereas from the super element-rigid joint model comparison, it ranges from 1.44 to 0.65.

#### 4.4.2 Roof Level

A visual inspection in Fig. 4.5 above, shows that the average of the peak in-time drift ratio for the super element model decreases appreciably when compared to the scissors and the rigid joint models at the roof level. In summary, in 13 out of 16 cases at the 5% significance level as well as all cases for the 10% significance level, the equivalency of the normalized super element-rigid joint model peak drift ratio may be rejected as seen in table 4.3. Hence, a better approach to assessing the impact of the super element joint model on the seismic demand of the hypothetical frames under study is by establishing confidence intervals on the population parameter (the mean of normalized responses). Under the assumption of a student t-distribution, the expected decrease in terms of the peak drift ratio for the super element joint model at the roof level can range from 16% to 70% of the drift demand of RC frames modelled under the conventional rigid joint approach of frame connectivity. However, from Table 4.3, for the scissor-rigid joint model cases, the equivalency of the peak drift ratios can be accepted at both the 95% and 90% confidence level. It should be interpreted that on average, in 90% or 95% of the cases, we expected the peak drift ratio of the scissors joint model and rigid joint model to be equal.

Observing that the scissors joint model dynamic responses approximating the rigid joint model, we expect the drift demand of the super element joint model to be less than the scissors model as seen in Table 4.4, with mean value distributed significantly below unity. The means of the drift ratios range from 0.4 to 0.68. On average, using the pooled set of record, a decrease in the range of 20%-70% is expected when compared to the scissors joint model.

Table 4.3. Ratio of mean and standard deviation of the normalized drift responses at the roof floor level

			CM-R1	CM-R2	CM-R3	CM-P
Three Storey	SM	Mean	1.06	1.01	1.07	0.95
		SD	0.12	0.18	0.31	0.22
	SEM	Mean	0.40	0.68	0.60	0.56
		SD	0.12**	0.22*	0.29*	0.23*
Six Storey	SM	Mean	1.05	1.01	1.03	1.03
		SD	0.12	0.17	0.24	0.20
	SEM	Mean	0.64	0.67	0.47	0.60
		SD	0.12**	0.22	0.27**	0.21**
Nine Storey	SM	Mean	1.05	1.07	1.05	1.06
		SD	0.14	0.22	0.25	0.21
	SEM	Mean	0.55	0.59	0.52	0.55
		SD	0.12**	0.22**	0.27**	0.22**
Pooled	SM	Mean	1.06	1.03	1.05	1.04
		SD	0.10	0.13	0.16	0.12
	SEM	Mean	0.53	0.64	0.53	0.57
		SD	0.10**	0.14**	0.20**	0.14**

\*CM-R1: Rigid joint model for record set 1; CM-R2: Rigid joint model for record set 2 ; CM-R3: Rigid joint model for record set 3; CM-P: Rigid joint model for pooled record set; SM: Scissors model; SEM: Super element model; SD: Standard deviation ; \*\* and \* signify the rejection of the null hypothesis at 5% and 10% significance levels respectively.

Table 4.4. Ratio of mean and standard deviation of the means of Z at the roof floor level

			SM-R1	SM-R2	SM-R3	SM-P
Three Storey	SEM	Mean	0.38	0.67	0.58	0.54
		SD	0.14**	0.21*	0.28*	0.22**
Six Storey	SEM	Mean	0.61	0.66	0.46	0.58
		SD	0.14**	0.22*	0.28**	0.20**
Nine Storey	SEM	Mean	0.53	0.55	0.50	0.53
		SD	0.14**	0.21**	0.27**	0.21**
Pooled	SEM	Mean	0.50	0.63	0.51	0.55
		SD	0.10**	0.14**	0.19**	0.13**

\*SM-R1: Scissors model for record set 1; SM-R2: Scissors model for record set 2 ; SM-R3: Scissors model for record set 3; SM-P: Scissors model for pooled record set; SEM: Super element model; SD: Standard deviation ; \*\* and \* signify the rejection of the null hypothesis at 5% and 10% significance levels respectively.

#### 4.4.3 General Case

The maximum inter-storey drift ratio observed in any storey of the building is basically the quantity is used in fragility assessment of RC frames. Table 4.5 shows that the estimate of this quantity in about 94% of the cases are equal when explicit joint models are compared to the rigid joint assumption at the 10% significance level. Furthermore the hypothesis of equivalence in maximum inter-storey drift ratio can be accepted for all cases under study at a 5% significance level. However upon comparing the scissors joint model with the super element model in table 4.6, for low intensity ground motions, the equivalency cannot be accepted at both the 5% and 10% significance level. More so for records in the moderate magnitude range, the hypothesis that the responses of the super element joint model being equal to the scissors and rigid joint model can be accepted at both the 90% and 95% confidence level.

Table 4.5. Ratio of mean and standard deviation of the normalized drift responses.

			CM-R1	CM-R2	CM-R3	CM-P
Three Storey	SM	Mean	1.03	0.99	1.03	1.02
		SD	0.11*	0.17	0.33	0.21
	SEM	Mean	0.77	1.11	0.95	0.94
		SD	0.14	0.21	0.33	0.23
Six Storey	SM	Mean	1.05	1.00	1.04	1.03
		SD	0.10	0.14	0.24	0.24
	SEM	Mean	1.02	0.86	0.63	0.84
		SD	0.13	0.18	0.32	0.23
Nine Storey	SM	Mean	1.09	1.03	1.06	1.06
		SD	0.16	0.18	0.19	0.27
	SEM	Mean	0.85	0.95	0.66	0.82
		SD	0.13	0.17	0.23*	0.26
Pooled	SM	Mean	1.05	1.01	1.04	1.03
		SD	0.08	0.10	0.16	0.14
	SEM	Mean	0.88	0.97	0.75	0.87
		SD	0.09	0.11	0.17	0.14

\*CM-R1: Rigid joint model for record set 1; CM-R2: Rigid joint model for record set 2 ; CM-R3: Rigid joint model for record set 3; CM-P: Rigid joint model for pooled record set; SM: Scissors model; SEM: Super element model; SD: Standard deviation ; \*\* and \* signify the rejection of the null hypothesis at 5% and 10% significance levels respectively.

Table 4.6. Ratio of mean and standard deviation of the means of Z.

			SM-R1	SM-R2	SM-R3	SM-P
Three Storey	SEM	Mean	0.75	1.11	0.95	0.94
		SD	0.14*	0.21	0.33	0.23
Six Storey	SEM	Mean	0.97	0.86	0.61	0.81
		SD	0.13	0.18	0.32	0.23
Nine Storey	SEM	Mean	0.78	0.93	0.63	0.78
		SD	0.13*	0.17	0.23*	0.26
Pooled	SEM	Mean	0.83	0.97	0.73	0.84
		SD	0.09**	0.11	0.18*	0.14

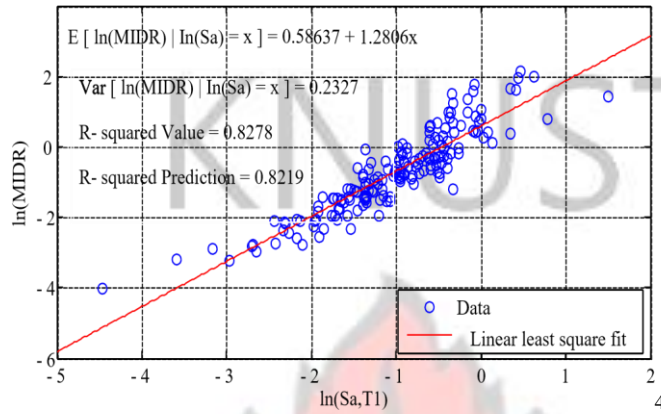
\*SM-R1: Scissors model for record set 1; SM-R2: Scissors model for record set 2 ; SM-R3: Scissors model for record set 3; SM-P: Scissors model for pooled record set; SEM: Super element model; SD: Standard deviation ; \*\* and \* signify the rejection of the null hypothesis at 5% and 10% significance levels respectively.

## 4.5 Seismic Vulnerability Assessment

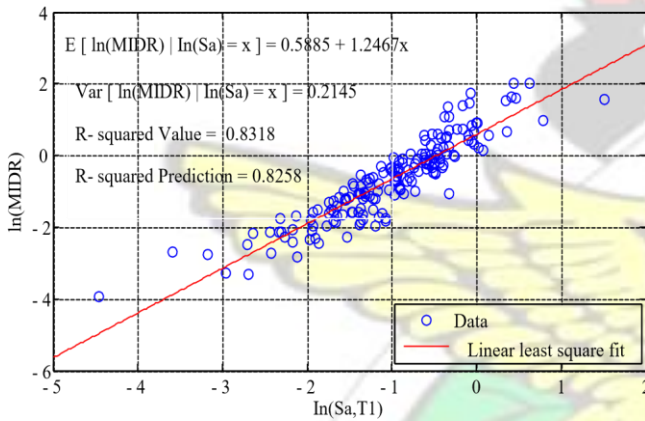
### 4.5.1 Probabilistic seismic demand model

A probabilistic seismic demand model (PSDM) as discussed in chapter 3-section 3.6 was developed to provide inputs for computing analytical fragility functions ( see Fig. 4.6). By comparing the mean function for the various joint models, which here represents the median drift response for a given intensity measure, the rigid joint model exhibited the highest degree of inelasticity. This is from the fact that the slope which is the coefficient of the intensity measure in the rigid joint PSDM, 1.2886, is far from unity relative to the explicit joint models (1.2467 for super element model and 1.1617 for scissors joint model. A slope of unity, signifies a perfect linear relationship between the intensity measure and the drift response in the basic space; —the equal displacement rule as noted by Veletsos and Newmark (1960). The mean functions from the various cases in combination with the estimated variance, can be used to establish the 16<sup>th</sup>, 50<sup>th</sup> and 84<sup>th</sup> percentile of the observed data at a particular intensity measure. It was found that the increase in MIDR when joint flexibility is incorporated is not directly proportional to the  $S_a(T_1)$ , and that this phenomenon may be valid for lower ranges of ground motion intensities. A typical

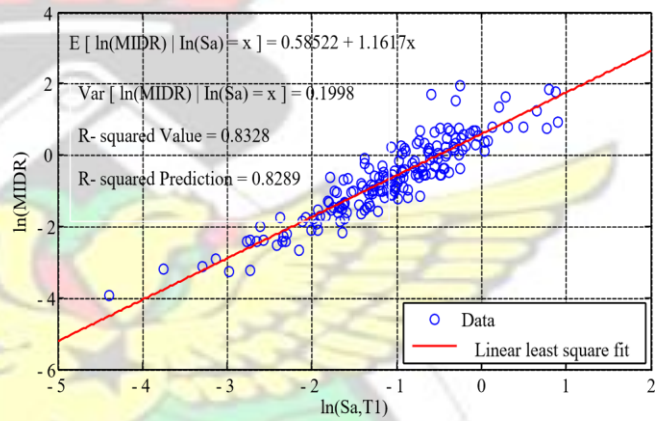
example is the median MIDR at  $S_a(T1)$  of 0.5g which yields 0.739%, 0.759% and 0.803% for the rigid, super-element and scissors joint modelling schemes respectively.



a P DM for rigid joint model



b P DM for super element joint model



c P DM for scissors joint model

Fig 4.6. Probabilistic demand model analysis of RC frame with different joint modelling schemes

However at  $S_a(T1)$  of 1.5g, the estimates of the median MIDR are 3.021%, 2.986% and 2.876% for rigid, super-element and scissors joint models. This observation is consistent with the work of Park and Mosalam (2012) that quantified the variation in the rigid and scissors joint model, concluding that for more flexible frames, the relative increase in the drift responses may drop at larger spectral acceleration. This could be attributed to the

fact that framing members may have then been subjected to large strain hardening in the rigid joint model.

#### 4.5.2 Fragility Functions

The probability of exceeding a prescribed limit state is usually a metric that is employed in computing the seismic reliability of a structure. This is usually lumped into a fragility curve which requires a functional relationship between the structural response and its associated ground motion intensity. The predefined limit state that reflects the extent of damage sustained by a structural component locally or a whole structural system from base excitation are typically treated as deterministic values, such as the immediate occupancy limit state with a threshold drift ratio of 1% from (FEMA 350, 2000), or as a random value when incremental dynamic analysis is employed. The HAZUS-MH (FEMA, 2003), mainly developed from expert opinions have outlined four damage states that can be used in estimating seismic losses. The median drift response are 0.5%, 0.8%, 2%, 5% corresponding to slight, moderate, extensive and complete limit state respectively with a dispersion of 0.3 and is adopted for computation. Adopting the cloud analysis demand model with variables assumed to be lognormally distributed, the limit state probability of exceedance can be computed as per Equation 4.1.

$$P[D \geq C | S_a = x] = 1 - \frac{1}{2} \left[ 1 + \frac{\ln C - \ln(ax^b)}{\sqrt{\ln^2 \mu_{D|x} + \ln^2 \mu_c + \ln^2 \mu_M}} \right] \quad (4.1)$$

where, here  $C$  and  $D$  are the limit state capacity and seismic demand,  $S_a$  is the spectral acceleration at the first mode,  $F$  is the cumulative Gaussian distribution function,  $a$  and  $b$ , are regression coefficients from regression analysis and  $\beta_{D|x}$ ,  $\beta_C$ ,  $\beta_M$  represent the dispersion in the demand model, limit state capacity and modelling uncertainties, respectively (assumed to be 0.2).

Following this procedure, Fig. 4.7 shows the generated analytical fragility functions for the hypothetical frame that incorporates the various joint modelling schemes at each damage state. It is observed that for the slight and moderate limit states, the spectral acceleration corresponding to the 50% probability of exceedance (median capacity) is relatively lower for the explicit joint models as compared to the rigid joint model. This reflects the increased vulnerability inherent in incorporating joint flexibility in the assessment framework. Following from the discussion made above, that the increase in MIDR when joint flexibility is incorporated is not directly proportional to the  $S_a(T1)$ , there is a significant vertical shift in the generated fragility curves at larger damage states. This is due to the fact that relatively lower intensity measures will be required to reach those damage limit states for the rigid joint model, hence increasing the conditional probability of exceedance. Hence, with the intuitive assumption that there will be an expected increase in the seismic vulnerability through increased fragility estimates when joint flexibility is incorporated, this may be valid for lower structural capacity limit states.

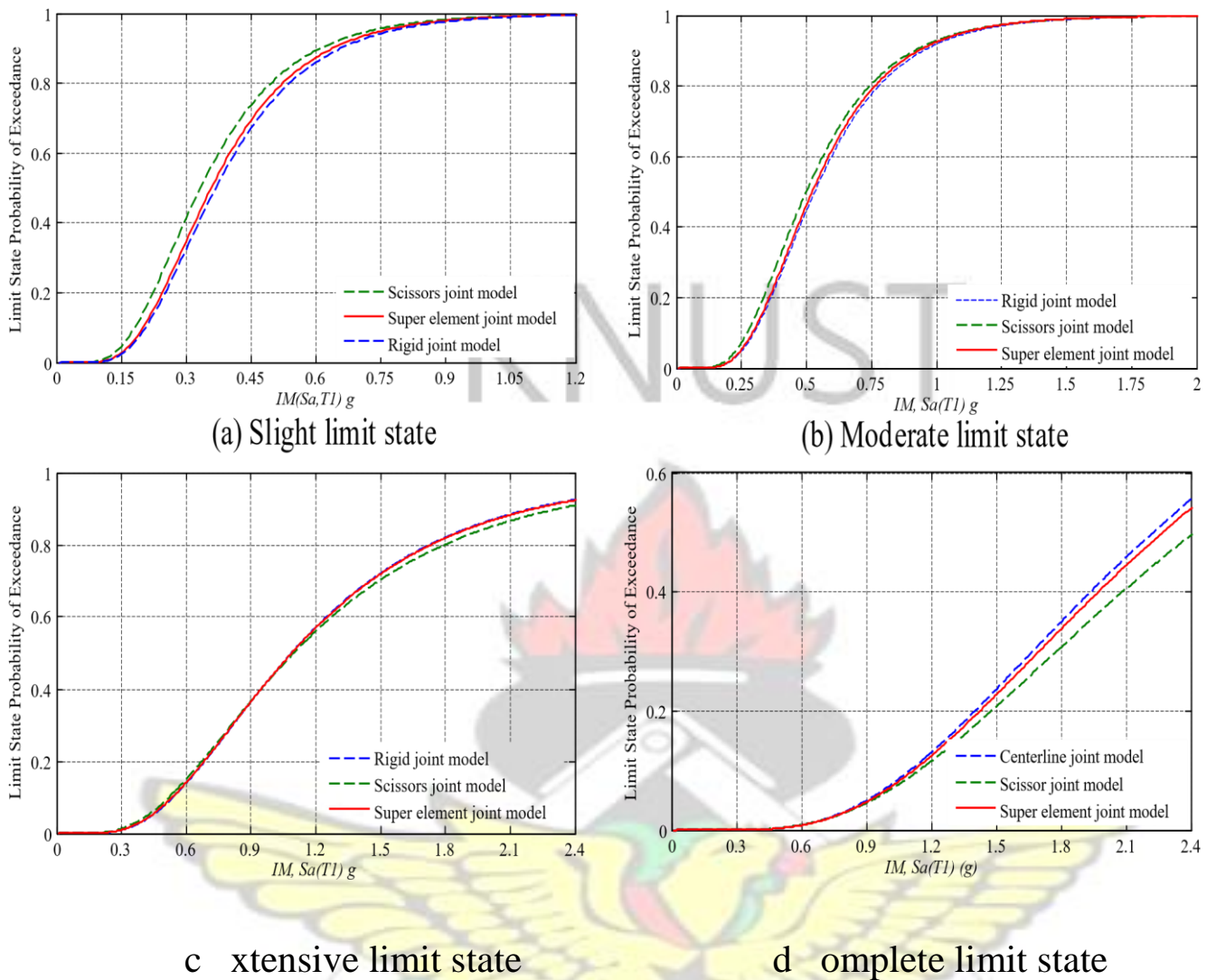
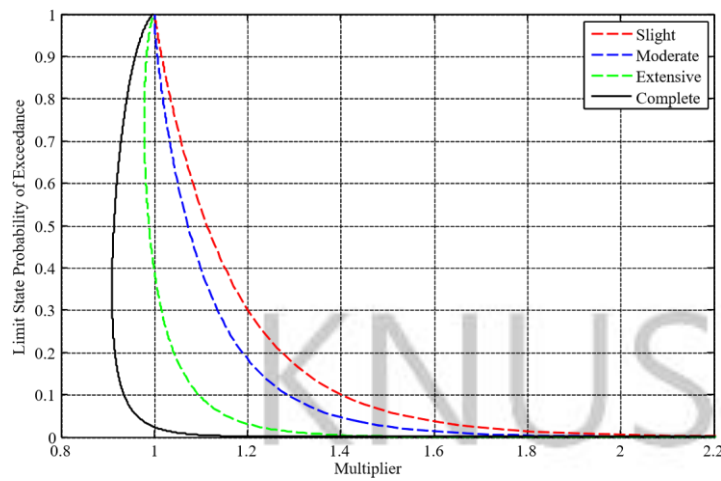
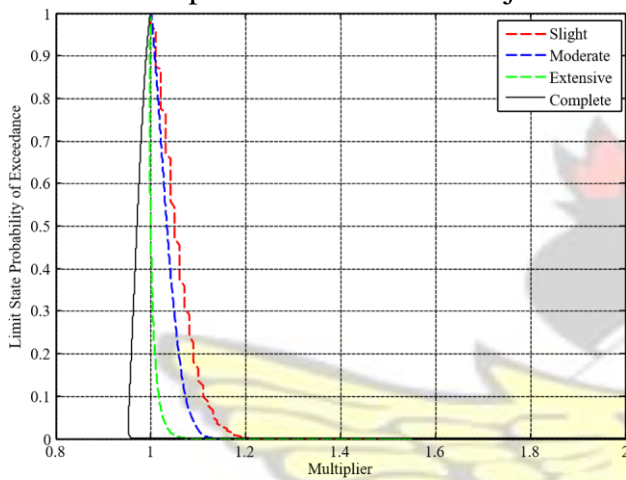


Fig. 4.7: Analytical fragility functions for various joint modelling schemes

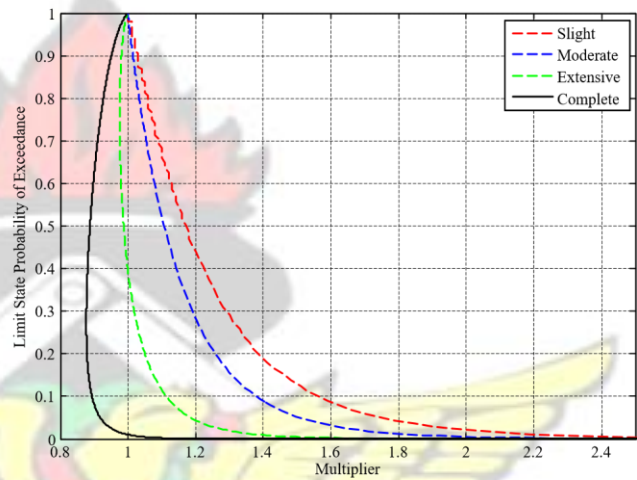
Fig. 4.8 illustrates the distribution of the shift in the vulnerability functions between the various modelling schemes for each limit state. It summarizes the extent to which there may be a significant increase in the limit state probability of exceedance by considering two joint modelling approaches at a time. We observe that the scissors model implementation of joint response apparently gives the most vulnerable estimate of our knowledge of the extent of damage for a particular ground motion intensity at lower damage states, and that in most of the cases, for the complete limit state capacity, the response from the rigid joint model may be critical.



a super element - scissors joint model



b rigid - super element joint model



c rigid - scissors joint model

Fig. 4.8: Relative shift in limit state probability between joint model.

It is seen in Fig. 4.8a, that to relate the fragility functions for the super element model to the scissors joint model, a multiplier greater than unity is required for transition when the performance objectives are the slight and moderate limit state. This emphasizes the increased vulnerability for the scissors joint model at lower limit state capacities. However, for the extensive limit state with an intensity measure that will produce a probability of exceedance above 40% as well as the complete limit state, the multiplier is below unity, hence making the super element model more vulnerable, relative to the

scissors joint model. One implication of this phenomenon is that, in performing seismic collapse risk assessment, the simulation of joint region with multicomponent deteriorating hysteretic models may cause an addition of global flexibility hence reducing the intensity measure required to cause collapse of the structural system compared to the popularly used single-component representation (zero –length rotational spring) joint behaviour.

#### **4.6 Summary of Findings**

The quantification of the additional inelastic deformation from inadequate shear and bond slip behaviour of joint has been found to be relevant for performing seismic vulnerability assessment. This has been evident in the responses of the rigid joint model schemes unreliably overestimating the lateral shear strength and it being unable to account for the reduced strength due to anchorage failure. Also, the amount of dissipated hysteretic energy may be well above the experimental responses of quasistatic reverse cyclic test.

An evaluation of the variation in the seismic response using either a multicomponent joint representation (super element model) and a single component representation (scissors joint model) has also shown that, in most cases, there may be equivalence in estimated maximum inter-storey drift. However, there exists large deviation in the drift responses at the roof when the super element joint model is implemented when compared to the scissors joint model and the conventional approach of fully fixed connection in nonlinear time history analysis of non-ductile RC frames.

Lastly, generated analytical fragility functions have also demonstrated that the expected added vulnerability that joint modelling of the primary inelastic mechanism produces, may be very critical when lower performance objectives, such as the slight and moderate limit state, are prescribed. The multi-component joint modelling scheme may

produce greater vulnerability than the scissor joint model when performing seismic collapse risk assessment.

# KNUST



## **CHAPTER 5: CONCLUSIONS AND RECOMMENDATIONS**

### **5.1 Conclusions**

The inelastic behaviour of reinforced concrete beam-column joints that lacks modern seismic detailing requirement is addressed. This stems from the fact that when such joints are subjected to high shear forces due to seismic excitations, the inelastic mechanisms that emanate may be detrimental to other framing members, that is, inadequate utilization of flexural capacities of beam and columns. Hence, this study sought to evaluate and quantify the inelastic behaviour and seismic performance of RC frames that do not have adequate joint shear capacity to maintain the conventional rigid joint assumption.

Three joint modelling schemes used for simulating the behaviour of joint response under nonlinear seismic analysis of RC frame structures were investigated. The rigid joint assumption (rigid joint model) which relies on framing members being able to maintain their orthogonality during analysis, a single component joint model (scissors joint model) where all the primary inelastic mechanism is concentrated into a rotational spring and a multi component joint modelling scheme (super element joint model) that allows for independent quantification of the various joint inelastic mechanism, were implemented in the nonlinear platform finite element platform, *Opensees*. These analytical joint modelling schemes were tested under three typical joint configurations using experimental results of quasi-static reverse cyclic loading of interior, exterior and knee joints with no transverse reinforcement. Both explicit joint models (scissors and super element joint models) were fairly able to capture the estimated horizontal shear strength as well as the highly pinched behaviour beamcolumn joint subassemblies under load reversals. The estimated shear capacities of the rigid joint model were much higher with a larger amount of hysteretic energy dissipated when compared to experimental results.

To evaluate the seismic performance of the various joint models, the demand from three hypothetical frames was evaluated for three classes of records. Based on this investigation, there is a large deviation in the drift responses of super element joint models at the roof level when compared to the scissors and rigid joint model. The equivalence in

the drift responses for the explicit joint modelling approaches also did not yield a significant correlation with selected class of records at varying intensities. For seismic risk assessment of RC building, the maximum inter-storey drift at any storey height is preferred for generating fragility functions. From this study, there is no consistent evidence to suggest that care should be taken in selecting either a single or multi component joint model for seismic risk assessment of buildings when the maximum inter-storey drift ratio is used as the engineering demand parameter.

Furthermore, an investigation of the appropriateness of incorporating joint response in nonlinear time history analysis of RC non ductile frames utilizing multi component spring model is performed, since concerns has been raised about it causing numerical divergence in the global solution algorithm. To this extent, the two other joint modelling schemes (rigid and scissors joint models) were also implemented in order to quantify their variations in the estimated seismic demand from a given ground motion intensity. A probabilistic seismic demand analysis was performed to quantify the functional relationship between the ground motion intensity measure (IM) and the seismic response (EDP). With these functional relationships as input, analytical fragility functions that can be used to assess the extent of vulnerability of various joint modelling schemes were constructed. Result showed that the single component joint model is the most vulnerable for lower limit state capacities, with the rigid joint model being the least. However, this trend reverses for higher limit state, such the complete limit state with a threshold of 5% median drift ratio. The super element joint model, where all the governing inelastic mechanisms are decoupled by employing a multi-component spring model, yielded responses that were in between the two other joint models, but rather skewed towards the rigid joint model. This trend emphasizes the appropriateness of using the super-element joint model which have been thought to cause numerical divergence during time history analysis of two-dimensional RC frames.

## 5.2 Recommendations for Future Research

The current study has emphasized the importance of including joint flexibility in nonlinear seismic vulnerability assessment. It has also shown the appropriateness of employing a multi-component spring model for quantifying joint behaviour. Hence further research advancement on the usage of this modelling scheme can be

- Incorporation into a full probabilistic collapse risk assessment of existing nonductile reinforced concrete frames.
- Investigate the adequacy of how current retrofitting strategies, such as column jacketing, reinforcement through epoxy injection, etc., provide additional shear resistance to unreinforced RC joints.
- Fragility analysis of several idealized archetype older RC building.
- Providing simplified extension to three dimensional analyses of irregular RC structures as well as accounting for bidirectional seismic effect.

## 6. REFERENCES

- Alath, S. and Kunnath, S. K. (1995). —Modelling inelastic shear deformations in RC beam-column joints. Engineering Mechanics Proceedings of 10th Conference, May 21–24, University of Colorado at Boulder, Boulder, Colorado, ASCE, 2: 822–825.
- Altoontash, A. (2004). — Simulation and damage models for performance assessment of reinforced concrete beam-column joints. Ph.D. Dissertation, Department of Civil and Environmental Engineering, Stanford University, Stanford, CA.
- Anagnostopoulos, S.A (1972). —Nonlinear dynamic response and ductility requirement for buildings subjected to earthquakes. Report No. R72-54, Department of Civil Engineering, Massachusetts Institute of Technology, Cambridge, MA.

- Anderson, J. and Townsend, W. H. (1977). —Models for RC frames with degrading stiffness, *Journal of the Structural Division, ASCE*, 103(ST12): 2361–2376.
- Anderson, M., Lehman, D., and Stanton, J. (2008). —A cyclic shear stress-strain model for joints without transverse reinforcement, *Engineering Structures*, 30(4): 941–954.
- Arias, A. (1970). — Measure of earthquake Intensity, in *Seismic Design for Nuclear Power Plants*. R. J. Hansen, Editor, M. I. T. Press, Cambridge, 438–483.
- Armelle A., (2006). — simple displacement control technique for pushover analyses, *Earthquake Engineering and Structural Dynamics*, 35:851–866.
- ACI 41/06, —Seismic Rehabilitation of Existing Buildings, American Society of Civil Engineers, Reston, Virginia, 2006.
- Aslani, H. (2005). —Probabilistic Earthquake Loss Estimation and Loss Disaggregation in Buildings, PHD Dissertation, Stanford University.
- Aycardi, L. E., Mander, J. B., and Reinhorn, A. M. (1994). — seismic resistance of reinforced concrete frame structures designed only for gravity loads: experimental performance of subassemblages, *ACI Structural Journal*, 91(5): 552-563.
- Baber, T., and Noori, M. N. (1985). —Random vibration of degrading, pinching systems, *ASCE Journal of Engineering Mechanics*, 111(8):1010-1026.
- Bakir, P. G., and Boduroğlu, H. M. (2002). — New Design Equation for Predicting the Joint Shear Strength of Monotonically Loaded Exterior Beam-Column Joints, *Engineering Structures*, 24:1105-1117.
- Baker, J.W and Cornell, C.A. (2003). —Uncertainty specification and propagation for loss estimation using FOSM methods, PEER Report, 2003/07, Pacific Earthquake Engineering Centre, University of California, Berkeley, CA.
- Baker, J.W and Cornell, C.A. (2006). —Vector-valued ground motion intensity measures for probabilistic seismic demand analysis, PEER Report, 2006/08, Pacific Earthquake Engineering Centre, University of California, Berkeley, CA.
- Baker, J. W. and C. A. Cornell (2007). "Uncertainty propagation in seismic loss estimation." *Structural Safety* 30(3): 236-252.
- Bazzurro, P. (1998). —Probabilistic seismic demand analysis.", PhD. Dissertation Department of Civil and Environmental Engineering, Stanford University, Stanford, CA.
- Belarbi, A. and Hsu, T.T.C. (1994). —Constitutive Laws of Softened Concrete in Biaxial Tension-compression, *ACI Structural Journal*, 9(4):465-474.

- Beres, A., White, R.N. and Gergely, P. (1992). — seismic performance of interior and exterior beam-to-column joints related to lightly RC frame buildings: Detailed experimental results, structural engineering Report 92-7, School of Civil and Environmental Engineering, Cornell University. Ithaca, NY.
- Birely, A.C., Lowes, L.N. and Lehman E. D. (2012). — model for the practical nonlinear analysis of reinforced-concrete frames including joint flexibility., *Engineering Structures*, 34: 455–465.
- Borghini, A., Gusella, F. and Vignoli, A. (2016). — seismic vulnerability of existing R. . buildings: A simplified numerical model to analyse the influence of the beamcolumn joints collapse, *Engineering Structures*, 121:19–29.
- Bouc, R. (1967). — forced vibration of mechanical systems with hysteresis., Abstract Proc., 4<sup>th</sup> Conference on Nonlinear Oscillation.
- Bracci, J. M., Reinhorn, A. M. and Mander, J. B. (1995). — seismic resistance of reinforced concrete frame structures designed for gravity loads: Performance of structural system., *ACI Structural Journal*, 92(5):597-608.
- BSI: CP 110: (1972). —The Structural Use of Concrete. Part I: Design, Materials and Workmanship., British Standards Institution, London
- Cornell, C.A. and Krawinkler, H. (2000). —Progress and challenges in seismic performance assessment., *PEER Centre News*, 3 (2).
- Celik, O. C. (2007). —Probabilistic assessment of non-ductile reinforced concrete frames susceptible to Mid-America ground motions., Ph.D. Thesis, Georgia Institute of Technology, Atlanta, 1–200.
- Celik, O. C. and Ellingwood, B. R. (2008). —Modelling beam-column joints in fragility assessment of gravity load designed reinforced concrete frames., *Journal of Earthquake Engineering*, 12(3):357-381.
- Chandler, A.M. and Lam, N.T.K (2001). —Performance-based design in earthquake engineering: a multi-disciplinary review., *Engineering Structures* 23(12):1525–1543.
- Chao-Lie, N., Bo, Y. and Bing L. (2015). —Beam-column joint model for nonlinear analysis of non-seismically detailed reinforced concrete frame., *Journal of Earthquake Engineering*, 20:476–502.

- Clough, R. W., and Johnston, S. B. (1966). — Effect of stiffness degradation on earthquake ductility requirements. Proceedings, Second Japan National Conference on Earthquake Engineering, 227-232.
- Deng, C.G., Bursi, O.S., and Zandonini, R. (2000). — hysteretic connection element and its application. *Computers and Structures*, 78(1-3):93-110.
- Deniz, D. (2014). — Stochastic prediction of collapse of building structures under seismic excitations, PhD. Dissertation, Department of Civil and Environmental Engineering, University of Illinois at Urbana-Champaign, IL
- El-Metwally, S.E and Chen, W.F (1988). — Moment rotation modeling of reinforced concrete beam-column connections. *ACI Structural Journal*, 85(4):384–394.
- Elwood, K.J. and Moehle, J.P. (2005). — Drift capacity of reinforced concrete columns with light transverse reinforcement, *Earthquake Spectra*, 12(1):71–89.
- FEMA 356 (2000). — Pre standard and commentary for the seismic rehabilitation of buildings”, FEMA Publication No. 356, prepared by the American Society of Civil Engineers for the Federal Emergency Management Agency, Washington, DC.
- FEMA (2000). — Recommended seismic design criteria for new steel moment-frame buildings. Report No. M - 350, SAC Joint Venture, Federal Emergency Management Agency, Washington DC.
- FEMA (2003). — HAZUS-MH MR4 technical manual, earthquake model, Federal Emergency Management Agency, Washington, DC.
- Haselton, C.B. (2006). — Assessing seismic collapse safety of modern reinforced concrete moment frame buildings, Ph.D. Dissertation, Department of Civil and Environmental Engineering, Stanford University, CA.
- Haselton, C.B., Liel, A.B., Deierlein, G., Dean, B.S., and Chou, J.H. (2011). — Seismic collapse safety of reinforced concrete buildings. I: Assessment of ductile moment frames, *ASCE Journal of Structural Engineering*, 137(4):481–491.
- Hassan, W. M. (2011). — Analytical and experimental assessment of seismic vulnerability of beam-column joints without transverse reinforcement in concrete buildings, PHD Dissertation, University of California, Berkeley.
- Hwang, S.J. and Lee, H.J. (2002). — Strength prediction for discontinuity regions by softened strut-and-tie model, *ASCE Journal of Structural Engineering*, 128(12):1519–1526.

- Hisada, T., Nakagawa, K., and Izumi, M., (1962). — earthquake response of structures having various restoring force characteristics. | Proceedings, Japan National Conference on Earthquake Engineering, pp. 63-68.
- Hoffmann, G.W, Kunnath, S.K, Reinhorn A.M and Mander, J.B (1992). —Gravity-load designed reinforced concrete buildings: Seismic evaluation of existing construction and detailing strategies for improved seismic resistance. | Technical Report NCEER- 92-0016, National Centre for Earthquake Engineering Research, State University of New York at Buffalo, Buffalo, NY.
- Hossain, M. R., Ashraf, M., and Padgett, J. E. (2013). —Risk-based seismic performance assessment of Yielding Shear Panel Device. | *Engineering Structures*, 56:1570-1579.
- Ibarra, L.F. and Krawinkler, H. (2005). —Global collapse of frame structures under seismic excitations |, Rep. No. TB 152, The John . Blume earthquake Engineering Centre, Stanford University, Stanford, CA.
- Ibarra, L.F., Medina R.A. and Krawinkler, H. (2005). —Hysteretic models that incorporate strength and stiffness deterioration |, *Earthquake Engineering and Structural Dynamics*, 34(12):1489-1511.
- Iervolino, I. (2004). —Record Selection for Nonlinear Seismic Analysis of Structures |, M.Sc. thesis, University of Pavia, Pavia, Italy.
- Iwan, W. D. (1966). — distributed-element model for hysteresis and its steady-state dynamic response, “ *Journal of Applied Mechanics*, 33(42):893–900.
- Jalayer F. (2003). —Direct probabilistic seismic analysis: Implementing non-linear dynamic assessments |, Stanford University, Ph.D. Dissertation, Stanford, CA,
- Jeon, J.S. (2013). — aftershock vulnerability assessment of damaged reinforced concrete buildings in California. | PHD Dissertation, Georgia Institute of Technology, Atlanta.
- Jeon, J.S., Lowes, L.N, DesRoches, R. and Brilakis, I. (2015). — fragility curves for nonductile reinforced concrete frames that exhibit different component response mechanisms. |, *Engineering Structures*, 85:127–143.
- Kaneko, Y., Mihashi, H., and Ishihara, S. (2001). —Entire load-displacement characteristics for direct shear failure of concrete: Modelling of inelastic behaviour of RC structures under seismic load Reston, VA: American Society of Civil Engineers.

- Kien, L.T, Kihak, L., Myoungsu, S. and Jaehong, L. (2012). — eismic Performance Evaluation of RC beam column connections in special and intermediate moment frames, *Journal of Earthquake Engineering.*, 17:187–208.
- Kim, J., and LaFave, J. M. (2009). —Joint shear behaviour of reinforced concrete beamcolumn connections subjected to seismic lateral loading. Report No. N L020, Department of Civil and Environmental Engineering, University of Illinois at Urbana-Champaign, IL.
- Krawinkler, H., and Zareian, F. (2007). —Prediction of collapse – How Realistic and Practical Is It, and What an We Learn from It? The Structural Design of Tall and Special Buildings, 16, 633-653.
- Laura, E., Eduardo M., Lignos D. (2016). — pectral shape metrics and structural collapse potential, *Earthquake Engineering and Structural Dynamics*, 45: 1643–1659.
- LeBorgne, M.R. (2012). —Modelling the post shear failure behaviour of reinforced concrete columns, Ph.D. Dissertation, The University of Texas at Austin, Austin, TX.
- Lee, D.H. and Elnashai, A.S. (2001). —Seismic analysis of RC bridge columns with flexure shear interaction:, *ASCE Journal of Structural Engineering*, 127(5): 546–553.
- Lehman, D.E., Moehle, J.P. (2000). —Seismic performance of well-confined concrete bridge columns., Pacific Earthquake Engineering Research Centre, University of California, Berkeley, CA.
- Liel, A.B. (2008) — ssuming the collapse risk of alifornia’s existing reinforced concrete frame structures: Metrics for seismic safety decisions, Ph.D. Dissertation, Department of Civil and Environmental Engineering, Stanford University, CA.
- Liel, A.B., Haselton, C.A., Deierlin G.G. and Baker J.W (2009). —Incorporating modelling uncertainties in the assessment of seismic collapse risk of buildings., *Structural Safety*, 31:197–211.
- Lignos, D. (2008). — ide-sway collapse of deteriorating structural systems under seismic excitations. Ph.D. Dissertation, Department of Civil and Environmental Engineering, Stanford University, CA.
- Lignos, D. and Krawinkler, H. (2012). — ide-sway collapse of deteriorating structural systems under seismic excitations. John A. Blume Earthquake Engineering Research Center Report No. 177, Department of Civil Engineering, Stanford University.

- Lowes, L. N. and Altoontash, A. (2003). —Modelling reinforced-concrete-column joints subjected to cyclic loadings.‖ *ASCE Journal of Structural Engineering*, 129(12): 1686-1679.
- Mackie K. and Stojadinovic B., (2003). —Seismic demands for performance-based design of bridges.‖, Pacific Earthquake Engineering Research Centre, University of California at Berkeley, PEER , 2003-16, Berkeley, California.
- Masi, A., Santarsiero, G., Lignola, G.P.and Verderame, G.M. (2013). — tudy of the seismic behaviour of external RC beam–column joints through experimental tests and numerical simulations.‖, *Engineering Structures*, 52: 207–219.
- McKenna, F., Scott, M. H., and Fenves, G. L. (2010). —Nonlinear finite-element analysis software architecture using object composition.‖ *ASCE Journal of Computing*, 24(1). 95-107.
- Menegotto, M. and Pinto, P (1973). —Method of analysis of cyclically loaded reinforced concrete plane frames including changes in geometry and inelastic behaviour of elements under combined normal geometry and inelastic behaviour of elements under combined normal force and bending.‖, Proceedings of the IABSE Symposium on the Resistance and Ultimate Deformability of Structures Acted on by Well-Defined Repeated Loads, Lisbon.
- Medina, R. (2002). — eismic demands for nondeteriorating frame structures and their dependence on ground motions.‖ Ph.D. Dissertation, Department of Civil and Environmental Engineering, Stanford University, Stanford, CA.
- Mehanny, S.S., and Deierlein, G.G. (2000). —Modelling and Assessment of Seismic Performance of Composite Frames with Reinforced Concrete Columns and Steel Beams”, Report No. 136, The John A. Blume Earthquake Engineering Center, Stanford University, Stanford, CA.
- Mirko, K.,Peter, F. and Matjaz,D (2014). — pproximate seismic risk assessment of building structures with explicit consideration of uncertainties‖, *Earthquake Engineering and Structural Dynamics*, 43:1483–1502.
- Mitra N. and Lowes, L.N (2007,) — valuation, alibration, and Verification of a Reinforced Concrete Beam– olumn Joint Modell, *Journal of Structural Engineering*, 139:105-20.
- Mitrani-Reiser, J. (2007). —An Ounce of Prevention: Probabilistic Loss Estimation for Performance Based Earthquake Engineering‖, PHD. Dissertation, California Institute of Technology.

- Moehle J. and Deierlein G.G., (2004). —A framework methodology for performancebased earthquake engineering, in Proceedings, 13th World Conference on Earthquake Engineering, Vancouver, Canada.
- Moehle, J. P. and Mahin, S. A. (1991). —Observations on the Behaviour of Reinforced Concrete Buildings during Earthquakes., arthquake-Resistant Concrete Structures—Inelastic Response and Design, SP-127, S. K. Ghosh, ed., American Concrete Institute, Farmington Hills, Michigan, 67-89.
- Nielsen, N.N., and Imbeault, F.A., (1971) —Validity of various hysteretic systems. Proceedings, Third Japan National Conference on Earthquake Engineering, 707714.
- Otani, S., and M.A. Sozen, (1972). —Behaviour of multi storey reinforced concrete frames during earthquakes. Structural Research Series No. 392, Civil Engineering Studies, University of Illinois, Urbana, 1972.
- Ortiz, I.R. (1993). —Strut-and-Tie Modeling of Reinforce Concrete Short Beams and Beam-Column Joints, PhD Dissertation, University of Westminster. London, UK.
- Ozbolt, J., Mayer U., and Vocke, H. (2001). —Smearred fracture FE-analysis of reinforced concrete structures – theory and examples. Modeling of Inelastic Behavior of RC Structures under Seismic Load., Reston, VA: American Society of Civil Engineers, 234-256.
- Pantazapoulou, S.J. and Bonacci, J.F. (1994). —On earthquake-resistant reinforced concrete frame connections., *Canadian Journal of Civil Engineering*, 21:307-28.
- Pantelides, C.P., Hansen, J., Nadauld, J., and Reaveley, L.D. (2002) —Assessment of reinforced concrete building exterior joints with substandard details., P R Report , 2002/18, Pacific Earthquake Engineering Centre, University of California, Berkeley, CA.
- Paulay, T., Park, R. and Priestley, M. J. N. (1978) \_\_Reinforced concrete beam-column joints under seismic actions,“ *ACI Structural Journal*, 75(11):585–593.
- Park, S. (2010). — xperimental and nalytical tudies on Old Reinforced oncrete Buildings with Seismically Vulnerable Beam-Column Joints., PHD Dissertation, University of California, Berkeley, USA.
- Park, Y.-J., and Ang, A.H.-S. (1985). —Mechanistic eismic Damage Model for Reinforced oncrete,“ *ASCE Journal of Structural Engineering*, 111(4): 722– 739.

- Park, S. and Mosalam, K.M (2012). —Experimental and analytical studies on reinforced concrete buildings with seismically vulnerable beam column joints.‡, P R Report, Pacific Earthquake Engineering Centre, University of California, Berkeley, CA.
- Pincheira, J. A., Dotiwala, . . and D' ouza, J. T. (1999). — eismic analysis of older reinforced concrete columns‡, *Earthquake Spectra*, 15(2): 245-272.
- Porter, K. A., J. L. Beck and R. V. Shaikhutdinov (2002). —Sensitivity of Building Loss Estimates to Major Uncertain Variables.‡ *Earthquake Spectra*, 18(4): 719- 743.
- Piyali S. and Bing L. (2014) — eismic fragility evaluation of lightly reinforced concrete beam-column joints‡, *Journal of Earthquake Engineering*, 18:1102–1128.
- Rahnama, M. and Krawinkler, H. (1993). — ffect of soft soils and hysteresis models on seismic design spectra.‡ John A. Blume Earthquake Engineering Research Centre Report No. 108, Department of Civil Engineering, Stanford University.
- Rezaeian, S. (2010). —Stochastic modelling and simulation of ground motions for performance-based earthquake engineering.‡ Ph. D. Dissertation, Department of Civil and Environmental Engineering, University of California, Berkeley, CA.
- Rice, J.A, (2007) —Mathematical tistics and Data nalysis‡, Third Edition, Duxbury, California, USA.
- Riddell, R. (2007). —On Ground Motion Intensity Indices.‡ *Earthquake Spectra*, 23: 147–173.
- Sucuoglu, H., and Erberik, A., (2004). — nergy-based hysteresis and damage models for deteriorating systems.‡ *Earthquake engineering and structural dynamics*, 2004, 33(1):69-88.
- Sezen, H. and Chowdhury, T. (2009). —Hysteretic model for the lateral behaviour of reinforced concrete columns including shear deformation‡, *ASCE Journal of Structural Engineering*, 135(2):139–146.
- Sezen, H., Elwood, K.J., Whittaker, A.S., Mosalam, K.M., Wallace, J.W. and Stanton, J.F. (2000). —Structural engineering reconnaissance of the August 17,1999 earthquake: Kocaeli, (Izmit) Turkey‡, PEER Report, Pacific Earthquake Engineering Centre, University of California, Berkeley, CA
- Sozen, M. A. (1981) —Review of earthquake response of reinforced concrete buildings with a view to drift control.‡ in State-of-the-Art in Earthquake Engineering, Turkish National Committee on Earthquake Engineering, Istanbul, Turkey, 383–418.

- Shafaei, J., Zarein, M.S., Hosseini, A. and Marefat, M. S. (2014). — Effects of joint flexibility on lateral response of reinforced concrete frames, *Engineering Structures*, 81: 412–431.
- Shing, P. B., and Spencer, B. (2001). —Modelling of shear behaviour of RC bridge structures: modelling of inelastic behaviour of RC structures under seismic load., Reston, VA: American Society of Civil Engineers.
- Shome, N. (1999). —Probabilistic seismic Demand analysis of Nonlinear structures, Ph.D. Dissertation, Dept. of Civil and Environmental Engineering, Stanford University, Stanford, California, USA.
- Song, J. and Pincheira, J. (2000). — Spectral displacement demands of stiffness and strength degrading systems. *Earthquake Spectra*, 16(4):817-851.
- Taylor, H.P.J. (1974). —The behaviour of in-situ concrete beam-column joints. Technical Report 42.492, Cement and Concrete Association, Wexham Springs, UK.
- Takeda, T., Sozen, M., Nielsen, N. (1970). —Reinforced concrete response to simulated earthquakes. *Journal of the Structural Division*, 96(12):2557-2573.
- Theiss, A.G. (2005). —Modelling the earthquake response of older reinforced concrete beam-column building joints, M c thesis, University of Washington.
- Tothong, P. and Cornell, C. A. (2008). — Structural Performance Assessment under Near-Source Pulse-Like Ground Motions Using Advanced Ground Motion Intensity Measures. *Earthquake Engineering and Structural Dynamics*, 37(7): 1013-1037.
- Thyagarajan, R. S. and Iwan, W. D. (1990). —Performance characteristics of widely used hysteretic model in structural dynamics. Proceedings, Fourth U.S National Conference on Earthquake Engineering, Earthquake Engineering Research Institute (EERI), 2:177-186.
- Vamvatsikos, D. and Cornell, C.A. (2002). —Incremental Dynamic analysis. *Earthquake Engineering and Structural Dynamics*, 31(3):491-514.
- Vecchio, F.J and Collins, M.P (1986). —The modified-compression field theory for reinforced concrete elements subjected to shear. *Journal of the American Concrete Institute* 83(2): 219–231.
- Vollum, R.L. (1998). —Design and Analysis of Exterior Beam Column Connections., PhD Dissertation, Imperial College of Science Technology and Medicine University of London, London, UK.

- Veletsos, A. S. and Newmark, N. M (1960). — Effect of inelastic behaviour on the response of simple systems to earthquake motions, Proceedings of the Second World Conference on Earthquake Engineering, Japan, Tokyo, 2: 895-912.
- Villaverde, R. (2007). —Methods to assess the seismic collapse capacity of Building Structures: State of the Art. *ASCE Journal of Structural Engineering*, 33(1):57-66.
- Wong, H.F. (2005). —Shear Strength and Seismic Performance of Non-Seismically Designed Reinforced Concrete Beam-Column Joints, PhD Dissertation, Hong Kong University of Science and Technology, Hong Kong.
- Yamamoto, Y. (2011). —Stochastic model for earthquake ground motion using wavelet packets, Ph.D. Dissertation, Department of Civil and Environmental Engineering, Stanford University, Stanford, CA.
- Youssef, M. and Ghobarah, A. (2001). —Modelling of RC beam-column joints and structural walls. *Journal of Earthquake Engineering*, 5(1):93–111.
- Zhang, P., Hou, S. and Ou, J. (2016). — “beam-column joint element for analysis of reinforced concrete frame structures”, *Engineering Structures*, 118:125–136.

